REMEDIATION OF SOILS CONTAMINATED WITH FLUORIDE USING SEAWEED-DERIVED MATERIALS: CASE OF SLOPES OF MOUNT MERU

Ruth Lorivi Moirana

A Thesis Submitted in Partial Fulfilment of the Requirements for the Degree of Doctor of Philosophy in Materials Science and Engineering of the Nelson Mandela African Institution of Science and Technology

Arusha, Tanzania

August, 2023

ABSTRACT

While exposure to low fluoride is essential for stronger bones and teeth, exposure to high concentration (> 3 mg/L/day) leads to hyperostosis and osteoporosis. This research evaluated the role of fertilizer application on soil's fluoride release, and assess the effectiveness of using seaweed (*Eucheuma cottonnii*) derived materials for remedial purposes. The soil characterization results in the study area, indicated the availability of diverse fluoride fractions and in different quantities in the soil such that; water-soluble (Ws-F) (39.5 ± 0.5 mg/kg), Exchangeable (Ex-F) (3.5 ± 0.5 mg/kg), bound to iron/manganese (Fe/Mn-F) (3.1 ± 1.0 mg/kg), and organic matter bound (Or-F) (9.1 ± 2.1 mg/kg) fluoride whereas the total fluoride (Tot-F) was 422 ± 52.9 mg/kg. The study further reports that the use of three studied fertilizers (diammonium phosphate (DAP), Urea, and farmyard manure) accelerates the bioavailability of fluoride in the soil by increasing Ws-F. These results deliver alerts to the plant health regulators suggesting proper management of the quality of fertilizers used for the enhancement of crop quality particularly those used in fluoride-contaminated agricultural soils. While fertilizer application accelerated the bioavailability of fluoride in the soil, soil amendment with dried seaweed (DSW) led to a decrement of Ws-F from 81.7 ± 3.1 mg/kg up to 28.5 mg/kg whereas the fermented seaweed (FSW) decreased Ws-F from 81.7 ± 3.1 mg/kg to 12 ± 1.3 mg/kg following 5 % (*w/w*) amendments. But unlike DSW and FSW, seaweed-derived biochar (SB) adsorbed fluoride at specific pH five (5) from 103.1 mg/kg to 91.2 ± 3.2 mg/kg whereas hydroxyapatite activated seaweed-biochar (HSB) exhibited defluoridation capabilities at varies pH (3 – 11) with a maximum Ws-F reduction from 103.1 mg/kg to 21.6 ± 2.1 mg/kg which is close to the recommended limit of 16.4 mg/kg. The DSW and FSW defluoridation was based on complexation reactions, alteration of soil properties, and increasing the soil-specific surface area, but SB and HSB defluoridation was through chemisorption. Therefore, seaweed-derived materials are capable of remediation of fluoride contaminated soils and the study recommends further investigation on fluoride uptake by crops in pot and field experiments post-amendment with seaweed derived materials.

DECLARATION

I, Ruth Lorivi Moirana, do hereby declare to the Senate of the Nelson Mandela African Institution of Science and Technology that this thesis is my work and that it has neither been submitted nor being concurrently submitted for degree award in any other institution.

Ruth Lorivi Moirana		24th August 2023
Name of Candidate	**Signature**	**Date**

The above declaration is confirmed by:

Prof. Kelvin Mtei		12th Sept 2023
Name of Supervisor 1	**Signature**	**Date**

Prof. Revocatus Machunda		04.09.2023
Name of Supervisor 2	**Signature**	**Date**

Dr. Marcos Paradelo		16.08.2023
Name of Supervisor 3	**Signature**	**Date**

Dr. Josephine Mkunda		04.09.2023
Name of Supervisor 4	**Signature**	**Date**

COPYRIGHT

CERTIFICATION

The undersigned certify that they have read and, with this recommendation for acceptance by the Nelson Mandela African Institution of Science and Technology, a thesis titled **"Remediation of Soils Contaminated with Fluoride using Locally Available Seaweed Derived Materials : Case of Slopes of Mount Meru"** in partial fulfilment of the requirements for the degree of Doctor of Philosophy in Materials Science Engineering of the Nelson Mandela African Institution of Science and Technology.

Prof. Kelvin Mtei		12th Sept 2023
Name of Supervisor 1	**Signature**	**Date**
Prof. Revocatus Machunda		04.09.2023
Name of Supervisor 2	**Signature**	**Date**
Dr. Marcos Paradelo		16.08.2023
Name of Supervisor 3	**Signature**	**Date**
Dr. Josephine Mkunda		04.09.2023
Name of Supervisor 4	**Signature**	**Date**

ACKNOWLEDGEMENTS

I am grateful to my father in heaven for without his favor through his son Jesus Christ and the Holy Spirit I wouldn't have accomplished the least of what I have accomplished. For that, all glory, honor, and praise, be to him and him only.

I would like to thank Nelson Mandela African Institution of Science and Technology (NM-AIST) who is my employer and host university for granting me study leave and providing an amiable research environment. I would like to extend my appreciation to the Natural Resource Institute (NRI) of the University of Greenwich, UK for hosting me during a sandwich program and providing access to the laboratory equipment for analysis. Thanks to Sokoine University (SUA) for offering analytical equipment for soil analysis. I gratefully acknowledge the Partnership for Skills in Applied Sciences, Engineering, and Technology (PASET) for offering financial support, the East and West Africa farming system-BELT (EWA-BELT) Horizon 2020 project No. 862848, and Research England 'Expanding Excellence in England' (E3) – FaNSI programme of the NRI.

Special thanks should go to my supervisors Prof. Kelvin Mtei, Prof. Revocatus Machunda, Dr. Marcos Paradelo, and Dr. Josephine Mkunda for their excellent teachings, mentoring, support, advice, and encouragement throughout the research period. Amid weaknesses, moral dilemmas, pain, and challenges, each of one you were too understanding to hurt, judge, or give up instead you looked up steadfastly towards bringing the best output out of this work.

I extend my deepest gratitude to the PASET-RSIF scholarship's entire team (Dr. Moses Osiru, Ms. Caroline Oremo, Mr. Bonface Nyangha, and Ms. Everlyn Nguku) who were always ready to listen and attend to the challenges I encountered. I appreciate the will and the effort observed from you. I extend my thanks to the NM-AIST laboratory technicians, Mr. Richard Komba, Mr. Wilson Mahene, and Mr. Idd Hussein for their technical support and to my comrades and friends Mr. Almas Kashindye, Mr. Kipruto Yegon, and Mr. Denis Mwalongo for their encouragement and moral support. Similarly, I would like to thank Dr. June Paul, Ms. Apple Espino, Ms. Lilian Treasure, Ms. Ruth Festus and Ms. Immaculate Mwangangi for offering me a shoulder to lean on both academically and emotionally during my stay in the United Kingdom (UK).

I wish to acknowledge the great love and support from my family, particularly my dearest husband Fred Simel Lolusu, whose love and support remained unshaken amid research stress.

I consider myself lucky and blessed to have you by my side. To my sons Jovan Fred and Etii-Osiligi Fred for keeping my smile, healing my heart, and giving me hope in your own simple ways. To my momma, for protecting me like a lioness through prayers and for cooking Loshoro unceasingly out of love. To my dad for being my motivation, I strive to do my best just to see a proud laugh on your face saying wordlessly "Yes, this is my little girl". My optimistic sister Elizabeth, the refuge I run to vent, my Sweet sister Salome who loves and cares for my sons like her own, and my Help Safina Mathias who has devoted her life into taking care of my two boys as I pursue this dream.

No one has greater love [nor stronger commitment]

than to

lay down his own life for his friends

(*John 15:13)*

DEDICATION

This work is dedicated to my dear friend Holy spirit, my mom (Frida Moirana), and my dad (Lorivi Moirana)

"And there shall come forth a rod out of the stem of Jesse,

and a Branch shall grow out of his roots:

[2] And the spirit of the Lord shall rest upon him,

the spirit of wisdom and understanding, the spirit of counsel and might, the spirit of knowledge and of the fear of the Lord.

[3] And shall make him of quick understanding in the fear of the Lord:

and he shall not judge after the sight of his eyes,

neither reprove after the hearing of his ears:

[4] But with righteousness shall he judge the poor and reprove with equity for the meek of the earth: and he shall smite the earth: with the rod of his mouth, and with the breath of his lips shall he slay the wicked.

[5] And righteousness shall be the girdle of his loins,

and faithfulness the girdle of his reins"

(Isaiah 11:1-10).

Table of Contents

LIST OF TABLES

LIST OF FIGURES

LIST OF APPENDICES

LIST OF ABBREVIATIONS

AEC	Anion Exchange Capacity
CEC	Cation Exchange Capacity
CFCs	ChloroFluoroCarbons
DAP	Diammonium Phosphate
DSW	Dried Seaweed
EADD	Estimated Average Daily Dosage
EARV	East African Rift Valley
ESP	Exchangeable Sodium Percentage
FAO	Food and Agriculture Organization
FCs	Fluorinated Compounds
FSW	Fermented Seaweed
GC-MS	Gas Chromatography-Mass Spectrometry
HCFCs	HydroFluoroChoroCarbons
HFCs	HydroFluoroCarbons
HMWOAs	High Molecular Weight Organic Acids
HR-MS	High Resolution-Mass Spectrometry
HSB	Hyadroxyapatite Activated Seaweed Biochar
LC-MS-MS	Liquid Chromatography -tandem-Mass Spectrometry
LMWOAs	Low Molecular Weight Organic Acids
PFCs	PerFluoroCarbons
PFOA	PerFluoroOctanoate
PFOS	PerFluoroOctaneSulfonate
SB	Seaweed Biochar
TBS	Tanzania Bureau of Standard
TVFAs	Total Volatile Fatty Acids
VFAs	Volatile Fatty Acids
WHO	World Health Organization

CHAPTER ONE

INTRODUCTION

1.1 Background of the Problem

Fluoride (F^-) is the ionic form of fluorine (F_2). Fluorine (F_2) is the 13th most abundant element in the environmental aspects of soil, air, and water. It does not occur in its elemental state naturally due to its high reactivity but exists as a fluoride ion (F^-) reacting with the electropositive elements (Hong *et al.,* 2016). Fluoride ion is among the essential trace element maintaining normal psychological activities in animals including humans. It is an important element responsible for stronger skeletal tissues in the body (Ma *et al.,* 2014; O'Hagan *et al.,* 2002). Regardless of its essentiality, fluoride is reported to cause teeth fluorosis in humans at levels higher than 1.5 mg/L, affect bones at 4 -10 mg/L, and crippling fluorosis at levels higher than 10 mg/L (Okamoto, 2001). Chronic fluorosis is reported in grazing animals due to ingestion of fluoride-containing volcanic ashes and intake of naturally polluted water, soil, and plants (Cronin *et al.,* 2000).

In the environment, fluoride is released naturally through weathering and volcanic activities however anthropogenic activities such as industrialization and agricultural practices accelerate its release rates (Jayarathne *et al.,* 2014). Initially, drinking water was considered a conventional fluoride exposure route. This led to the establishment of several water defluoridation techniques such as membrane separation, ion exchange, adsorption, nanofiltration, and flocculation which have been proved effective and efficient. These water defluoridation techniques are currently being implemented for water defluoridation in a different parts of the world (Waghmare & Arfin, 2015). Although water defluoridation is generally settled, fluorosis is yet to be settled because there is more to fluoride exposure sources apart from drinking water (Rizzu *et al.,* 2020b). Oral care products, seafood, vegetables, tea, meat, and even air in industrialized countries are reported to contain a momentous amount of fluoride which human beings are exposed to, daily exceeding the recommended limit (Rizzu *et al.,* 2021; Singh *et al.,* 2018). Symptoms of fluorosis was discovered in 18% of the population in Ethiopia with fluoride concentration in drinking water as low as 0.2 - 0.3 mg/L (Olsson, 1978). Another study reported the prevalence of fluorosis in children in Sudan consuming drinking water with 0.25 mg/L fluoride of which 91% of the children revealed the symptoms of fluorosis (Ibrahim *et al.,* 1995) suggesting the existence of multiple fluoride exposure routes.

Therefore, human beings living in fluoride contaminated areas will always be exposed to fluoride above the recommended limit unless all exposure sources are managed accordingly.

Fluoride exposure through food is linked to soil-fluoride directly or indirectly as most food originates from the soil (Hong *et al.,* 2016). Naturally, to reduce or mitigate fluoride exposure through plants, low fluoride accumulators are grown in contaminated soils, and high accumulators are grown in contamination-free soils, however, this cannot be implemented in real-life situations (Banerjee *et al.,* 2019). Another approach is to limit fluoride uptake by plant roots through immobilization/adsorption of the fluoride found in the soil (Suzuki *et al.,* 2013; Tafu & Manaka, 2016; Wyszkowski *et al.,* 2014).

Unlike water, natural soil-fluoride originates from the underlying parent rock material and therefore soil-fluoride distribution is linked to the soil formation process (Baunthiyal & Sharma, 2012; Hong *et al.,* 2016; Zhao *et al.,* 2015). Soils with fluoride-free parent rocks can contain fluoride concentrations in the range between 20 - 1,000 µg/g whereas fluoride-contaminated soils can contain concentrations as higher as several thousand µg/g (Chatterjee *et al.,* 2020; Larsen & Widdowson, 1971). While there are different forms of fluoride in the soil, it is the soluble-fluoride content in the soil that is biologically important to plant and animals. This is the amount of fluoride in soil that is biologically available to the soil biota. Several studies have reported fluoride uptake by plants and its toxicity. Plants absorb fluoride ions through their roots and accumulate in their different edible parts but the amount taken by the plant depends on the type of the plant, soil properties, and the amount of soluble-fluoride (Hong *et al.,* 2016). Since plants are at the bottom of the food chain, they potentially expose all other higher members of the food chain with human beings at the top to fluoride (Rizzu *et al.,* 2020a). Therefore, it remains important to find ways to minimize the bioavailability of fluoride in the soil.

Bio-adsorbents have been used for fluoride removal purposes (Bashir *et al.,* 2015). These adsorbents have functional groups such as hydroxyl, carboxyl, thiol, amine, and sulfate, which are susceptible to modification to acquire efficient defluoridation capabilities (Evangeline & Pragasam, 2015). Although effective, the majority of these bio-adsorbents have been tested for water defluoridation (Bashir *et al.,* 2015; Nehra *et al.,* 2020; Qiu *et al.,* 2020; Tomar *et al.,* 2014), but literature on its application particularly those derived from seaweed for soil remediation is limited and requires further investigations.

This study aimed to exploit seaweed (*Eucheuma cottonii*) for minimizing the bioavailable fraction of soil fluoride thereby preventing its mobilization and accumulation into the plants, vegetables, sea biota, grazing animals, and other living things. The seaweed contains Carrageenan polysaccharide as its major structural component in the cell wall which contains important functional groups crucial for fluoride trapping and locking in the soil. The same functional groups can also be manipulated using different techniques to further enhance their defluoridation performance in the soil.

1.2 Statement of the Problem

While several defluoridation techniques are dedicated to defluoridation of drinking water, less attention is directed towards other potential fluoride exposure routes particularly soil which harbors most of the fluoride present in the ecosystem. Although most of the fluorides in the soil are sparingly soluble in the presence of water, some such as SiF_4, NaF, and HF are quite soluble constituting the bioavailable fluoride fraction (Cronin *et al.,* 2000; Pickering, 1985). The bioavailable fluoride in the soil ends up in the food chain directly through uptake and accumulation by plants who are the bottom members of the food chain exposing the rest of the chain to fluoride toxicity (Fig.1). For-example a study by Rizzu *et al.* (2020a) reported the cumulative estimated average daily dosage (EADD) to be in the range of 0.026 - 0.165 mg/kg. The EADD was calculated from the edible parts of maize (*Zea mays L.*), bean (*Phaseolus vulgaris L.*), tomato (*Lycopersicon esculentum Mill.*), and kale (*Brassica sp. pl.*) grown in soils encompassing the bioavailable fluoride concentration of 63 – 133 mg/kg (Rizzu *et al.,* 2020b). These results are of significant importance as they present an exposure rate from single source and suggests that exposure to multiple sources could surpass the maximum recommended limits of 1.5 mg/L/day and 4 mg/L/day set by WHO and TBS, respectively (Ligate, 2023). Moreover, the bioavailable fluoride in the soil ends up being distributed into surface waters (lakes, rivers, and oceans) through surface runoff, groundwater through leaching, and in uncontaminated soils through erosion widening the exposure routes (Ibrahim *et al.,* 1995; Jayarathne *et al.,* 2014). While this is a case, techniques such as electrokinetic (Prabhu *et al.,* 2023), soil washing , biological remediation (del Socorro Santos-Díaz & Zamora-Pedraza, 2010; Suzuki *et al.,* 2013), and immobilization/adsorption have been investigated for soil defluoridation but majority of these techniques are either not economical, have unsatisfactory results or unrealistic for implementation in actual environment calling for more feasible remedial approaches which is the main focus of this study.

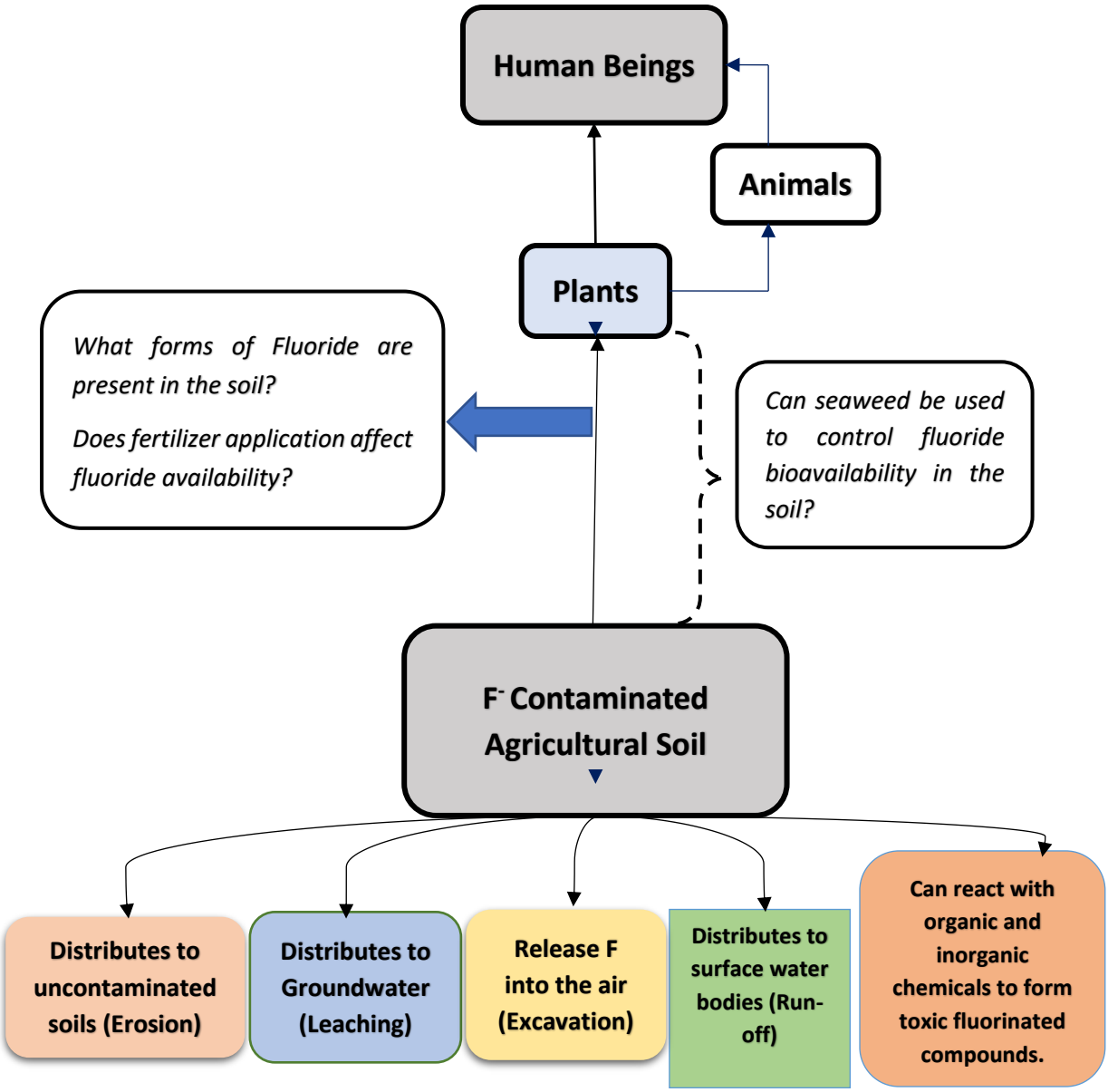

Figure 1: Distribution of soil fluoride into different parts of the ecosystem

1.3 Rationale of the Study

The free fluoride in the soil is normally taken up and accumulated into edible parts of crops which end-up reaching human beings who are the top members of the food chain (Rizzu *et al.,* 2020b). While it is necessary to add fertilizer into the agricultural soils to enhance soil fertility, these fertilizers particularly diammonium phosphate (DAP) has significant quantities of fluoride which is released into the soil following its application. Furthermore, application of these fertilizers in fluoride contaminated zones minimizes the fluoride absorption efficiency of the soil (Hong *et al.,* 2016; Jha *et al.,* 2008; Murray, 1984). While fertilizer application is important, reducing the amount fluoride exposure through soil remains important as well.

Therefore, this study intends to limit the bioavailability of fluoride in the soil using seaweed derived materials. The seaweed used is *Eucheuma cottonii* because it contains 30% carrageenan which is a high molecular weight organic compound (HMWOC) which can easily be manipulated for defluoridation purposes (Susilorini *et al.,* 2014). But this seaweed is chosen specifically because it contains plant growth hormones and can therefore play the role of fertilizer. Although the seaweed has been investigated for adsorption of cationic species such as uranium, cadmium, and arsenic (Chang & Teo, 2016; Distantina & Fahrurrozi, 2011; Guntur *et al.*; Susilorini *et al.,* 2014), handful information is available on its use for adsorption of anionic species like fluoride particularly the one found in the soil. Therefore, this study provides a more feasible remedial alternative in terms of defluoridation efficiency, improvement of crop health and soil fertility in fluoride-contaminated soils.

1.4 Objectives of the Study

1.4.1 General Objective

The overall objective of this study is assessment of fluoride contamination status of the soils and exploration of remediation approaches using seaweed (*Eucheuma cottonii*)-derived materials employing soils along the slopes of Mount Meru as a case study.

1.4.2 Specific Objectives

The study aimed to achieve the following specific objectives:

(i) To quantify the bioavailable fluoride fractions in the fluoride-contaminated soil along the slopes of Mount Meru.

(ii) To evaluate the responsive behavior of the bioavailable fluoride fractions towards the commonly used fertilizers in the contaminated agricultural soils.

(iii) To formulate and evaluate the efficiency of dried and fermented seaweed *Eucheuma cottonii* for remediation of fluoride-contaminated soil.

(iv) To formulate and evaluate the defluoridation efficiency of seaweed-derived biochar and its activated product with hydroxyapatite.

1.5 Research Questions

The study intended to answer the following questions:

(i) What are the bioavailable fluoride fractions present in the agricultural soils along the slopes of Mount Meru?

(ii) How does fertilizer application practice influence fluoride adsorption/release behavior of the soil?

(iii) Do seaweed derived materials have the potential for remediation of fluoride contaminated soils?

(iv) Which seaweed seaweed-derived material has the highest defluoridation efficiency?

1.6 Significance of the Study

Most of the population (both Plantae and Animalia kingdoms) living in fluoride-contaminated areas will be exposed to high fluoride concentrations unless all exposure routes and precursors are identified and managed accordingly. This study holds soil as a principal source of fluoride distribution and accumulation into the food chain and therefore intends to limit its mobility through the ecosystem by reducing the amount of the bioavailable fraction in the soil using seaweed-derived materials. The use of seaweed-derived materials for remediation purposes of fluoride-contaminated soils is crucial for long-term sustainability of soil properties, fertility, and productivity. Therefore, the results of this study will be helpful in:

(i) Providing information about the bioavailable fluoride fraction in the soil as well as the role of agricultural practices, particularly fertilizer application, in the enhancement of the fluoride bioavailability in the agricultural soils.

(ii) Promoting awareness on the existence of fluoride in the soil, and the role it plays in fluoride exposure through food.

(iii) Evaluating the effectiveness of using the locally available seaweed and its derived materials for remedial purposes of fluoride-contaminated agricultural soils.

(iv) Reporting the appropriate dosages for effective remediation purposes of contaminated soils.

1.7 Delineation of the Study

The current study was undertaken from January 2020 to January 2023. The case study involved collecting the soil and farmyard manure obtained from one of the agricultural farms located on the slopes of Mount Meru. The soil collected was used for the investigations reported in this study. The first objective intended to uncover whether the agricultural practices (this case being fertilizer application) accelerate or decelerate fluoride release in the soil and to what extent. The second and third objectives focused on identifying the most effective seaweed preparation method for remedial of fluoride contaminated agricultural soil. Effective in this study refers to the ability of the amended material to reduce the amount of bioavailable/soluble fluoride in the soil. The bioavailable fluoride fraction in this study was equivalent to the extractable fluoride fractions. All the experiments were conducted at a laboratory scale rather than field due to constrains of funds and time. This study has not covered the investigation of fluoride uptake by the plants after amendment with the seaweed materials. Even though the pot experiments intended to investigate the efficiency in limiting fluoride uptake by plants after amendments was conducted, the results could not be acquired due to unsuccessful seed germination. But also, this study did not cover the socio-economic aspect of the use of seaweed-derived materials and therefore, recommends for further studies.

CHAPTER TWO

LITERATURE REVIEW

2.1 Fluorine and Fluorides

The determination and quantification of biologically and environmentally essential ions have caught the attention of researchers globally. Amongst these ions is fluorine (F_2) which is a univalent, irritating, pale yellow-green gaseous halogen with a sharp odor It is the most electronegative element and the most reactive of all. Because of this property, elemental F_2 rarely exists in nature (Fig. 2), instead, it exists as a fluoride (F^-) ion which readily reacts with other elements to form fluoroinated compounds (WHO, 1984, 2003; Yuan *et al.,* 2019).

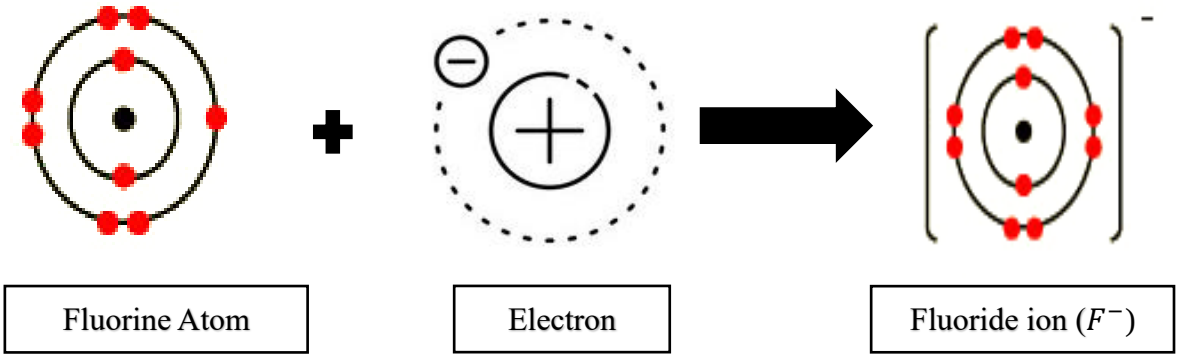

Figure 2: The electron configuration of a fluorine atom and fluoride ion (F^-)

Fluorinated compounds are referred to as "fluorides" and have dissimilar properties to the similar compounds of the other halogens. Fluorides such as SrF_2 and CaF_2 are sparingly soluble in water while $CaCl_2$, $CaBr_2$, $SrCl_2$, and $SrBr_2$ are readily soluble in water whereas the case is reversed for AgF, $AgCl$, and $AgBr$ (Fuwa, 1986). The fluoride ions react strongly with heavy metals to form complex metallic ions such as AlF_6^{3-}, FeF_6^{3-}, ZrF_6^{2-}, ThF_6^{2-}. It also reacts strongly with organic and inorganic compounds and forms insoluble fluorinated compounds (Yuan *et al.,* 2019). Therefore, while fluorine rarely exists in nature, fluorides/fluorinated compounds (FCs) are abundant in nature.

2.1.1 Sources of Fluoride in the Environment

Fluorides occur naturally on the earth's crust but are released onto the earth's surface through natural activities like weathering and volcanic activities or anthropogenically through agricultural practices and industrial activities (Hong *et al.,* 2016; WHO, 2003). Naturally,

fluorides are found in phosphate rock deposits and minerals that are sedimentary. The main fluoride-containing minerals are fluorite (CaF_2), fluorapatite (($Ca_5(OH,F)(PO_4)_3$), and cryolite (Na_3AlF_6). Fluorite (CaF_2) contains about 49% fluoride, fluorapatite ($Ca_5(OH,F)(PO_4)_3$) about 4% fluoride, and cryolite (Na_3AlF_6) has 54%, fluoride (Fuge, 1988). Among the three main minerals, fluorite (CaF_2) is considered a commercial source of fluoride whereas fluorapatite ($Ca_5(OH,F)(PO_4)_3$) is mined for commercial fertilizer purposes, and cryolite (Na_3AlF_6) is rarely found in nature but used during aluminum smelting process (Jha *et al.,* 2011). It is estimated that the annual release of fluorides inform of hydrogen fluoride (HF) from the volcanic activities alone to range between 60 – 6 000-kilotons (Symonds *et al.,* 1988). Oskarsson reported rapid fluoride release in the form of $Ca_5(PO_4)_3F$, NaF, AlF_3, $CaSiF_6$, and CaF_2, in the volcanic ash (Óskarsson, 1980) and another study further concluded the presence of fluoride within the glassy fraction of volcanic ash and the soluble fluoride salts attached to the top layer of the volcanic ash (Delmelle *et al.,* 2007). The amount of fluoride concentration in the crystalline fraction was later found to range between 280 - 480 mg/kg in the form of $F-Si$ and $F-Al$ whereas the top layer existed in $F-Na$ and $F-Ca$ salts which were far from those inside a glassy fraction (Bia *et al.,* 2020). Unlike volcanic eruption, fluoride release into the soil through weathering is associated with pH and the amount of $NaHCO_3$ present in either rock or the passing water, temperature, depth of the rock, and the climatic conditions and contributes to about 400 mg/kg total fluoride (Tot-F) of the soil (Chae *et al.,* 2006; Mondal & Gupta, 2015; Rafique *et al.,* 2015).

The major and common anthropogenic sources of fluoride are agriculture and industrialization. Industrial activities such as aluminum smelting (Kvande & Drabløs, 2014), coal-burning (Fidanci, 2001), steel production (Blanco-Flores *et al.,* 2018), chemical production (Alexander *et al.,* 2003), glass manufacture (Ono *et al.,* 2022), fertilizer , pesticides (Kim *et al.,* 2011), as well as brick and ceramics manufacturing (Sun & Su, 1985), enriches the topsoil with fluoride. For example, the aluminum smelting process uses cryolite (Na_3AlF_6) which emits fluoride in the form of HF in the atmosphere and further deposits on the topsoil (Kvande & Drabløs, 2014). In 1995, Arnesen and coworkers investigated the soil fluoride pollution caused by the aluminum smelters in Norway. This study reported that soil fluoride pollution could be traced to more than 30 km away from the smelters and fluoride concentration increased with increasing soil depth (Arnesen *et al.,* 1995). On contrary, soils around 3 to 5 km away from brick and ceramics industries were reported to contain 0.6 - 3 mg/kg fluoride higher than the soils 30 km away (Jha *et al.,* 2008).

The highest anthropogenic soil fluoride source in unindustrialized countries is fertilizer application. Phosphate fertilizers contain about 1.5 to 3% fluoride and therefore, continuous application of phosphate fertilizer hypothetically increases the amount of fluoride in agricultural soils. Therefore, on every occasion, 1 ton of phosphate fertilizer addition to the agricultural soil contributes to 0.01 tons of fluoride. According to the 2021/2022, FAO, the current world phosphate fertilizer demand is estimated to be 49 096 000 tons equivalent to 490 960 -1 472 889 tons of fluoride enrichment into the agricultural soil. The fluoride released during the manufacture of fertilizer is far more dangerous as it is released in form of gaseous HF into the atmosphere which later deposits itself in plant leaves, topsoil, and human skin and mixes with the inhaled air.

2.1.2 Fluoride Uses and Toxicity

The toxicity of fluoride may be acute, chronic, or mild depending on the exposure route and rate. The routes of fluoride exposure include ingestion, inhalation, and absorption through the skin (Fuge, 1988; WHO, 2003). For human beings, acute toxicity normally results from the ingestion of fluoride salts or solutions (NaF, SiF_4). Chronic toxicity is associated with occupational exposures to dusts, gaseous HF, ingestion of foods or water containing fluoride (Hodge & Smith, 1977). Chronic toxicity is characterized by osteosclerosis, a disorder characterized by irregular hardening of bone and an advancement in bone density reliant on the duration and magnitude of exposure. It has also been estimated that exposure to 32 – 64 mg/kg fluoride is lethal to people weighing 70 kg and above (WHO, 2003).

Fluorosis is a common fluoride toxicity reported. Dental fluorosis shows mild exposure to fluoride whereas skeletal fluorosis is caused by ingestion of high fluoride levels (Hodge & Smith, 1977). These two conditions are common in areas with excessively high fluoride levels in water and soil (Singh *et al.,* 2018). In adults, fluoride facilitates the growth of abnormal bone at tendon and ligament insertion sites which causes ossification and also increases bone density a condition called osteosclerosis. These two conditions are characterized by excessive joint pain as well as stiffness in adult life associated with neurological complications (Gupta & Ayoob, 2016; Jarvis *et al.,* 2013). Fluorosis in children manifests by bone deformities especially when the child's diet has inadequate calcium and proteins. When calcium is insufficient, fluoride exacerbates the calcium demand by chelating with calcium causing secondary hyperthyroidism and sclerosis of the bones (Jarvis *et al.,* 2013).

Once exposed to fluoride, it is absorbed immediately into the blood where 50% of it is excreted via urine in the next 24 h, and the remaining 50% is deposited into the skeleton tissue delaying the mineralization process and altering its crystal structure (Hodge & Smith, 1977). The earlier fluoride toxicity signs include molted teeth and skeletal fluorosis (Maadid *et al.,* 2017). Herbivores were more susceptible to toxicity compared to carnivores and other animals because their eating is not selective (Chatterjee *et al.,* 2020).

Plants are exposed to fluoride through soil, water, and air. From the soil, fluoride is absorbed by plant roots and is accumulated in different parts of the plant depending on the plant type (Hong *et al.,* 2016). It travels in the plant tissue through transpiration or can move through the stomata finding its place at the margins of the leaves (Chatterjee *et al.,* 2020; Hong *et al.,* 2016; Jha *et al.,* 2008). Depending on the fluoride accumulation rate in the plant, it stops the photosynthesis process from taking place through the alteration of metabolic pathways, inhibiting enzymes that require cofactors like Ca^{2+}, Mn^{2+}, and Mg^{2+} ions and lowering the amount of chlorophyll in the leaves (Jha *et al.,* 2011). Necrosis is an early sign of fluoride toxicity in the plant however it doesn't kill the plant, it weakens it affecting its production quality and quantity (Chatterjee *et al.,* 2020; Jha *et al.,* 2008).

Human industrial activities have established a wide variety of fluorinated precursors which creates novel toxic fluorinated compounds (FCs) once they interact with the environment. The novel fluorinated chemical structures make up to 60 – 90% of total FCs in biological and environmental conditions (Yeung & Mabury, 2015). In 1975 for-example, Teflon, a fluorinated compound used to coat non-stick cookware was found to enhance the amount of fluoride 3 folds in foods compared to other cookware handing the lives of Americans to cancer risks to date (Mack, 1961).

The high electronegativity of fluorine gives it a strong oxidizing property which favors its reaction with most organic and inorganic materials below and at room temperature (Fidanci, 2001). Henceforth, FCs are utilized in production processes or embedded in many products utilized in our day-to-day activities. Although there are numerous minerals containing fluoride, only three minerals are fit for commercial utilization due to their high fluoride concentration. These minerals are, cryolite ($AlF_3 3NaF$), fluorite/ fluorspar (CaF_2), and fluorapatite ($Ca_5(PO_4)_3F$) (Hong *et al.,* 2016).

Initially, the use of fluorides was limited to its salts only whereby during this period, salts such

as fluorite and cryolite were used as fluxing agents for iron and steel furnaces and welding (Asakawa *et al.,* 2007). Cryolite was also used as an electrolyte in the aluminum production process (Hall-Heroult electrolytic process). Further up, uranium hexafluoride (UF_6) was in demand for uranium production during world war (II). Uses in ceramics and glass manufacture were reported but were considered as insignificant rate during this period (Arnesen *et al.,* 1995; Asakawa *et al.,* 2007; Fung *et al.,* 2003; Jha *et al.,* 2011; Villalba *et al.,* 2007). By 1920, a new process (floatation process) was developed. This process enabled the production of more than 97% pure fluorite named Acid spar distinguishing it from metspar which was the impure fluorite. This was a major milestone in the use of FCs as acid spar gave way to the production of a pure hydrofluoric acid (HF) used in the production of chlorofluorocarbons (CFCs) used as refrigerants, deodorants, cleaning agents, propellants for spray cans in paints, solvents, foaming agents, to mention a few (Asadi *et al.,* 2018; Villalba *et al.,* 2007).

By far, the second most worldwide use of fluorinated compound apart from fluorite is fluorapatite which is used in the fertilizer industry to manufacture phosphoric acid (H_2PO_4) which contains 2 – 3%, fluoride (Hong *et al.,* 2016; Yi *et al.,* 2017). During the production of phosphoric acid, fluorapatite is dissolved into sulfuric acid a process that releases fluoride in form of hydrogen fluoride gas (HF) into the atmosphere (Villalba *et al.,* 2007). In the 1990s the international phase-out of CFCs led to the establishment of hydrofluorocarbons (HFCs) and hydrochlorofluorocarbons (HCFCs) which widened the uses of FCs and hence the demand for hydrofluoric acid (HF). Today, the use FCs is not limited to the above-mentioned uses but is used in healthcare (as parts of drugs and inducing anesthesia) (Mahmić-Kaknjo & Marušić, 2015). In food security (herbicides, fungicides, insecticides) (Harsanyi & Sandford, 2015), materials (enhancement of thermostability, non-stick cookware (Teflon, Dupont), protective clothing and textile treatment (Goretex®, WL Gore)) (Ameduri & Boutevin, 2004), and Energy (as fuel for atomic energy industries, (Flemion®, Asahi Glass)) (Hoogers, 2002). All of these fluoride uses are the main reasons leading to fluoride excavation and extract from its rocks.

2.1.3 Fluoride in Soil

Fluoride in soils is normally contained within minerals fluorite and micaceous clay minerals. But fluoride in the soil can also be found adsorbed in ions and compounds (Bowen & Rood, 1966). While natural soil fluoride is a function of the soil parent material, it is high in volcanic areas with active fluoride-rich volcanic ash (Cronin *et al.,* 2000). Where the soil is form of quartzo-feldspathic rocks, older igneous rocks, and phosphate-free carbonate rocks the

quantities of natural soil fluoride are generally lower (Bowen & Rood, 1966; Cronin *et al.,* 2000; Rooeda-van-Eysinga, 1974). In the soil, fluorine exists as fluoride ions (F^-) which is lithophile (has a high affinity to silicates and oxides of the soil). Its lithophilic character favors its retention in the soil through the formation of ligand exchange reactions with the soil minerals and elements such as Al or H. Normally the total fluoride (Tot-F) concentration in uncontaminated soil range between 200 – 300 mg/kg (WHO, 2003) however some uncontaminated soils were reported to contain Tot-F concentration of 1000 – 3500 mg/kg (Ranjith *et al.,* 2017). In the soil, fluoride is mostly found locked with soil elements, particularly aluminum, ammonium, potassium, iron, or clay. Fluoride attaches to the clay by displacing the hydroxide ion found at the surface of the clay (Ranjith *et al.,* 2017). If the soil contains calcareous properties fluoride leaching and dispersion will be limited by the formation of CaF_2 precipitate (Jha *et al.,* 2011) whereas sodic soils are characterized by high soluble fluoride concentration due to the formation of a highly soluble NaF. Therefore, sandy soils contains lesser fluoride compared to clay soils, but if the sandy soil is sodic, it is likely to contain high fluoride concentration (Li *et al.,* 2020). Apart from the soil properties and composition, fluoride concentration and release into the soil depends on other external factors such as weathering, climate, and altitude.

High variability is reported between soils that are uncontaminated which is associated with the soil particle size and properties. High total fluoride in the soil is associated with an increasing clay content of the soil, depth of the soil (due to the low affinity of fluoride to organic matter, increasing clay content and long-term fluoride leaching) (Bowen & Rood, 1966; Hani, 1978; Larsen & Widdowson, 1971; Omueti & jones, 1980).

Unlike total fluoride, the labile form of fluoride considered bioavailable is made up of soluble compounds of fluoride. It forms its most stable bonds with Al, $Ca,$ and Fe but forms unstable compounds with soil components that contain these elements, and clay minerals. At low quantities, both Fe and Al oxides and hydroxides have high fluoride adsorption whereas clay minerals, halloysite, and kaolinite have a natural tendency to absorb high fluoride quantities (Bowen & Rood, 1966; Larsen & Widdowson, 1971).

The fluoride in water (ground and surface water) originates from the natural rock's dissolution through weathering and volcanic processes. Anthropogenic activities such as fertilizer and industries as well as volcanic activities release fluoride on to the soil and atmosphere which is also deposited on the earth's surface (topsoil) (Asadi *et al.,* 2018; Hong *et al.,* 2016). On the

earth's surface fluoride can be transferred into the ground water through leaching or to the surface water by erosion or surface water runoff. Fluoride in groundwater depends on the aquifer fluoride enrichment which further depends on its physical characteristic, rock types, pH of the water, water residence time soil properties as water reacts (Chidambaram *et al.,* 2018).

Although with the cycle it's normally tricky to identify the source, with fluoride though, the source could be identified as the soil. It is the soil that holds the initial fluoride whether in total or soluble form. Altering the soil properties and its interaction with other environmental aspects leads to the soil-fluoride release either into the atmosphere, surface water, groundwater, or into fluoride-free soil. Therefore, the main question remains: will control the solubility of soil-fluoride limit its release into the environment?

In the soil, fluoride undergoes a diversity of complex reactions with the soil elements to form massive fluorinated complexes. It undergoes precipitation-dissolution, complexion-dissociation, or adsorption-desorption reactions to balance itself in the soil system as shown in Table 1 (Jha *et al.,* 2008; Pickering, 1985). It forms reversible reactions with soil elements such as Al^{3+}, Ca^{2+}, Mg^{2+}, and Fe^{2+} to form precipitates that accumulate in the soil. At different pH, fluoride reacts selectively with soil elements to form complexes. At pH below 6 for example, fluoride reacts with aluminum to form $Al-F$ complexes (AlF_3, AlF^{4-}, AlF^{2+}, AlF^{3+}) (Jha *et al.,* 2011; Lindsay & Walthall, 2020). In strong acidic soils, fluoride tends to form complexes with free iron (Fe) ions in the soil and therefore fluoride will exist as $Fe-F$ complexes such as (FeF_2^+, FeF^{2+}, FeF_3) (Perrott *et al.,* 1976; Pickering, 1985). The presence of wastes of animal origin in the soil, organic matter and its decomposition products such as volatile organic acids, phenols, and alcohol also reacts with fluoride through adsorption to form organic/inorganic-fluoride complexes. The main fluoride adsorption mechanism with the organic soil components is through exchange with the $-OH$ group in the organic acids (Chen *et al.,* 2013; Jha *et al.,* 2011; Perrott *et al.,* 1976).

Based on chemical extraction methods, fluorides can be grouped as water-soluble (Ws-F), Exchangeable (Ex-F), bound to iron and manganese (Fe/Mn-F), bound to organic matter (Or-F), and residual fluorides (Res-F) presented in Fig. 3 (Chen *et al.,* 2013). The concentration of each form of fluoride is different from one soil to the other depending on the soil properties such as clay content, pH, organic matter, elemental composition as well as climatic conditions (Chen *et al.,* 2013).

Table 1: The main fluoride chemical reactions in the soil

Reaction type	Chemical reaction
Precipitation – dissolution	$CaF_2 \leftrightarrow Ca^{2+} + 2F^-$
	$MgF_2 \leftrightarrow Mg^{2+} + 2F^-$
	$AlF_3 \leftrightarrow Al^{3+} + 3F^-$
	$FeF_3 \leftrightarrow Fe^{3+} + 3F^-$
	$KF \leftrightarrow K^+ + F^-$
	$Na_3AlF_6 \leftrightarrow 3Na^+ + Al^{3+} + 6F^-$
	$ZnF_2 \leftrightarrow Zn^{2+} + 2F^-$
Adsorption-Desorption	$(H_2O - Fe - OH)^0 + F^- \leftrightarrow (H_2O - Fe - F)^0 + OH^-$
	$(HO - Fe - OH)^- + F^- \leftrightarrow (HO - Fe - F)^- + OH^-$
	$(H_2O - Fe - OH)^0 + F^- \leftrightarrow (HO - Fe - F)^0 + H_2O$
	$(Fe - OH - Fe)^0 + F^- \leftrightarrow (Fe - F)^{-\frac{1}{2}} + (Fe - OH)^{-\frac{1}{2}}$
	$-COOH + F^- \leftrightarrow COF + OH^-$
	$-CH_2OH + F^- \leftrightarrow CH_2F + OH^-$
	$-OH + F^- \leftrightarrow F + OH^-$
Complexation-dissociation	$Al^{3+} + F^- \leftrightarrow AlF^{2+}$
	$Al^{3+} + 2F^- \leftrightarrow AlF^{2+}$
	$Al^{3+} + 3F^- \leftrightarrow AlF_3$
	$Al^{3+} + 4F^- \leftrightarrow AlF^{3-}$
	$Al^{3+} + 5F^- \leftrightarrow AlF_3^{2-}$
	$Al^{3+} + 6F^- \leftrightarrow AlF_3^{3-}$
	$Fe^{3+} + F^- \leftrightarrow FeF^{2+}$
	$Fe^{3+} + 2F^- \leftrightarrow FeF^{2+}$
	$Fe^{3+} + 3F^- \leftrightarrow FeF_3$
	$Fe^{2+} + F^- \leftrightarrow FeF_2$
	$Mn^{2+} + F^- \leftrightarrow (MnF)^+$
	$Zn^{2+} + F^- \leftrightarrow (ZnF)^+$
	$Zn^{2+} + 2F^- \leftrightarrow (ZnF_2)^0$

Water-soluble fluoride (Ws-F) and Exchangeable fluoride (Ex-F) are the two fluoride fractions easily found in the soil solution interface (Rizzu *et al.,* 2020b). It is attached to the soil-solid interface, clay, or soil exchangeable cations through electrostatic adsorption and released back

into the soil through desorption (Yi *et al.,* 2017; Zhao *et al.,* 2015). The two forms can easily be removed from the soil through phytoextraction, adsorption/immobilization, leaching, or electrokinetic as they are sensitive to pH changes in the soil system.

Fluoride bound to iron and manganese (Fe/Mn-F) is the fluoride fraction that is attached to either aluminum (Al^{X+}), iron (Fe^{X+}), or Manganese (Mn^{2+}) elements in the soil (Chen *et al.,* 2013). Unlike the first two, the reaction of fluoride with these elements involves complex formation and dissociation and its amount is dependent on pH and the number of targeted cations present in the soil (Li *et al.,* 2020; Yi *et al.,* 2017). For example, low pH favors the formation of $Al-F$ or $Fe-F$ complex however its concentration cannot exceed the concentration of these elements present in the soil. minimization of the bioavailability of this fluoride fraction involves immobilization by the introduction of another stable element with a stronger affinity to fluoride (Li *et al.,* 2020).

There are two classes of organic acids in the soil, low molecular weight organic acids (LMWOA) such as oxalic acid which originates from plant material decomposition, microbial metabolism, or root exudates. The second is high molecular weight organic acids (HMWOA) like Humic acids (Jones, 1998; Strobel, 2001). Both of these organic acid classes together with their decomposition products participate in adsorption-desorption reactions with fluoride or the formation of complexes with fluoride (Chen *et al.,* 2013). If the organic acids participate in adsorption-desorption or unstable complex reaction with fluoride, it forms an organic matter bound-fluoride (Or-F) fraction (Wang *et al.,* 2007), but if it forms a stable complex it contributes to residual fluoride (Res-F) (Chen *et al.,* 2013).

Unlike the first four fluoride fractions, residual fluoride (Res-F) represents complex fluoride compounds. This fluoride fraction is yet to be extracted like the other fractions but is calculated as the difference between the total fluoride (Tot-F) in the soil and the four fluoride fractions (Equation 1) (Chen *et al.,* 2013).

Res-F = Total fluoride (Tot-F) – ((water-soluble (Ws-F) + Exchangeable (Ex-F) + bound to iron and manganese (Fe/Mn-F) + bound to organic matter (Or-F))……..(01)

These residual fluorinated compounds can either be attached to organic or inorganic compounds of the soil. Although Res-F could originate naturally into the soil, a significant part of it is caused by anthropogenic activities like pesticide and fertilizer application as well as

industrialization (Bolan *et al.,* 2021). The Res-F could be potentially harmful at very low concentrations compared to the four fractions (Harada & Koizumi, 2009) and includes harmful fluorinated compounds such as specific forms of organic-F particularly perfluorinated compounds (PFCs), perfluorooctanoate (PFOA), and perfluorooctanesulfonate (PFOS) (Fiedler, 2007).

Analytical chemists have been working on ways to analyze these fluoride complexes not only in biological samples but in environmental samples as well. A limited number of Res-F is quantified using liquid chromatography-tandem mass spectrometry (LC-MS-MS) (Schröder, 2003), ionic or gas chromatography-mass spectrometry (GC-MS) (Bose *et al.,* 2019; Percival, 1957), and high-resolution-mass spectrometry (HR-MS) (Asadi *et al.,* 2018; Blondel *et al.,* 1989). These techniques though, although effective, yet, cannot capture all the Res-F compounds due to a lack of authentic standards. Therefore, the question of how many Residual fluorinated compounds is present in the environment and are missed during analysis remains a puzzle.

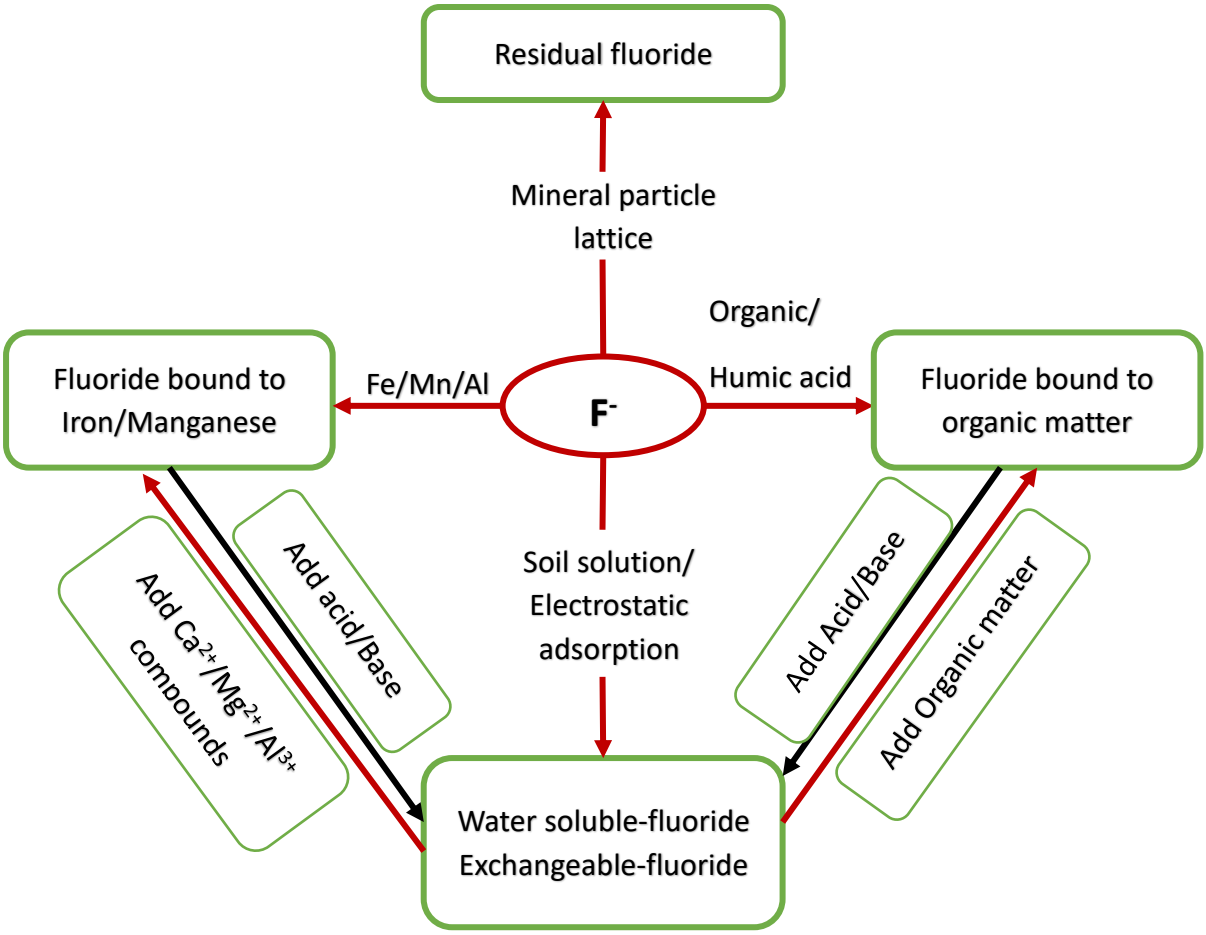

Figure 3: The bioavailable soil-fluoride fractions and their interaction

Normally, fluorosis is associated with fluoride in drinking water because this is the most direct fluoride exposure pathway (Rizzu *et al.,* 2020b). Exposure to water is through ingestion of fluoride-contaminated water which is absorbed into the blood stream and deposited into the skeletal tissue (Díaz-Nava *et al.,* 2002). Water was identified as the main fluoride exposure source up until other exposure sources were reported. Olsson discovered symptoms of fluorosis in 18% of the population in Ethiopia with fluoride concentration in drinking water as low as 0.2 - 0.3 mg/L (Olsson, 1978). Another study by Ibrahim and coworkers investigated the prevalence of fluorosis in children in Sudan consuming drinking water with 0.25 mg/L fluoride of which 91% of the children revealed the symptoms of fluorosis (Ibrahim *et al.,* 1995). The results from these studies suggested the availability of other potential fluoride exposure sources apart from drinking water (Malde *et al.,* 1997). Following the discoveries, Malde *et al.* (1997) decided to investigate alternative fluoride exposure sources in the food web apart from drinking water. The results of fluoride concentrations were dreadful such that sardines from the Indian Ocean contained 144 mg/kg, shrimp contained 17 mg/kg, spinach had 6.8 mg/kg dry weight, and tea contained 132 - 249 mg/kg dry weight (Malde *et al.,* 1997). The fluoride concentration in fish ranged from 4.4 - 21.5 mg/kg depending on the type of fish but fish bones contained 1000 - 2300 mg/kg dry weight (Malde *et al.,* 1997). Seawater biota uptake their fluoride from the sea water and over time, they accumulate a significant amount of fluoride in different parts of their bodies which end-up accumulating in human tissue after consumption.

Plants grown in fluoride uncontaminated soil contained fluoride concentrations of less than 10 mg/kg (Hong *et al.,* 2016). Although the soil contains a high amount of total fluoride (Tot-F), Plant roots are capable of taking water-soluble fluoride (Ws-F) fraction only. Other fluoride fractions (exchangeable (Ex-F, bound to iron and manganese (Fe/Mn-F), bound to organic matter (Or-F), and residual fluoride (Res-F)) cannot be taken up by the plant roots however can be taken up indirectly (Rizzu *et al.,* 2020b). Indirect uptake involves the conversion of the fluoride fractions into water-soluble fluoride (Ws-F) by changing the soil properties of pH, clay content, Organic matter, or elemental composition (Arnesen *et al.,* 1995; Hong *et al.,* 2016). Therefore, the amount of soil fluoride accumulated by the plant through roots depends on the amount of water-soluble fluoride (Ws-F) in the soil, soil properties, and the type of plant species, the latter being the major limiting factor (Camarena-Rangel *et al.,* 2015; Rizzu *et al.,* 2020b; Shu *et al.,* 2003).

2.2 The Geographical and Geochemical Fluoride Distribution

2.2.1 Global Fluoride Belts

High fluoride concentration in water is associated with extensive geographical and geological belts which are associated with either tectonic zones, marine sediments, granites, and gneissic rocks as well as volcanic rocks appearing at linear elasticities linking different countries (Gupta & Ayoob, 2016). Based on these factors, the distribution of fluoride is divided into five major fluoride belts (Fig. 4).

The first belt runs south; it starts from Turkey to Tanzania. This belt starts from Turkey and cuts across Syria, Egypt, Jordan, Somalia, Sudan, Ethiopia, Kenya, Tanzania, Mozambique, and South Africa. Fluorosis observed from this belt is mainly caused by geological sources which contaminate both the topsoil and water. Higher levels of fluoride in the groundwater in the vicinity of the rift valley are observed in Ethiopia, Kenya, Tanzania, Mozambique, and South Africa (Chowdhury *et al.,* 2019).

The second belt runs from Egypt to Mauritania. It starts from Egypt through Libya, Algeria, Morocco, and Western Sahara ending at Mauritania. The significantly high geological fluoride concentration in this belt is contributed by granites and Precambrian basement gneisses (Chowdhury *et al.,* 2019). While the latter is true for Libya and Algeria, fluoride in the groundwaters of Mauritania is associated with meta-rhyolites whereas the elevated fluoride levels in Morocco and Western parts of the Sahara are mainly contributed by the mining of phosphate rocks for fertilizer manufacturing, application, and exportation (Adesiyan *et al.,* 2018; Maadid *et al.,* 2017).

The third fluoride belt runs from Turkey through China. Its starting point is Turkey followed by Iraq, Iran, Afghanistan, Pakistan, India, and North Thailand, through China (Chowdhury *et al.,* 2019). High fluoride concentrations in Iraq and Iran have been associated with the weathering and dissolution of gypsum, calc-alkaline rocks, and volcanic activities, unlike Afghanistan whose fluoride is associated with pegmatite veins and granites, and Pakistan which is enhanced by dry climate as well as alkaline water (Dehbandi *et al.,* 2017). Unlike other countries in its belt, India's fluorosis is contributed to several factors including granites and its aquifers, the manufacture, and application of phosphatic fertilizers, and fracture-controlled hydrology (Kumar *et al.,* 2016) whereas Fluoride in China and Thailand are associated with hot springs accompanied by the above-mentioned factors (Gupta & Ayoob, 2016).

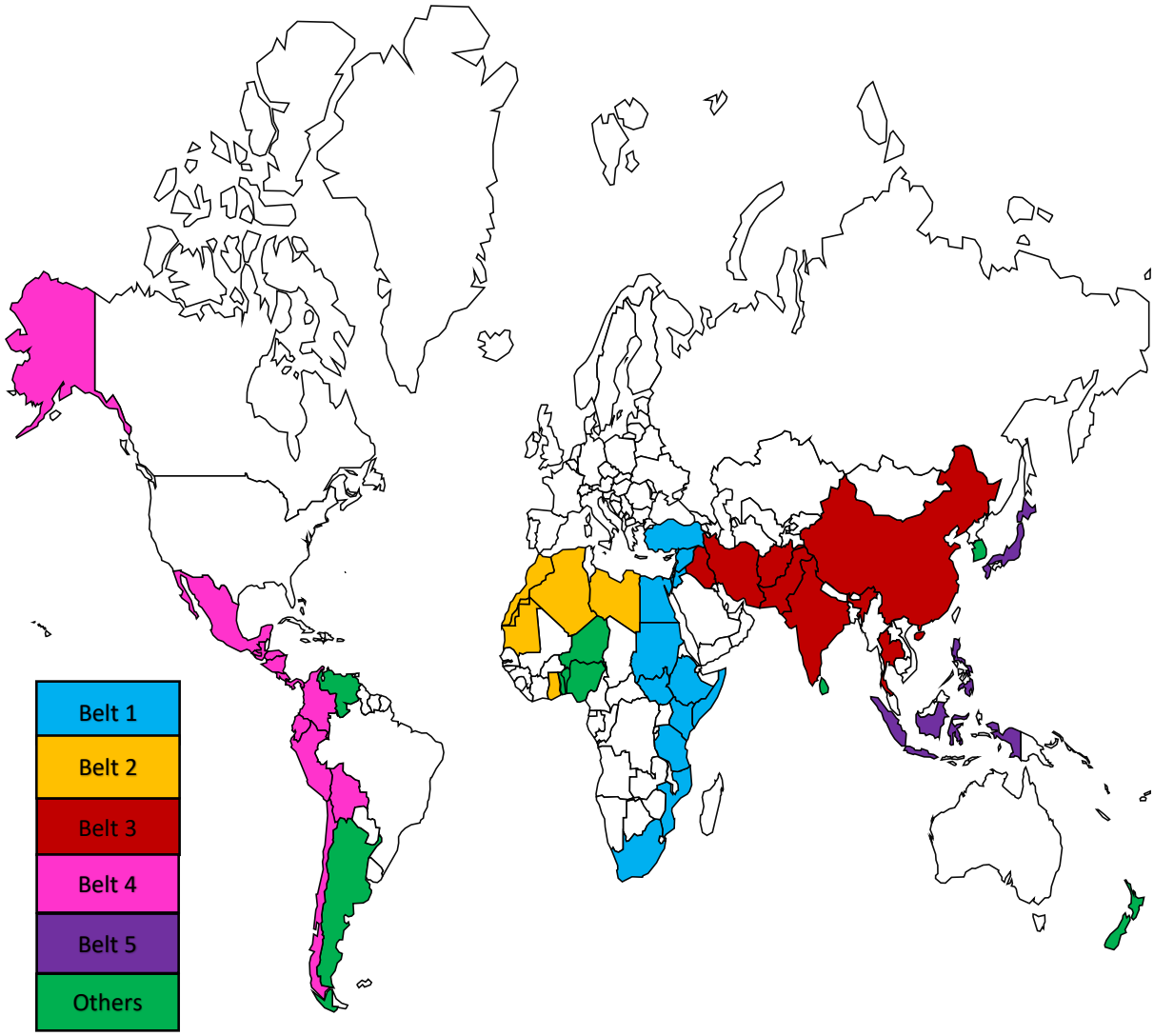

Figure 4: The geographical distribution of fluoride in the world agro-ecosystem (Chowdhury *et al.*, 2019)

The fourth belts stretch from the Sierra Nevada to the Andes Mountains. The belt starts from the Sierra Nevada, USA Rocky Mountains, Mexico, central America, Peru, Columbia, and Bolivia, ending at the Andes Mountains. This belt is also characterized by a tropical climate and the major soil type is Andisols (Chowdhury *et al.,* 2019). It connects a significant number of volcanoes and therefore it's a volcanic fluoride belt. Fluoride at the surface and ground water as well as soil is caused naturally by volcanic eruption and ash. Fluoride enrichment in South America and Columbia is contributed solely by hot springs and volcanic craters whereas in Sierra Nevada and Bolivia, fluoride is also contributed by granitic aquifers and the Andes mountains contain volcanic ash which through leaching and runoff it feeds fluoride to ground and surface water as well as the topsoil.

The fifth and last belt runs from Japan to the Volcanic islands of Indonesia. Japan is the starting point then the Philippines through Indonesia and is dominated by Andisols soil (Chowdhury *et al.,* 2019). Like the fourth belt, this belt is also connected by a series of active and dormant volcanoes but with tectonic activities included. Although volcanic ash, rocks, and subduction are the principal causes of high fluoride concentration in Japan and Indonesia, the Philippines receive extra influence from the hot springs rising its fluoride concentration in the lake to > 1266 mg/L.

2.2.2 Fluoride in Tanzania

Fluorosis is reported prevalent in more than 25 countries worldwide (Fawell *et al.,* 2006). Most of these countries occur in volcanic areas such as the east African rift valley (EARV) which Tanzania is part of. It is reported that 87.4% of children aged 9 – 13 at Maji ya Chai exhibited severe dental fluorosis (Fawell *et al.,* 2006).

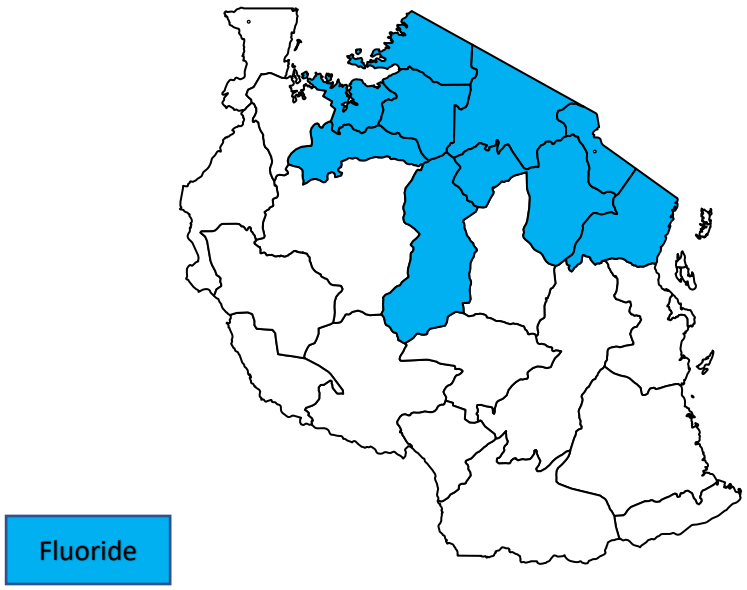

Figure 5: Map showing reported Tanzanian regions affected by fluoride

In 1999, Awadia reported 83 – 95% of native people living in the Arusha and Kilimanjaro regions exhibited severe dental fluorosis (Awadia *et al.,* 1999). On the other hand, the prevalence of skeletal fluorosis has been reported in Arusha, Kilimanjaro, Singida Shinyanga Mwanza, and Mara, regions, the leading regions being Arusha region situated at the foot of Mount Meru and Moshi situated at the foot of Mount Kilimanjaro (Fig. 5) (Awadia *et al.,* 1999; Fawell *et al.,* 2006; Mjengera & Mkongo, 2003). These regions contain fluoride concentrations ranging from 12 – 690 mg/L in surface waters (Fawell *et al.,* 2006).

2.3 Remediation Technologies for Fluoride-Contaminated Soils

2.3.1 Electro-Kinetic Remediation

The electrokinetic remediation technique is an in-situ technology for the cleanup of sludge, sediment, and soil that has been contaminated with organic and inorganic contaminants. It works by supplying direct electric currents to the contaminated soil (Virkutyte *et al.,* 2002). The contaminants can be removed by two transport mechanisms; electro-osmosis or electro-migration. Electro-osmosis involves the movement of pore water towards the cathode when the zeta potential of the soil surface is negative whereas electro-migration causes cations to move from anode to cathode (Baek & Yang, 2009; Zhu *et al.,* 2009). In an electrokinetic system, the electrolysis reaction near electrodes facilitates the extraction and desorption of pollutants from the soil. For example, during the removal of cationic contaminants, the hydrogen ion produced at the anode moves to the cathode, and the cationic contaminants are extracted and desorbed from the soil by cation exchange with hydrogen which then moves towards the cathode. These processes make the soil acidified and contaminants are then removed.

Electrokinetic technology has been effectively used to remove contaminants such as organic pollutants and heavy metals from contaminated soils. But remediation of fluoride-contaminated soils using conventional electrokinetic technology has yielded unsatisfactory results (Zhu *et al.,* 2009). To effectively remove fluoride from the soil using the electrokinetic method, the pH of the system needs to be controlled. This is because fluoride is strongly held at pH 5.5 - 6.5 and then desorbed intensely at one unit higher or lower (Jha *et al.,* 2011). At high pH, fluoride cannot form complexes with aluminum or iron instead fluoride is desorbed by the soil and exist as free fluoride (Baek & Yang, 2009; Costarramone *et al.,* 2000). At low pH fluoride forms complexes with aluminum inhibiting its effective adsorption by other stable soil ions.

In response to the pH control challenge, studies proposed using anolyte to enhance the performance of the electrokinetic method for the remediation of fluoride (Hu *et al.,* 1997; Kim *et al.,* 2009; Pomes *et al.,* 1999). The anolyte application was said to increase the electro-osmotic flow which enhances the electro-osmotic fluoride transport of the system however Zhu *et al.* (2009) when investigating the two different concentrations of anolyte solution circulated with a strong base solution and three different electric potentials suggested electro-migration to be a major transport process and the fluoride removal efficiency of 73% was attained (Zhu

et al., 2009). On the other hand, Zhou *et al.* (2014) identified the unsatisfactory fluoride remediation results obtained during conventional electrokinetic was because anionic pollutants such as fluoride are easily desorbed from the soil at high pH more than at neutral pH and acidic conditions. The approaching cathode releases more OH^- which accelerates pH rise favoring fluoride desorption from the soil (Zhou *et al.,* 2014). Following their observation, the authors employed electrokinetic with several approaching cathodes to remediate fluoride-contaminated soil. Their proposed method enhanced fluoride removal efficiency from 69.8 to 75% while serving 16% of the operating energy consumption (Zhou *et al.,* 2014). Although efficient, the utilization of electrokinetic in situ is rather technical, and manipulating it to acquire selectivity is of importance.

2.3.2 Biological Remediation

Biological remediation involves the use of living organisms both naturally occurring or genetically modified to absorb and accumulate fluoride that is present in the contaminated areas. These living organisms can either be microorganisms (bacteria and fungi) or plants.

(i) Microbial remediation

Table 2 presents microorganisms that have been investigated for fluoride absorption and accumulation. The commonly used microorganisms are bacteria and fungi. These microbes utilize the contaminant during their metabolism process. The high reactivity property of fluoride, adds to the advantage of fluoride reacting with the microbial enzymes, by forming alumino-fluoride and beryllium fluoride complex which are phosphate analogs, or by acting as a trans-membrane proton transporter through the formation of HF (Poulsen, 2011). Although fluoride exposure has been reported to decrease 80% of the bacterial biomass, some bacteria protect themselves by secreting an outer covering layer that is hydrophobic assisting its adaptation to fluoride toxicity (Hussein *et al.,* 2003; Tscherko & Kandeler, 1997). The bacteria capable of secreting the hydrophobic layer are mass-produced and utilized for the remedial purpose against fluoride contamination but their defluoridation efficiency is still low and not cost-effective. Recently, the employment of micro-organisms for defluoridation has been widely reported but the majority of the studies focus on water leaving a handful of data for soil research.

Table 2: Defluoridation efficiency of different microorganisms reported in literature using different initial fluoride concentration

Microbial spp.	Microbial dosage (g)	F^- dosage (mg/L)	F^- removed (%)	Reference
Aspergillusniger FS18	1.5	2, 4, and 6	100	Annadurai *et al.* (2019)
Starria zimbabweensis	0.089	10	66.6	Biswas *et al.* (2018)
Padina sp.	3	3	94	Mohamed *et al.* (2020)
Phormidium sp.	4.5	3	60	Mittal *et al.* (2020)
Ulva fasciata	0.5	5	97	Kalyani *et al.* (2009)
Spirogyra sp. IO1	0.05	5	64	Mohan *et al.* (2007)
Acinetobacter sp. GU566361	0.04	5	57	Shanker *et al.* (2020)
Bacillus cereus	-	730	22	Banerjee *et al.* (2016)

(ii) Phytoremediation

Table 3 presents plants that have been reported to accumulate high fluoride concentrations. Phytoremediation involves the use of plants to clean fluoride-contaminated soil. while the majority of plants depend on the soil to obtain its nutrients for growth and development, scientists have invested in utilizing this approach to identify plants that a capable of taking up fluoride and tolerate to its toxicity (hyperaccumulators) (Baunthiyal & Ranghar, 2015). Santos-Díaz and Zamora-Pedrazaa (2010) investigated the water defluoridation efficiency of 17 different plant species at fluoride concentration of 2.5 – 10 mg/L, however, it was three species only (*Saccharum officinarum* (40% removal), *Pittosporum tobira* (15% removal) and *Camellia japonica* (7.5% removal)) that proved effective at 4 mg/L initial fluoride concentration (del Socorro Santos-Díaz & Zamora-Pedraza, 2010). Even though this approach could be cost-effective, it has limitations such as the immobility of plants, disposal after harvest, and taking time to grow (Wang *et al.,* 2002).

Table 3: Fluoride absorption efficiency of different plants as reported in literature

Plant spp.	Fluoride removal	Reference
Oryza sativa	25 mg/L	Banerjee *et al.* (2020)
Solanum lycopersicum	0 – 100 mg/L	Ahmad *et al.* (2018)
Portulaca grandiflora	22.96 mg/mL	Patil *et al.* (2014)
Camellia sinensis	1442 mg/kg	Camarena-Rangel *et al.* (2015)
Vachellia tortilis	592.24 µg/g	Baunthiyal and Sharma (2012)
Amaranthus gangeticus	20.9 g/kg	Khandare and Rao (2006)

2.3.3 Chemical Remediation

Immobilization/Adsorption is among the most effective methods for the remediation of contaminated soils (Tafu & Manaka, 2016). It controls pollutant dispersion to the surroundings or prevents its movement to the water sources both ground and surface water (Bolan *et al.,* 2021; Udeigwe *et al.,* 2011). Compared to washing treatment or soil removal, immobilization is cost-effective to inhibit contaminants in the environment (Asakawa *et al.,* 2007; Tafu & Manaka, 2016). This process involves the incorporation of hazardous elements into a stable matrix through cementing reactions locking it from dispersion into the environmental matrix (He & Suito, 2001). Table 4 presents adsorbents investigated for the remediation of fluoride-contaminated soils.

Gao *et al.* (2012) investigated the soil defluoridation influence of wood and bamboo charcoal in tea plants cultivated soils. Their results suggested that both wood and bamboo charcoal could effectively adsorb the bioavailable fluoride in the soil and thereby prevent its uptake and accumulation by the tea roots. Both charcoals are equipped with active sites capable of holding the free fluoride in the soil solution making it unavailable for the plant roots to absorb (Gao *et al.,* 2012). In 2013, Suzuki and coworkers investigated the efficiency of fluoride immobilization in artificially contaminated kaolinite using commercial-grade magnesium oxide (MgO). The results suggested that MgO could sufficiently immobilize fluoride if a sufficient amount of MgO is added. Fluoride could be removed from 100 - 0.8 mg/L at MgO a dosage of 100 mg/20 mL following the mechanism of Equations 2 - 4 (Suzuki *et al.,* 2013). Even though immobilization of fluoride with MgO proved to be effective, it is not economical and rises the soil pH which is a crucial factor for crop germination and development.

$$MgO + H_2O \leftrightarrow Mg^{2+} + 2OH^- \ldots \quad (02)$$

$$Mg^{2+} + 2OH^- \leftrightarrow Mg(OH)_2 \ldots \quad (03)$$

$$Mg(OH)_2 + 2F^- \leftrightarrow MgF_2 + 2OH^- \ldots \quad (04)$$

Another study investigated two low molecular weight organic acids (LMWOA), Humic and citric acid. Humic acid was found to decrease water-soluble fluoride but increase the amount of exchangeable fluoride. This study, therefore, concluded that the presence of low molecular organic acids in the soils activates the release of fluoride into the soil and therefore accelerates its uptake and accumulation by crops (Chen *et al.*, 2013). When LMWOA was mixed with hydroxyapatite and tested for fluoride adsorption, it was found to increase the number of active sites in hydroxyapatite and therefore enhanced fluoride adsorption capacity (Wang *et al.*, 2011).

The pH of the soil is one of the methods investigated for fluoride uptake. Ruan *et al.* (2004) investigated the impact of pH on fluoride uptake by tea plants where the highest fluoride uptake was observed at a pH of 5.5 and low uptake was observed at a pH of 4.0. However, pH is not a reliable method since pH is not always consistent. The inconsistence of pH is attributed to changes in soil properties such as CEC, EC, elemental composition, and organic matter which are normally subject to change. On the other hand, liming has been found to limit fluoride uptake in plants by 47%, however, higher concentrations of lime in soil rises pH and as a result facilitates further fluoride release (Ruan *et al.*, 2004).

Synthetic adsorbents such as $polyphenol\text{–}Ce$ derived from plants were used to suppress fluoride accumulation in plants by controlling its uptake. Polyphenol contains end-to-end phenolic hydroxyls which chelate with Al^{3+}in the soil and therefore prevent plant uptake of fluoride in the form of AlF_3, a fluoride complex taken by tea plants easily. Also Ce^{4+}could accommodate two fluoride ions and therefore hold them for uptake (Zhao *et al.*, 2015). Most of these reported fluoride immobilization technologies have proved effective but could not limit fluoride to the levels permissible for plant uptake.

Table 4: Fluoride remediation efficiency of different adsorbents

Adsorbent	F^- removal (%)	Reference
Hydroxyapatite	37.3 − 87.8	Gan *et al.* (2021)
Wood and bamboo charcoal	5 – 30	Gao *et al.* (2012)
CaO	37.2	Ruan *et al.* (2004)
MgO	effective	Suzuki *et al.* (2013)
$polyphenol-Ce$	74.5	Zhao *et al.* (2015)
$Al_2\ (SO_4)_3$	40 - 69	Zang *et al.* (2022)

In another study, hydroxyapatite ($Ca_{10}(PO_4)_6(OH)_2$) was used to immobilize fluoride. Hydroxyapatite which is a stable calcium of phosphate easily exchanges its OH^- ion with fluoride ion. The 2% *w/w* hydroxyapatite amendment could immobilize up to 37.3 - 87.8% water soluble-fluoride (Ws-F) at an initial concentration of 14.3 - 124.5 mg/kg by a mechanism presented by Equation 5 (Gan *et al.,* 2021).

$$Ca_{10}(PO_4)_6(OH)_2 + 2F^- + 2H^+ \rightarrow Ca_{10}(PO_4)_6F_2 + 2H_2O \quad \ldots\ldots\ldots\ldots\ldots\ldots\ldots\ldots\ldots\ldots (05)$$

The challenge with using hydroxyapatite is that it requires higher calcium concentration and in its supersaturated state, hydroxyapatite precipitates into particles that are very small and difficult to handle. To overcome this challenge, dicalcium phosphate dihydrate (DCPD, $CaHPO_4 \cdot 2H_2O$) was further investigated for 20 mg/L fluoride immobilization. Although there was no reaction within the first 4 h contact time between fluoride and DCPD, fluoride was abruptly removed in the next 1 h (5^{th} hour) to attain a final fluoride concentration of 3 mg/L (Equation 6) (Tafu & Chohji, 2006).

$$10CaHPO_4H_2O + 2F^- \rightarrow Ca_{10}(PO_4)_6F_2 + 4HPO_4^{2-} + 10H^+ + O_2 \quad \ldots\ldots\ldots\ldots\ldots\ldots (06)$$

2.4 The use of Biomaterials

In agricultural activities, biomaterials have been used to improve the soil quality which in turn enables farmers achieve high quality agricultural products (Shaji *et al.,* 2021). Fertilizers derived from biomaterials is mostly organic and due to its low decomposition process the nutrient leaching process is slowed (Craigie, 2011; Krishnamoorthy & Malek, 2022). Therefore biomaterials are considered useful soil amendments (Chew *et al.,* 2019). Seaweed materials and extracts has a variety of bioactive compounds which are beneficial for plant growth and development (Craigie, 2011). The extraction of these bioactive compounds is executed using

water, acids or bases, physical methods or by heat (Sharma *et al.,* 2014). Amongst biomaterials, seaweeds have been reported to contain a wide variety of bio-stimulants for agricultural purposes (Krishnamoorthy & Malek, 2022).

Seaweed *Eucheuma cottonii* is one of the seaweeds that has high value economically and it is also known as *Kappaphycus alvarezii* (Supriyono *et al.,* 2022). This seaweed contains a high molecular weight organic compound called carrageenan which has several industrial applications ranging from gelatin of seaweed, medicine, textile, woof, cosmetics, food, shampoo, toothpaste, paper, and even lubricating oil on Petro-gas industries (Sharma *et al.,* 2014). But unlike many other seaweeds, this seaweed contains plant growth hormones such as auxin, cytokinin, gibberellin, kinetin, and zeatin contributing to its application as fertilizer into the soil (Cahyaningtyas *et al.,* 2021; Sedayu *et al.,* 2014). The use of *Eucheuma cottonii* for commercial purposes have been effective due to its availability which is abundant and its short growth circle which grows ten times its initial weight in just six weeks (Cahyaningtyas *et al.,* 2021).

The use of biomaterials for defluoridation purposes has the advantages of environmental pleasantness, abundance, and economics. Some of the biomaterials investigated for defluoridation purposes include algae (El-Said *et al.,* 2018), leaves (Dehghani *et al.,* 2018), husks (Gebrewold *et al.,* 2019) as well as biowastes. The biomaterials could be used in their natural states or modified. A study investigated a defluoridation efficiency of a biomaterial derived from *Luffa cylindrica* integrated with nano-cerium oxide which was found effective in offering better interaction between its active sites and free fluoride ions ensuing higher fluoride adsorption (Nehra *et al.,* 2020). Another study investigated the use of rice husk coated with aluminum hydroxide which revealed a fluoride adsorption capacity of 9 – 10 mg/g (Ganvir & Das, 2011). Natural biomaterials are packed with essential adsorption components such as lignin, tannins, cellulose, and pectin responsible for ionic reactions and sorption behaviors (Nehra *et al.,* 2020). With these essential adsorption components, modification of biomaterials with inorganic compounds guarantees its highest defluoridation capacities at affordable expenses (He *et al.,* 2020).

There are micro and macro-algae species in the marine environment both of which have been investigated for contaminant removal. Seaweeds also termed macro-algae are marine species with no true roots, leaves, or stems. Seaweed serves as food, fertilizer, fodder/feed to fish and poultry, as well as a source of active ingredients in phytochemicals (alginates, carrageenan,

ulvan, and agar) (Krishnamoorthy & Malek, 2022). Lately, seaweed-derived bio-materials for removing pollutants in water and soil have drawn the attention of researchers globally. This is attributed to its abundance, cost-effectiveness, short growth period, and high binding capacity (He *et al.,* 2020).

Remediation of contaminated soils using seaweed depends on the interaction between the target contaminant in the soil and the engineered mechanism of the amended algae. These interactions can either be physical, electrostatic, ion exchange, precipitation, or complexation. Seaweed has high exchangeable nutrient content (N, P, K, Mg, and Ca) which contributes to soil fertility compared to most other biomaterials (He *et al.,* 2020; Singh *et al.,* 2021). Depending on the type of seaweed, it can also neutralize the pH, CEC, carbon content, and specific surface area (SSA) of the soil (Enriquez, 2017). Seaweed biochar has also been investigated for contaminant removal in the soil. the seaweed-derived biochar contains lower lignin. Lower lignin content reduces volatilization which further lessens weigh loss during pyrolysis thereby producing more biochar compared to the same amount of wood-based biomass (Singh *et al.,* 2021).

Even though the use of seaweed-based bio-adsorbents for soil remediation has been exhausted for the removal of cationic pollutants such as copper, nickel, and lead and has shown great potential, its use for anionic pollutants such as fluoride calls for further research.

2.5 Mechanisms of Fluoride Removal

The fluoride removal depends on an interaction between fluoride and the surface of the amended adsorbent. This interaction is a function of the characteristic of the surface of the adsorbent. These interactions can be:

2.5.1 Electrostatic Attractions

This involves an interaction between cation-π and C = C bond and C - C. The interaction between cations and protons in the electrolyte solution determines the rate of dynamics taking pace in a scatter system like coagulation, flocculation, interaction with the boundary surface (adsorption), and aggregation (Adamczyk & Warszyński, 1996). Dugyala *et al.* (2016) investigated the impact of particle charge and concentration on the adsorption dynamics of silica nanoparticles to the fluid-fluid interface where the interfacial tension decreased was more when the particles were weakly charged meaning more adsorption but when particles were highly charged, the interfacial tension change was negligible (no adsorption). When the

particles are highly charged, the net energy barrier prevents the adsorption of ions into the interface however the addition of a sufficient amount of $NaCl$ decreases the net energy barrier facilitating easy adsorption (Dugyala *et al.,* 2016). Normally the electrostatic attraction depends on the point-zero-charge (pH_{pzc}) of the adsorbent. If the pH_{pzc} of the adsorbent is higher than the solution interface the surface of the adsorbent becomes protonated thereby promoting electrostatic interaction with the contaminant. This was reported while investigating the defluoridation mechanism of chitosan and composite magnesia/chitosan (MgOC) (Sundaram *et al.,* 2009a; Viswanathan *et al.,* 2009)

2.5.2 Physisorption

Physical sorption involves the diffusion of the ionic forms into the pores of the adsorbent materials without participating in any chemical reactions/bonds. This fluoride removal process was observed during the fluoride removal by hydrothermally modified limestone powder using phosphoric acid. The study results suggested that the Langmuir plots were poor than those of the Freundlich adsorption plots signifying that the fluoride removal process was primarily physisorption (Gogoi & Dutta, 2016).

2.5.3 Complexation

Once the soil encounters a polar solution, the elements within are dissolved into the interface as cations, neutral, complexes, or anions. The anions and cations are solvated (they are surrounded by a hydration shell of water molecules) forming dipole-ion bonds with the dissolved ions. Sometimes the anions and cations or other molecules can bond with each other forming aqueous complexes in which a central cation is surrounded by anions/ligands (Koretsky, 2000). Complexation can contribute to contaminant adsorption through complex formation or competing for the surface for available adsorption sites, causing no perceptible change in the degree of adsorption if the ligand has weak complex formation ability/ displays a lack of affinity for the solid surface or it may enhance adsorption if the ligand is capable of strong complex formation and strong affinity to the solid phase of the adsorbent and soil (Elliott & Huang, 1979).

2.5.4 Ion Exchange

This mechanism involves an exchange reaction between a contaminant and anions/cations attached to the adsorbent. For this removal method to be effective, the newly formed

component post ion-exchange should be insoluble/stable. Exchange resins such as Amberllte IRA 400, Polyanion (NCL), and Deacedite FF (IP), have been investigated for fluoride removal through ion exchange (Bose *et al.,* 2019; Popat *et al.,* 1994). Ion exchange is 90 -95% effective however its efficiency is highly affected by the presence of other anions and cations (Ingle *et al.,* 2014).

2.6 Factors Affecting Fluoride Adsorption

2.6.1 Soil Properties

Total fluoride is reported to vary greatly among soils. This variability is correlated to the soil texture, pH, and organic matter. High fluoride content is associated with an increase in the clay content of the soil as it increases the solid surface area of the soil for fluoride ions to attach. The most interesting soil property controlling the soil's ability to fluoride adsorption is the soil pH. at pH 6 fluoride adsorption is reported to be at its maximum and dropped drastically at one unit higher or lower pH value (Gilpin & Johnson, 1980; Larsen & Widdowson, 1971). pH is also associated with the dissolution of fluorapatite mineral (Cronin *et al.,* 2000) and low pH favors the formation of $Al-F$ complexes increasing soil's fluoride adsorption. Unlike low pH, high pH increases the electrostatic potential of the soil which decreases the soil's ability to retain fluoride thereby increasing fluoride concentration in the soil solution interface which becomes bioavailable. High pH also works by increasing the concentration of OH^- ions in the soil solution interface which inturn displaces the adsorbed fluoride ions in the soil (Larsen & Widdowson, 1971). Similarly, fluoride adsorption in calcareous soils is low in acidic soils limited by the rate of formation and dissolution of CaF_2 and $Ca_5F(PO_4)_3$ promoting swift fluoride leaching. Also the formation and dissolution of is slow, other studies have reported these soils to retain 98% of the formed fluoride for over 10 years unlike NaF and Na_3AlF_6 which retained most fluoride at the topsoil (Murray, 1984).

pH is not only the mastermind controlling the soil properties but also controls the defluoridation performance of the remedial material. A vast of studies have reported that the defluoridation efficiency of the adsorbents was contingent on pH, while some adsorbents performed well at a wide pH range, some could only perform at a solitary pH. for this reason, pH has been an important monitored parameter during analysis. Pumice was modified with HCl and $NaOH$ to enhance its defluoridation efficiency, the results observed defluoridation increase from pH 2 – 6 and a decrease from pH 6 – 10. High fluoride removal was noticed in acidic conditions than

in alkaline conditions the maximum being at pH 6. pH of the solution and the adsorbent pHpzc affects the anionic structure of fluoride and the dispersion of negative and positive charges at the adsorbent surface (Yousefi *et al.,* 2019). When the solution pH is less than the pHpzc of the adsorbent, the surface of an adsorbent becomes positively charged attracting more fluoride ions but when the solution pH is more than the pHpzc of the adsorbent, its surface becomes negatively charged repulsing the fluoride ions. Therefore, defluoridation is low when the initial pH is close to or higher than the adsorbent pH_{pzc} due to proton release (deprotonation) (Sawangjang *et al.,* 2021).

A study by Bower and Hatcher which investigated fluoride adsorption in acidic and alkaline soils reported fluoride adsorption to decrease in an order $Al(OH)_3$ precipitate on bentonite > $Al(OH)_3$ >> hydrated halloysite & dehydrated halloysite > a weakly acidic soil >> kaolinite > gibbsite > alkaline soils > goethite > bentonite and vermiculite. The conclusion from this study suggested that fluoride adsorption occurs by an exchange reaction between the $-OH$ groups of the $Al(OH)_3$ and Al polymers rather than by exchange with crystal lattice $-OH$ groups of the clay minerals (Bower & Hatcher, 1967).

2.6.2 Initial Fluoride Concentration

The amount of fluoride adsorbed is directly related to the amount of fluoride present in the soil solution interface. Even if the adsorbent still contains several active sites for fluoride adsorption, if it is not available in the soil solution then none will be adsorbed (Khandare & Rao, 2006). Commonly, to understand the saturation point of the adsorbent, the initial fluoride concentration is varied. At the highest initial fluoride concentration, all the active sites as well as exchangeable ions in the adsorbent material are saturated reaching an equilibrium indicating the maximum defluoridation efficiency of the adsorbent (Dong & Wang, 2016).

2.6.3 Contact Time

Contact time is the amount of time an adsorbent material is kept in contact with the solution containing fluoride ions. This provides ample time for the exchange reactions or adsorption process to take place. While some adsorbents require sufficient time to react with the fluoride ions, some adsorbents exert abrupt reactions. The contact time data are normally used to define the adsorption kinetics of the adsorbent fitted in pseudo-first and pseudo-second-order kinetic models discussed in Chapter three (He *et al.,* 2016).

2.6.4 Adsorbent Surface Area

The surface area of the adsorbent defines the number of fluoride ions it will hold. It is defined by the porosity of the adsorbent material. A porous material provides more adsorption sites for the interaction with the fluoride ions through physisorption or chemisorption (Hegde *et al.,* 2020; Madera-Parra, 2016). While natural biomaterials which contains activated carbon contains a reasonable surface area for adsorption, crosslinking it with metal oxides increases its surface area and hence adsorption efficiency. A study by Mukherjee and Halder (2016) compared the defluoridation efficiency of raw biomass and activated carbon of *Colocasia esculenta* in which, raw biomass had a surface area of 49.33 m^2/g with fluoride adsorption efficiency of 33% and its activated biochar almost doubled to 89. 98 m^2/g surface area and fluoride adsorption of 78.8% which is a significantly large improvement in both surface area and defluoridation efficiency a study later supported by Bibi *et al.* (2017) while using rice husk and potato peel (Bibi *et al.,* 2017; Mukherjee & Halder, 2016).

2.6.5 Presence of Co-Existing Ions

Both anions and cations are known to affect fluoride adsorption. The presence of these ions can facilitate fluoride adsorption but could also hinder its adsorption by competing for the active sites. The order in which anions interfere with fluoride removal is HCO_3^- > SO_4^{2-} > Cl^-under the use of different biomaterials (Kamathi, 2017; Sharmila *et al.,* 2019). A study Investigating the alumina-based defluoridation examined the interference profiling of Cl^-, SO_4^{2-}, CO_3^{2-}, OH^-anions in the surface water where CO_3^{2-} and OH^- was found to interfere fluoride removal more compared to Cl^- and SO_4^{2-} (Bavda *et al.,* 2018). While there is a handful of literature on the effect of cations on fluoride adsorption, some studies have reported that the presence of Ca^{2+} had no significant influence on fluoride adsorption into TiO_2 adsorbent while Mn^{2+} was found to enhance the fluoride adsorption into Zeolite material (Hegde *et al.,* 2020).

2.6.6 Adsorbent Dosage

In most cases, the increase in adsorbent dosage increases fluoride adsorption. This is due to the increment in the adsorption sites in contact with the fluoride ions. But as adsorbent dosage increases, the adsorption rate decreases as the interaction between the unsaturated adsorption sites of the material with the fluoride ions decreases (Mbugua *et al.,* 2020).

CHAPTER THREE

MATERIALS AND METHODS

3.1 Study Area

The soil used for this study was collected at Ngarenanyuki which is one of the 17 wards of Meru district, Arusha, Tanzania (Fig. 6). Its geological setting is latitude 3° 8' 59" S and longitude 36° 51' 0" E and is located between Mount Meru and Mount Kilimanjaro. It is part of the East Africa Rift Valley surrounding Mount Meru which is an active Volcano. Ngarenanyuki ward has five villages (Uwiro, Olkung'wado, Ngabobo, Kisimiri chini and Kisimiri juu). The annual mean temperature is between 20 ± 2 and 29 ± 2°C. The study area has an Afro-Alpine semi-arid climate characterized by a wet and dry season (Kihampa *et al.,* 2010). The major wet season begins from June through September and accounts for approximately 70% of the annual rainfall while another wet season which is minor accounts for the remaining 30% of annual rainfall from mid-February through mid-May and the mean annual rainfall is estimated to be 535 mm (Ghiglieri *et al.,* 2010; Kihampa *et al.,* 2010). The significant part of the soil is characterized as sandy loam and the main source of food and income in this area is small-scale farming whereby people are involved in the cultivation of food and cash crops some of which includes, tomatoes, cabbage, potatoes, onions, maize, and beans (Mkungu *et al.,* 2014). The volcanic activities in this area have led to the accumulation of volcanic material containing fluoride at the topsoil, surface water, and groundwater and have attracted the majority of fluoride research activities (Kihampa *et al.,* 2010).

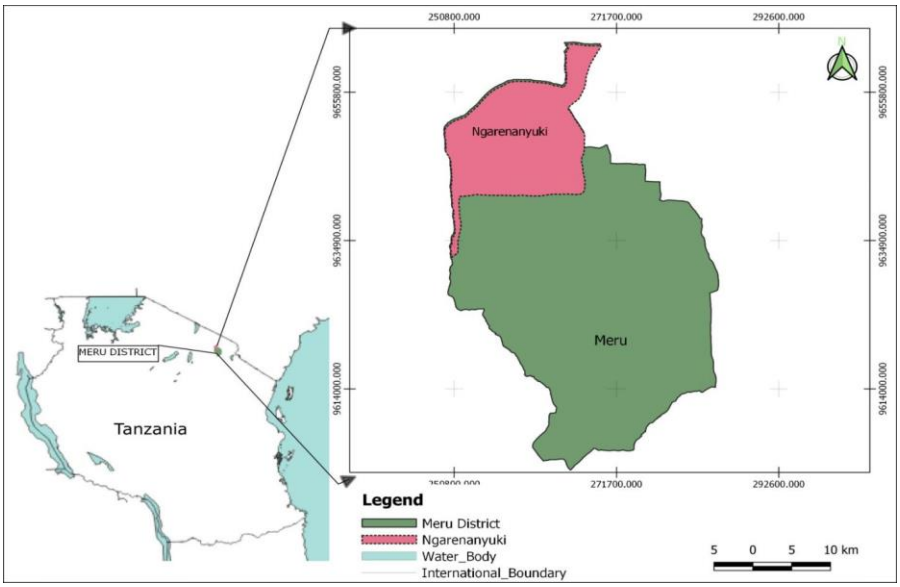

Figure 6: A map showing the location of the study area

3.2 Materials

The important materials used for this study were, Seaweed *Eucheuma cotonnii,* and fertilizers (diammonium phosphate (DAP), urea and farmyard manure). The seaweed was collected along the coastal area at Tanga region, Tanzania. The DAP and urea fertilizers were bought from local fertilizer suppliers in Arusha region. The farmyard manure was collected from the cattle house in one of the houses at the study area. The materials investigated for defluoridation purposes were dried seaweed (DSW), fermented seaweed (FSW), seaweed-derived biochar (SB) and hydroxyapatite-activated seaweed biochar (HSB). All the chemicals used for this study were of analytical grade and distilled water was used throughout the study.

3.3 Soil Sampling and Sample Preparation

To identify the soil used for the experimental purposes of this study, a preliminary study was conducted. The soil samples were randomly collected from four different villages of the Ngarenanyuki ward (Ngabobo, Olkung'wado, Uwiro, and Kisimiri Chini). After sample collection, the amount of total fluoride and the fluoride fractions were determined for each soil as well as pH and electric conductivity (EC) (preliminary data are available in Appendix 1). The data from this preliminary study established the use of cultivated soil from the Olkung'wado area located at coordinates 3°10'35" S 36°51'35" E throughout the study. Maize and beans were cultivated during the rainy season and horticultural production (Tomato, kale, cabbage, and onions) under irrigation during the dry season. According to the farm owners, the soil has regularly been supplied with DAP, Urea, and manure fertilizers for more than 2 decades to supply plant nutrients.

The topsoil (0 - 20 cm), was randomly collected from the same farm using a hand spade during the dry season to represent the root zone of most cultivated crops in the area. The soil was then mixed thoroughly, air-dried for 2 days, and then passed through a 2 mm sieve to eliminate grit and other debris. The soil was stored in plastic containers that were cleaned with nitric acid (HNO_3) before laboratory analysis. The selected soil parameters measured were pH, particle size distribution, soil organic matter (SOM), cation exchange capacity (CEC), electrical conductivity (EC), water holding capacity, soil specific surface area (SSSA), fluoride fractions (water-soluble (Ws-F), Exchangeable-fluoride (Ex-F), fluoride-bound to iron/manganese (Fe/Mn-F), organic matter bound-fluoride (Or-F), and residual-fluoride (Res-F)), phosphorus (P) interms of phosphorus pentoxide (P_2O_5), and the exchangeable bases (calcium (Ca^{2+}),

magnesium (Mg^{2+}), potassium (K^{+}) and sodium (Na^{+}). These parameters were monitored before and after amendment with each of the investigated materials.

3.4 Laboratory Analysis

The hydrometer method was used to measure the soil particle size distribution (Pickering, 1985). The content of SOM was calculated using the loss-on-ignition (LOI) method (Chen *et al.,* 2013). An electrical conductivity meter and pH meter were used to measure the electric conductivity (EC) and pH of the experimental soil. The cation exchange capacity (CEC) was measured using the barium chloride-triethanolamine method (pH 8.2) (Purnamasari *et al.,* 2021). The water absorption capacity was measured by the centrifugation method (Jumaidin *et al.,* 2017). The specific surface area of the soil was determined using the ethylene glycol monoethyl ether (EGME) method according to procedures by Yeliz and Abidin (Yukselen & Kaya, 2006). The exchangeable bases were quantified using the flame atomic absorption spectrophotometer (FAAS) (Selassie *et al.,* 2020) and X-ray fluorescence (XRF) was used to analyze the total elemental composition (Bibi *et al.,* 2017). The Point-zero-charge (pHzpc) of the composite material was determined using a pH drift method (Chai *et al.,* 2013). The carbon (C), hydrogen (H), nitrogen (N), sulfur (S), and oxygen (O) were determined using a micro-element analyzer (Saeed *et al.,* 2020). For the analysis of moisture content, 2 g of the air-dried seaweed and seaweed biochar were oven dried at 105℃ for 3 h, stored in the desiccator, and weighed when cooled to room temperature. The scanning electron microscope (SEM-EDX) was used to observe the morphology of the adsorbents, X-ray diffraction (XRD) was used to capture the crystal structure of the adsorbents (Qiu *et al.,* 2020).

3.4.1 Total Fluoride

Total fluoride was determined according to McQuaker and Gurney's procedure. The 0.5 g of the soil sample was weighed into the crucibles and then moistened with 5 mL of distilled water. A 6 ml of concentrated $NaOH$ (17 M) was then added and placed into the oven set to 150°C for 1 h. After 1 h the samples were moved into the muffle furnace set at 600°C for 30 min and then left to cool to room temperature. Distilled water was added to allow the dissolution of the $NaOH$ cake then moved to a 100 mL centrifuge tubes where the pH was adjusted to around 8 by using HCl. Subsequently, the samples were shaken and centrifuged and the supernatant was collected for analysis using a fluoride ion-selective electrode (F-ISE) mixed with TISAB II as an ionic strength adjustment buffer at 1:1(Dagnaw *et al.,* 2017; Loganathan *et al.,* 2001;

McQuaker & Gurney, 1977).

3.4.2 Sequential Extraction of Fluoride Fractions

Species of fluoride were extracted sequentially following a procedure reported by Chen and coworkers (Chen *et al.,* 2013). A 2.5 g of soil sample was sieved using 0.2 mm mesh and placed into a 50 ml centrifuge tube and various species of fluoride were extracted by adding 25 ml of the extracting solutions as summarized in Table 5. Sequential extractions were also used to extract the forms of fluoride present in the fertilizer's seaweed material.

Table 5: Procedures for sequential extraction of fluoride fractions from the soil (Chen *et al.,* 2013)

Fluoride spp.	Extract Solution	Settings
Ws-F	Distilled water	agitate for 0.5 h at 60ºC
Ex-F	1.0 mol/L $MgCl_2$ (pH = 7)	agitate for 1 h at 25ºC
Fe/Mn-F	0.04 mol/L $NH_2OH.HCl$	agitate for 1 h at 60ºC
Or-F	1st: 3 mL, 0.02 mol/L, HNO_3 + 10 mL 30% H_2O_2	After both steps: agitate for 0.5 h at 25ºC
	2nd: 12 mL, 3.2 mol/L ammonium Oxaloacetate (NH_4OAc)	
Res-F	A difference between Tot-F and a sum of the 4 forms	
Complex-F	X-Ray Diffraction technique	

3.4.3 Analysis of Volatile Fatty Acids (VFAs)

Gas chromatography (GC) was used to analyze the amount of volatile fatty acids (VFAs) present in the fermentative sap using the flame ionization detector (FID) and acetic acid as the standard solution. For analysis, the samples were collected from the fermented sap and then centrifuged at 1,500 rpm for 10 minutes to obtain a clear liquid. The liquid was acidified to pH 1.8 with formic acid to ensure that the pH of the sample is below its dissociation value (pKa) (Huq *et al.,* 2021). Due to analytical limitations, the VFAs results were given as the total volatile fatty acids (TVFAs) expressed as g acetic acid/l (gAc/l). The C: N ratio of the seaweed was measured using the CHNS analyzer (Saeed *et al.,* 2020).

3.4.4 Proximate and Ultimate Analysis

The proximate and ultimate analyses of soil and seaweed derived materials were conducted as follows. The empty crucibles were initially fired at 600℃ in a muffle furnace for 2 h and then cooled to room temperature in a desiccator and weighed.

For determination of moisture content (Equation 7), 2 g (wet weight (A)) of dried seaweed (DSW) was added into a crucible and oven dried at 105℃ for 3 h to remove free water from the sample followed by re-weighing to obtain the dry weight of sample (B).

$$(\%) Moisture\ content = \left(\frac{A-B}{A}\right) x\ 100 \ldots\ldots\ldots\ldots\ldots\ldots\ldots\ldots\ldots\ldots\ldots\ldots\ldots\ldots\ldots\ldots\ldots\ldots\ldots\ldots..(7)$$

The samples were then transferred into a muffle furnace set at 970℃ for 3 h cooled in a desiccator and weighed (C) to obtain the volatile matter content as per Equation 8.

$$(\%)\ Volatile\ Matter = \left(\frac{B-C}{B}\right) X\ 100 \ldots\ldots\ldots\ldots\ldots\ldots\ldots\ldots\ldots\ldots\ldots\ldots\ldots\ldots\ldots\ldots\ldots\ldots\ldots\ldots (8)$$

The sample was again transferred into a muffle furnace which was now heated at 850℃ for 3 h, cooled and weighed (D) to obtain the ash content as per Equation 9 and the fixed carbon content was calculated as a difference between 100 and the weighed values ae per Equation 10 (Krishnamoorthy & Malek, 2022).

$$(\%)\ Ash = \frac{B-D}{B} X\ 100 \ldots\ldots\ldots\ldots\ldots\ldots\ldots\ldots\ldots\ldots\ldots\ldots\ldots\ldots\ldots\ldots\ldots\ldots\ldots\ldots\ldots\ldots\ldots\ldots..(9)$$

$$(\%)\ Fixed\ Carbon = 100 - (\%)\ Moisture - (\%) Volatile\ matter - (\%) Ash \ldots\ldots\ldots (10)$$

For ultimate analysis, the DSW and its biochar samples were analyzed using the organic elemental analyzer, Thermo Scientific Flash 2000 series CHN/S analyzer using a thermal conductivity detector (TCD). Initially, a blank cup was loaded into the CHNS-O equipment to establish the C, H, and N values that were present in the combustion and carrier gas followed by an introduction of 0.4 mg of the samples. The amount of C, H, N, S, and Ash was obtained but the amount of oxygen (O) was obtained as per Equation 11.

$$(\%) O = 100 - \big((\%) C + (\%) H + (\%) N + (\%) S + (\%) Ash\big) \ldots\ldots\ldots\ldots\ldots\ldots\ldots\ldots\ldots\ldots (11)$$

3.4.5 Determination of Exchangeable cations, Cation Exchange Capacity (CEC), and Exchangeable Sodium Percentage (ESP)

To determine the number of exchangeable bases present in the soil, 5 g of the soil sample was placed into a flask followed by slow addition of 50 ml of ammonium oxaloacetate (NH_4OAc) at pH 7. The suspension was kept shaking for 30 minutes and thereafter was filtered by a Whatman paper. The extracted solutions were injected with cesium chloride solution to suppress the ionization of the exchangeable bases and were used for the determination of exchangeable bases in the atomic absorption spectrophotometer (AAS).

On the other hand, CEC presents a quantity of negatively charged sites at the surface of the soil particles able to retain the positively charged ions. Therefore, higher soil CEC presents a greater holding capacity of exchangeable bases and vice versa. Because the pH of the soil used for this study was strongly alkaline, the CEC was determined by the barium chloride-triethanolamine method (pH 8.2). To measure CEC, 2 g of the experimental soil was added into weighed empty falcon tubes followed by the addition of 20 mL of 0.1 $M\ BaCl_2.2H_2O$ and shaken for 2 h. the mixture was centrifuged at 5000 rpm and decanted. Thereafter, 20 mL of 2 m$M\ BaCl_2.2H_2O$ was added and shaken for 1 h, centrifuged, and the supernatant was discarded. The process was repeated several times to obtain a slurry pH thereafter added 10 mL of 5 m$M\ MgSO_4$ and shaken for 1 more hour where distilled water was continuously added up until the conductivity of the solution reaches that of 1.5 m$M\ MgSO_4$ and weigh the tube with the contents. The CEC was determined as Equations 12 (a-d):

(i) Total solution (S_{tot}) (mLs) ($assuming\ 1\ mL\ weighs\ 1\ g$) ... ... (12)
= $W_f\ - W_{\ i} - W_s$

Where:

W_f -Final weight of the tube (g)

W_i - Initial weight of the tube (g)

W_s- the weight of the soil used (2 g)

(ii) Mg in solution = S_{tot} (mLs) x 0.003 (meq/mL) *(1.5 mM $MgSO_4$ has 0.003 meq/mL)*

(iii) Total Mg added (meq) = 0.1 meq (meq in 10 mL of 5 m$M\ MgSO_4$) + meq added in 0.1

$M\ MgSO_4$(mL of 0.1 M $MgSO_4$ X 0.2 meq/mL (0.1 M $MgSO_4$ has 0.2 meq/mL))

(iv) CEC (meq/100 g) = (Total Mg added – Mg in final solution) X 50*(50 is from converting the 2 g of soil into 100 g)*

The exchangeable sodium percentage (ESP) which explains the quantity of soil cation exchange sites occupied by sodium was calculated as per Equation 13:

$$\text{ESP} = \frac{Exchangeable\ Na^{+}}{(Ca^{2+} + Mg^{2+} + K^{+} + Na^{+})}\ X\ 100 \ldots\ldots\ldots\ldots\ldots\ldots\ldots\ldots\ldots\ldots\ldots\ldots\ldots\ldots\ldots\ldots\ldots\ldots\ldots\ldots\ldots\ldots..(13)$$

3.5 Adsorption Experiments and Isotherms

The efficiency of a remediation technique is normally measured by analyzing its ability to remove a targeted contaminant. The ability to remove fluoride is termed defluoridation capacity and is presented as a mass of fluoride adsorbed per unit mass of an adsorbent (*m/m*). The defluoridation capacity varies from time to time depending on the initial fluoride concentration, adsorbent dosage, temperature, pH, and contact time. For proper design and understanding of the adsorption mechanism, one needs to understand and interpret the adsorption isotherm. It is used to quantify the adsorbate, analyze the behavior of the adsorption system, and verify the consistency of the theoretical assumption in the experimental study.

In this study, fluoride adsorption into the seaweed-derived materials was fitted into three selected adsorption isotherm models namely, Langmuir, Freundlich, and Temkin. The adsorption experiments were conducted in batches at room temperature 24 ± 3°C. The experimental soil (5 g) was mixed with different concentrations of fluoride (25, 50, 100, 200, and 300 mg/L) together and 50 ml of 0.01 mol/l $CaCl_2$ solution. Thereafter, the synthesized material was added and the mixture was kept shaking in a shaker at 110 rpm for 72 h. After 72 h the mixture was centrifuged and the amount of fluoride remaining in the supernatant was measured potentiometrically using the fluoride ion selective electrode (F-ISE). The amount of fluoride absorbed by the soil (q_e) was determined as a difference between the initial concentration (C_0) and the final concentration (C_e) using the following Equation 14:

$$q_e = \frac{(C_0 - C_e)}{W}V \ldots\ldots\ldots\ldots\ldots\ldots\ldots\ldots\ldots\ldots\ldots\ldots\ldots\ldots\ldots\ldots\ldots\ldots\ldots.\ldots\ldots\ldots\ldots\ldots\ldots\ldots\ldots\ldots..(14)$$

where:

q_e - fluoride adsorbed by the soil (mg/g),

C- concentration (mg/L),

W- the weight of the soil (kg),

V- the volume of the solution (l).

To understand the adsorption behavior of fluoride to the materials, the experimental data were fitted on the Langmuir (15), Freundlich (16), and Temkin (17) models.

The basic assumption of the Langmuir Theory is that adsorption occurs at the homogeneous sites which are specific inside the adsorbent. Once a fluoride ion occupies that specific site no additional fluoride adsorption happens to generate monolayer adsorption (Walsh *et al.,* 2020).

$$\frac{1}{q_e} = \frac{1}{K_L Q_{max}} \cdot \frac{1}{C_e} + \frac{1}{Q_{max}} \quad (15)$$

$$q_{max}\left(\frac{mg}{g}\right) = \frac{1}{Intercept} \quad (15a)$$

$$K_L\left(\frac{L}{mg}\right) = \frac{1}{slope * q_{max}} \quad (15b)$$

$$R_L = \frac{1}{1 + C_i K_L} \quad (15c)$$

Freundlich's Theory works in an assumption that there exists an interaction between the fluoride ions and the adsorbent sites as well as with the adsorbed fluoride ions generating the multilayer adsorption (Sundaram *et al.,* 2008)

$$Log q_e = Log K_f + \frac{1}{nLog C_e} \quad (16)$$

$$\log K_f = Intercept \quad (16a)$$

$$\frac{1}{n} = Slope \quad (16b)$$

Whereas Temkin isotherm assumes that as the adsorbent surface coverage increases, the adsorption heat of molecules decreases linearly and that adsorption is categorized by the unvarying dispersal of binding energies to a supreme binding energy (Piccin *et al.,* 2011)

$$q_e = \frac{RT}{B_T lnK_T} + \left(\frac{RT}{B_T}\right) \ln C_e \ldots \ldots \ldots \ldots \ldots \ldots \ldots \ldots \ldots \ldots \ldots \ldots \ldots \ldots \ldots \ldots \ldots \ldots \ldots \ldots \ldots \ldots \ldots \ldots (17)$$

$$B_T\left(\frac{J}{mol}\right) = Slope \ldots \ldots \ldots \ldots \ldots \ldots \ldots \ldots \ldots \ldots \ldots \ldots \ldots \ldots \ldots \ldots \ldots \ldots \ldots \ldots \ldots \ldots (17a)$$

$$K_T\left(\frac{L}{mg}\right) = \exp\left(\frac{Intercept}{B_T}\right) \ldots \ldots \ldots \ldots \ldots \ldots \ldots \ldots \ldots \ldots \ldots \ldots \ldots \ldots \ldots \ldots \ldots \ldots (17b)$$

where:

q_e - Amount of fluoride adsorbed by the soil (mg/g),

C_e - Fluoride concentration at equilibrium (mg/L),

K_L - Langmuir constant representing the maximum adsorption capacity (L/mg),

R_L- Indicates wether the shape of the isotherm is favorable (R_L < 1), linear (R_L = 1) or unfavorable (R_L > 1)

Q_{max} - Maximum fluoride concentration adsorbed by the soil (mg/g),

K_f - Freundlich constant,

$\frac{1}{n}$ - Adsorption intensity (The value of $\frac{1}{n}$ defines whether the adsorption process is favorable ($0.1 < \frac{1}{n} < 0.5$) or unfavorable ($\frac{1}{n} > 2$)) (Ayub *et al.,* 2020).

R - Universal gas constant (8.314 J/mol K),

T - Temperature (K),

K_T -Temkin isotherm equilibrium binding constant (L/mg), and

B_T - Temkin isotherm constant (The positive B_T the value indicates the adsorption process is exothermic and if negative the adsorption is endothermic).

3.6 Kinetic Study

The data obtained from the kinetic experiments were fitted into the two common kinetic models; the pseudo-first (Yang & Al-Duri, 2005) and the pseudo-second (Ho, 2006) models shown by Equations 18 and 19.

$$\log(q_e - q_t) = \log q_e - \left(\frac{K_1}{2.303}\right) t \ldots\ldots(18)$$

$$\frac{t}{q_t} = \frac{1}{K_2 q_e^2} + \left(\frac{1}{q_e}\right) t \quad \ldots\ldots(19)$$

Where:

q_t and q_e are the fluoride concentration at time (t) and at equilibrium, (mg/g) respectively.

The pseudo-first-order parameters were obtained by drawing the linear plots of ln (q_e-q_t) Vs t whereas the pseudo-second-order parameters were obtained by drawing a linear plot of $\frac{t}{q_t}$ Vs t.

3.7 Analysis of Microbial Community

The soil microorganisms were quantified by the agar plate dilution method (Al-Dhabaan & Bakhali, 2017). Bacteria were cultured using a buffered peptone enrichment medium and later transferred to the nutrient agar where it was sub-cultured into blood agar and MacConkey agar. The Sabouraud Dextrose agar was used for culturing fungi and starch casein agar (SCA) was used for culturing actinomycetes.

3.8 Material Synthesis

This study investigated the efficiency of four different seaweed-derived materials for reducing the amount of bioavailable fluoride fraction in the agricultural soil. The four preparation methods investigated were dried seaweed, fermented seaweed, seaweed-derived biochar and hydroxyapatite activated seaweed biochar. The seaweed used for these studies is *Eucheuma cottonii* collected from the Tanga region, Tanzania. The seaweed was collected and preserved in plastic containers with some seawater, then transported to the laboratory where it was washed thoroughly with fresh water to remove any salts deposited on the surface, rinsed with distilled water, and was then sun-dried.

3.8.1 Dried Seaweed (DSW)

The seaweed was collected at the coast, washed thoroughly with seawater, packed into plastic containers, and transported to the laboratory. In the laboratory, the seaweed was rinsed with

distilled water and air-dried for 1 week. The seaweed was then ground into a fine powder using a mechanical grinder to obtain a fine powder which was sieved to pass through a 2 mm sieve for homogeneity. The now-dried seaweed was stored at room temperature in a shaded area and labeled DSW.

3.8.2 Fermented Seaweed (FSW)

To obtain the fermented seaweed, 500 g of the seaweed powder was transferred to a container where it was mixed with 500 mLs of the inoculum (anaerobic sludge from the septic tank), 1 L distilled water, and 100 ml molasses. The molasses contains high quantities of sucrose and fructose which is an easily available food source for the anaerobic biomass. Subsequently, 4 ml of iodoform was added to prevent the methanogenesis process from taking place, thereby encouraging acidogenesis and acetogenesis processes (Plácido & Zhang, 2018). After mixing, the container was closed to stimulate the fermentation process. The container was kept in a shaker (110 rpm) at 37℃, free from light until the seaweed was entirely soft (5 weeks). The now fermented seaweeds were oven-dried at 50℃ to obtain a hard solid which was again milled into a fine powder and sieved through a 2 mm sieve. This powder was stored and labeled FSW.

3.8.3 Seaweed-Biochar (SB)

The powdered seaweed was pyrolyzed in a tube furnace at 450℃ for 2 h under continuous N_2 flow. The temperature ramp was maintained at 10℃/min up until the desired temperature was reached. The pyrolysis temperature was selected to recover high biochar yield and moderate cation exchange capacity (CEC) (Liang *et al.,* 2016). Thereafter, the carbonaceous materials which were now seaweed biochar (SB) were recovered. In order to facilitate the reaction, SB was first dipped with 1M HCl, washed with distilled water followed by dipping into 1M $NaOH$ solution, and thereafter rinsing it several times (Qiu *et al.,* 2020).

3.8.4 Hydroxyapatite-Activated Seaweed-Biochar (HSB)

The hydroxyapatite-activated seaweed-derived biochar (HSB) was prepared by taking 5 g seaweed biochar (SB) and dissolved in a 200 mL solution of 1M diammonium phosphate $(NH_4)_2PO_4$, stirred at 200 rpm for 12 h. After the 12 h, the SB was filtered out by centrifuging at 4000 rpm for 15 minutes, rinsed, and transferred to a 1.67 M solution of $Ca(NO_3)_2$ maintained at a minimum pH of 10 using an ammonia solution (NH_3OH). The contents were allowed to mature by stirring for 24 h at room temperature (24 ± 2℃). Afterward, the

hydroxyapatite-activatedseaweed biochar (HSB) was separated from its mother solution by centrifugation and rinsed several times with distilled water. The material was then oven-dried at 70℃ for 2 days and crushed into a fine powder using a mortar and pestle.

3.9 Experimental Setup

3.9.1 Determination of the Influence of Fertilizers on the Soil Fluoride Fractions

To investigate the influence of fertilizer on the forms of fluoride in the soil, the three different fertilizers were mixed with the experimental soil at a laboratory scale for homogeneity. A 100 g sample of fluoride-contaminated soil (39.5 ± 0.5 mg/kg, Ws-F) was thoroughly mixed with 80 mg of DAP or Urea or 500 mg of cow manure based on calculations of Food and Agriculture Organization (FAO) regulations. The samples were then incubated in a shaded area at room temperature (27 ± 2°C) and 70% moisture. The experiment was conducted in a completely randomized design. The blank samples were prepared within each series of sampling and analysis for quality assurance and detection of possible contaminations. The analysis of the amount of Ws-F, Ex-F, Fe/Mn-F, and Or-F on the soil-fertilizer mixtures together with pH was monitored every 30 days for 5 months. For analysis, a small amount of soil was taken, oven-dried at 40 °C then stored in a desiccator.

3.9.2 Determination of the Defluoridation Efficiency of Dried and Fermented Seaweed

The fluoride-containing soil samples (1 kg) were packed into the experimental pots and then mixed thoroughly with either 1.25, 3, or 5% (*w/w*) of either dried seaweed (DSW) or fermented seaweed powder (FSW) equivalent with the control samples labeled 0% in triplicates. Thereafter, the soil was humified to approximately 70 - 75% saturation and incubated in a shaded area, at room temperature (24 ± 3℃). The first soil sample was collected within 24 h of inoculation, and the fluoride fractions, as well as pH, were extracted, measured and quantified. The incubation process continued for 4 months while sampling and analysis were conducted every 30 days. The samples for each amendment was prepared in triplicates and the results are presented as mean values.

3.9.3 Determination of the defluoridation efficiency of Seaweed Biochar (SB) Hydroxyapatite-Activated Seaweed Biochar (HSB)

The natural fluoride-containing soil was used to study the influence of adsorbent dosage,

contact time, and pH on the defluoridation efficiency of the adsorbents. The impact of initial fluoride concentration on HSB defluoridation efficiency was studied by spiking the soil with 25, 50, 75, and 100 mg/L fluorides in form of NaF in order to obtain different fluoride concentrations and incubating for 1 month before the experiment.

In each of the batch experiments, 5 g of the soil sample was mixed with the selected adsorbent dosage, moistened, and incubated for 12 h before the test experiment begins. Five different adsorbents dosages were investigated for soil fluoride lock-off efficiency (0.1, 0.2, 0.3, 0.4, and 0.5 g together with the controls), the kinetic study comprised of 30 min, 1,1.5, 2, and 2.5 h contact time intervals whereas the impact of pH was investigated from (pH 3 - 11) at an interval of 2. All the experiments were conducted in triplicates and the results were reported as mean values.

3.10 Statistical Data Analysis, Quality Assurance and Control

Statistical data analysis was computed using Origin Pro 8.5 software and Excel. For quality assurance, the experiment was conducted in triplicates and two samples were drawn from each replicate for analysis. Values are given as mean ± standard deviation. To calculate the statistical significance levels, ANOVA tests were conducted using XLSTAT followed by Tukey's multiple pairwise comparison tests. Replicates of the samples were used for the ANOVA test, and a significant level of 5% was used in the statistics. For quality control, the soil samples were collected in composite manner to obtain a representative soil sample, and the analytical instruments were calibrated prior quantification.

CHAPTER FOUR

RESULTS AND DISCUSSION

This section presents and discusses the major findings of this study. The major findings of this section include the characterization of the investigated materials, the influence of the investigated materials on the experimental soil properties, defluoridation efficiency, mechanism, and kinetics. The amount of fluoride in the experimental soil reported in this section may vary from objective to objective. This is because it is very unlikely to get the same fluoride concentration in the soil each time you collect the soil samples even though the soils were collected in a composite manner to ensure that the soil obtained is a representative sample. The bioavailable fluoride in this study represents a total of the four extracted fluoride fractions water soluble-fluoride (Ws-F), Exchangeable fluoride (Ex-F), fluoride bound to Iron and manganese (Fe/Mn-F), and organic matter bound fluoride (Or-F). Therefore, bioavailable in this section is equivalent to the extractable fluoride and are bioavailable in an order Ws-F > Ex-F >>Fe/Mn-F>>>Or-F.

4.1 Materials Characterization

4.1.1 Dried Seaweed (DSW) and Fermented Seaweed (FSW)

The properties of interest for dried seaweed (DSW) and fermented seaweed (FSW) for this study are presented by Table 6. During the fermentation process, the anaerobic biomass converts the insoluble high molecular weight organic compounds (HMWOCs) such as polysaccharides, proteins, and lipids which are the main components in the seaweed into soluble low molecular weight organic compounds (LMWOCs) such as monosaccharides, amino acids, and other simple organic compounds which exists as a source of energy and carbon to the other group of micro-organisms (Justo *et al.,* 2016; Plácido & Zhang, 2018). The simple organic acids produced are further assimilated to produce short-chain organic acids like acetic acid, propionic acids, butyric acids, and alcohols which can either be fatty acids (FAs), amino acids, or simple sugars as shown by Equations 20 - 25 (Anukam *et al.,* 2019; Plácido & Zhang, 2018). These processes are accountable for the 0.3 gAc/l TVFAs obtained. The role of fermentation in defluoridation is to increase the number of reaction sites responsible for fluoride adsorption through breaking down the HMWOCs into LMWOCs. One HMWOC can absorb only a number of fluoride ions in a soil solution interface but breaking one HMWOC into several LMWOAs which are unstable and reactive increases its reaction sites and surface

are and hence the number of fluoride ions absorbed.

Table 6: The selected properties of dried seaweed and fermented seaweed

Parameter	DSW	FSW
Carbohydrate	59%	
Lipids	0.9%	
Protein	6.7%	
pH	7	5.9
The fixed carbon	21%	
C	48%	
H	7%	
N	1.12%	
S	0.9%	
Total organic carbon (TOC)	23%	
Moisture	5.98%	
Water absorption (g/g)	2.5	2.7
Total volatile fatty acids concentration (TVFAs) (gAc/l)		0.3
Ash	24%	
Volatile matter content	49%	
phosphorus (P) (mg/kg)		4.1
potassium (K) (mg/kg)		3.7
calcium (Ca) (mg/kg)		14.7
sodium (Na) (mg/kg)		21.0

$$(C_6H_{10}O_5)_n + 2nH_2O \rightarrow nC_6H_{12}O_6 + nH_2O \quad \ldots\ldots\ldots\ldots\ldots\ldots\ldots\ldots\ldots\ldots\ldots\ldots\ldots\ldots\ldots\ldots\ldots\ldots\ldots\ldots (20)$$

$$C_6H_{12}O_6 \rightarrow 2CH_3CH_2OH + 2CO_2 \quad \ldots\ldots\ldots\ldots\ldots\ldots\ldots\ldots\ldots\ldots\ldots\ldots\ldots\ldots\ldots\ldots\ldots\ldots\ldots\ldots\ldots (21)$$

$$C_6H_{12}O_6 + 2H_2 \rightarrow 2CH_3CH_2COOH + 2H_2O \quad \ldots\ldots\ldots\ldots\ldots\ldots\ldots\ldots\ldots\ldots\ldots\ldots\ldots\ldots\ldots\ldots\ldots\ldots\ldots\ldots\ldots (22)$$

$$CH_3CH_2COOH + 3H_2O \rightarrow CH_3COOH + CO_3^- + 4H_2 \quad (23)$$

$$C_6H_{12}O_6 + 2H_2O \rightarrow 2CH_3COOH + 2CO_2 + 4H_2 \quad (24)$$

$$CH_3CH_2OH + H_2O \rightarrow CH_3COOH + 2H_2 \quad (25)$$

The use of iodoform prohibited the acetic acid conversion (Equations 26 - 28) into methane but promoted the accumulation of the evidenced TVFAs as reported by Jung *et al.,* (Jung *et al.,* 2015).

$$CH_3COOH \rightarrow CH_4 + CO_2 \quad (26)$$

$$CO_2 + 4H_2 \rightarrow CH_4 + 2H_2O \quad (27)$$

$$2CH_3CH_2OH + 2CO_2 \rightarrow 2CH_3COOH + 0.5O_2 \quad (28)$$

4.1.2 Seaweed Biochar (SB) and Hydroxyapatite-Activated Seaweed Biochar (HSB)

The moisture, ash, and volatile matter content of the seaweed (DSW) was 5.98 ± 1%, 24.3 ± 1%, and 49.1 ± 2% compared to its biochar (SB) which was 0.9 ± 0.3%, 22.9 ± 1%, and 32 ± 2%, respectively. The moisture, ash, and volatile matter of SB biochar decreased compared to dried seaweed matter which is crucial for increasing the absorption surface area of the biochar. The amount of fixed carbon, C, H, N, S and O for seaweed was 19.3 ± 4, 48.2 ± 1%, 7 ± 0%, 1.1 ± 0%, 0.9 ± 0%, and 41 ± 2% whereas that for SB was 43.7 ± 1, 56.2 ± 2%, 6 ± 1%, 1.2 ± 0%, 1.3 ± 0%, 21 ± 2%, respectively. Both seaweed and its biochar had high contents of C and O but the carbonization process lead to an increment of C and a decrement of oxygen (O). The increment in carbon is influenced by the pyrolysis process which leads to a more concentrated carbon material whereas a decrement of oxygen highlights the presence of aromatic compounds in the seaweed. Therefore, these results suggest that pyrolysis concentrates the amount of carbon in the seaweed leading to an increment in the adsorption active sites.

The XRD patterns of SB, and HSB, are shown in Fig. 7. The SB represented by a black line is branded by a significant amount of amorphous materials and crystalline peaks of calcite ($CaCO_3$) at 23°, 29°, 36°, 40°,43.5°,48°, and 49° *2θ*, quartz (SiO_2) at 21° and 26.5° *2θ* and calcium hydroxide ($Ca(OH)_2$) at 34° *2θ*. Activation to HSB represented by a red line, reveals additional peaks to the SB at 31° – 35° *2θ*. The additional peaks observed match the hydroxyapatite ($Ca_5(PO_4)_3(OH)_2$) peaks produced during the addition of diammonium

phosphate ($(NH_4)_2PO_4$) and calcium nitrate ($Ca(NO_3)_2$) into the SB and therefore confirms the formation of hydroxyapatite in the adsorbent. The width of the peaks suggests that the attached hydroxyapatite in the SB has a small crystallite size (10 *nm*). But there was no noticeable alteration of the XRD pattern of HSB after treatment with the fluoride soil solution and these results are coincidental with results reported by Díaz-Nava *et al.* (2002). The XRD pattern of HSB did not change after fluoride adsorption showing that meaning fluoride ion exchanges with the OH^- in the hydroxyapatite rather than in its crystal lattice.

The SEM micrographs of SB and HSB at 50.0 μm are presented in Fig. 8 (a) and 8 (b), respectively. The figures demonstrate that the hydroxyapatite attaches itself to the surface of SB and constitutes rod - like structures. The elemental composition of SB was observed to change after activation with the hydroxyapatite where HSB displayed an extended concentration of Ca and P compared to the rest of the elements projecting a shift in the weight (%) of the elements within the adsorbent.

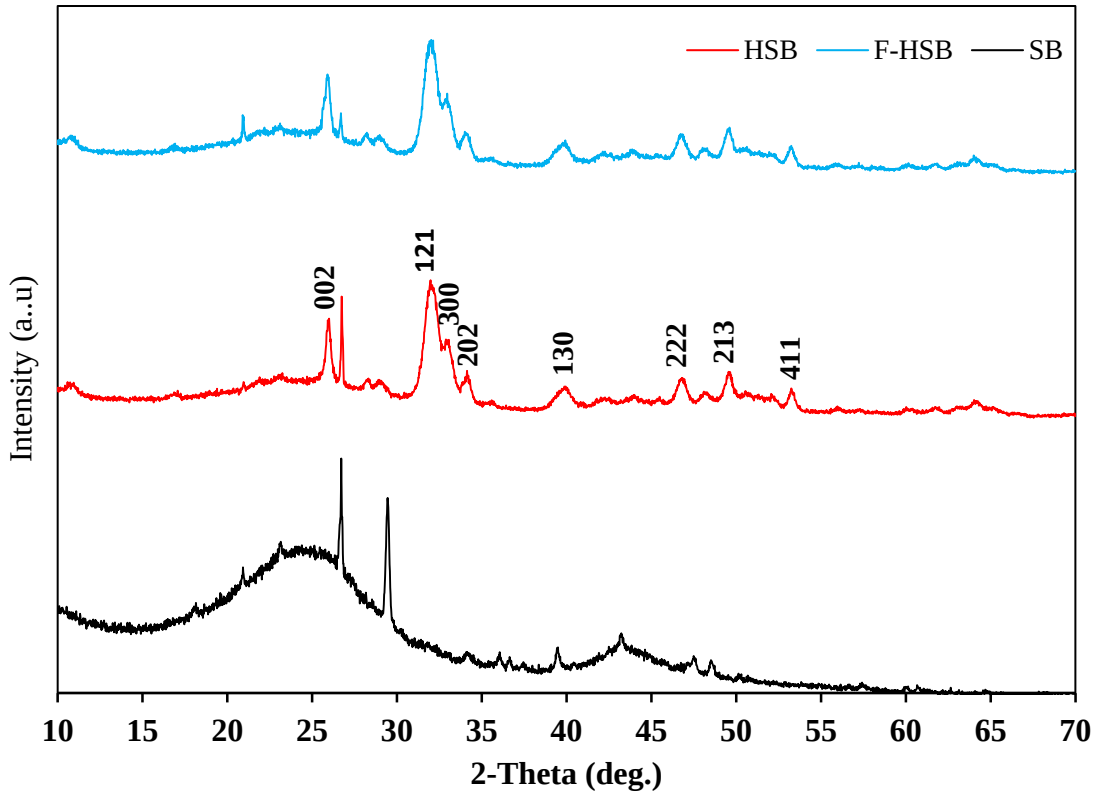

Figure 7: The XRD pattern for seaweed biochar (SB), hydroxyapatite-activated seaweed biochar (HSB), and fluoride-treated HSB (F-HSB) conforming the formation of hydroxyapatite and its resemblance succeeding fluoride adsorption

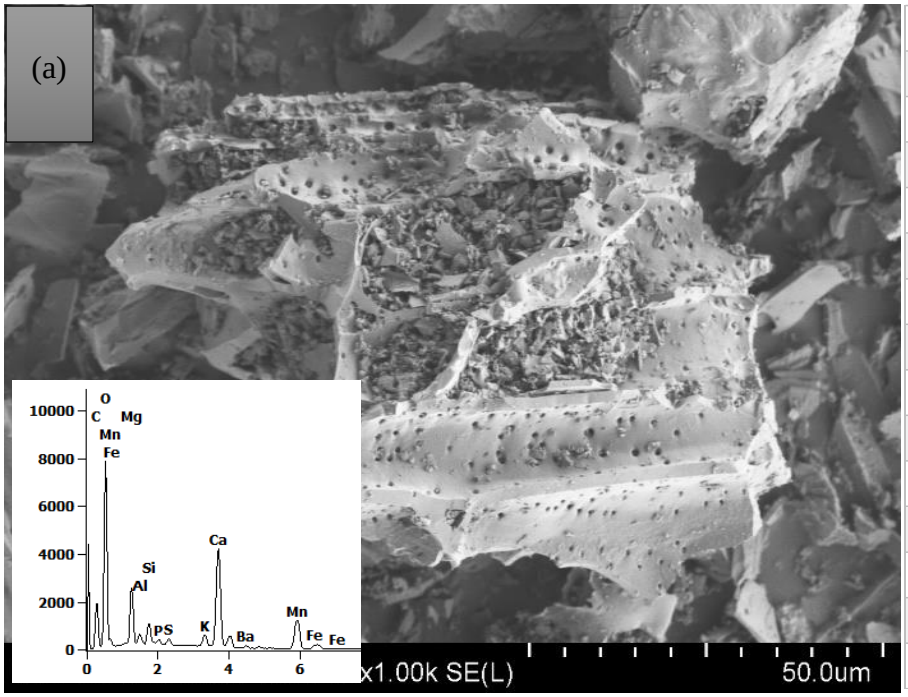

Element	Wt%
C	87.11
O	10.69
Na	0.12
Mg	0.14
Al	0.23
Si	0.24
P	0.06
S	0.24
K	0.52
Ca	0.49
Mn	0.04
Fe	0.04
Cu	0.09
Total	100.00

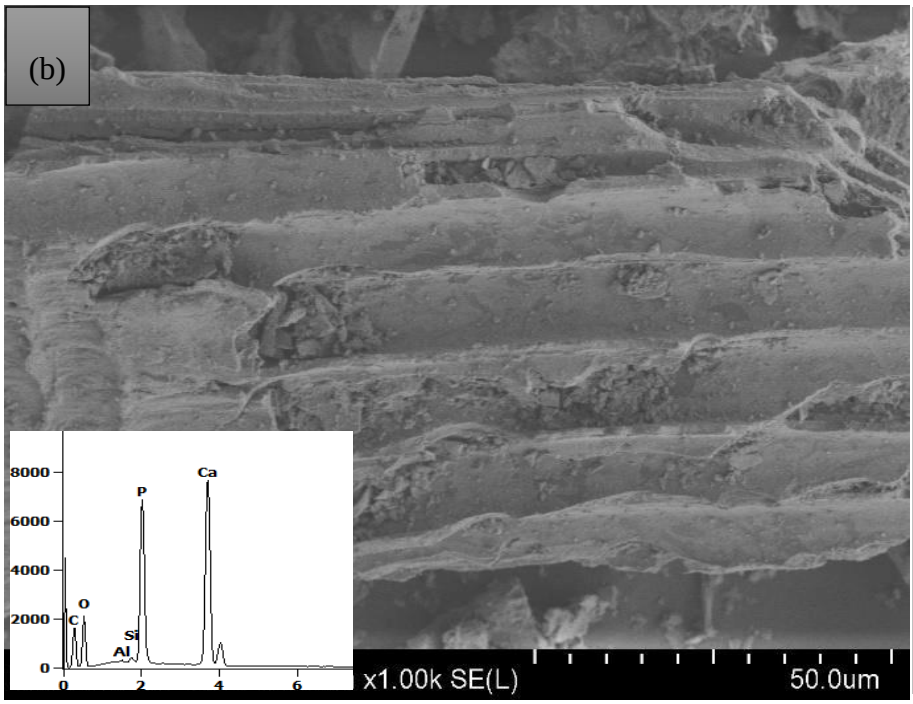

Element	Wt%
C	78.57
O	15.68
Na	0.15
Al	1.16
Si	0.13
P	1.12
S	0.26
K	0.04
Ca	2.71
Fe	0.02
Cu	0.17
Total	100.00

Figure 8: The SEM micrograph and EDX spectra for (a) seaweed biochar (SB), and (b) Hydroxyapatite activated seaweed biochar (HSB) at 50.0 µm

Furthermore, Fig. 9 shows EDX analysis showing the distribution of Carbon (C), phosphorus (P), and calcium (Ca) in both SB and HSB. Both EDX spectra present high C enrichment as seaweed is a carbon-based material but in contrast to SB, the HSB spectra present a substantial enrichment of P and Ca which are the main components of the hydroxyapatite suggesting its presence in high concentration in the fabricated HSB material.

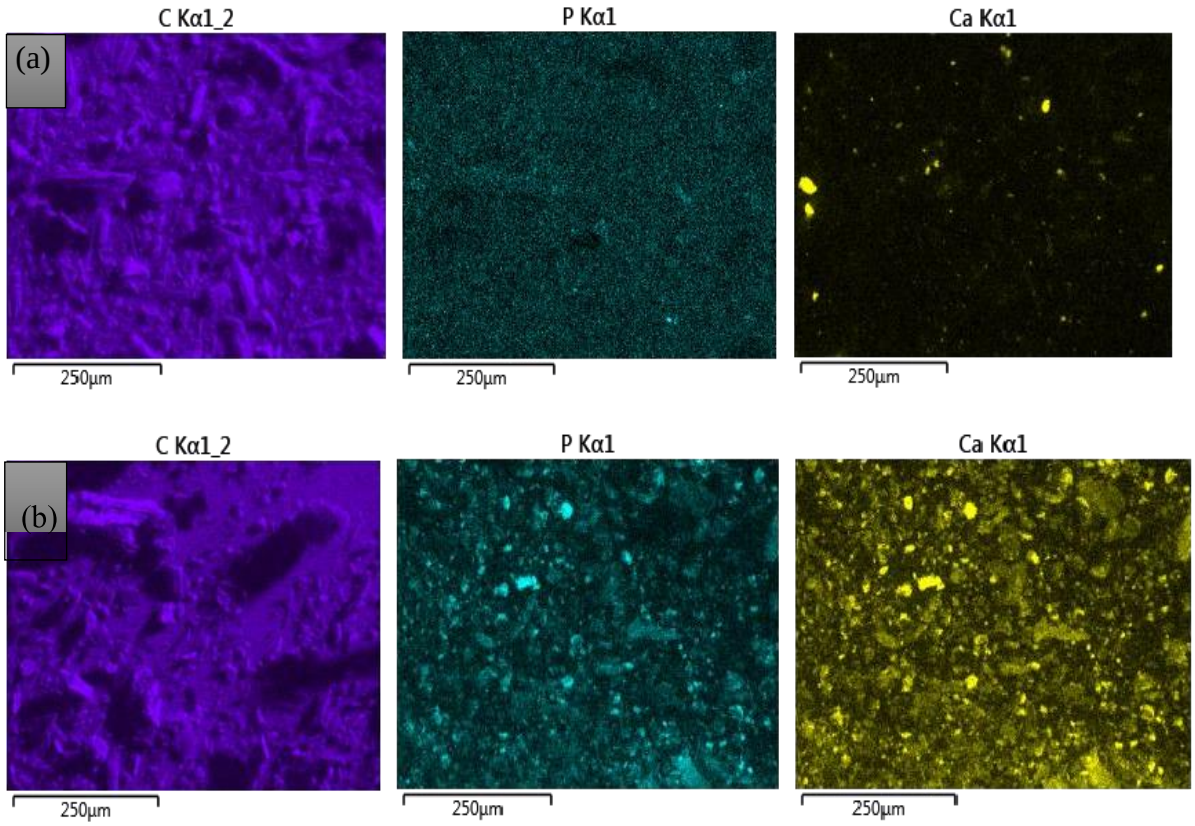

Figure 9: The EDX maps showing the spatial distribution of phosphorus and calcium in the (a) seaweed biochar before activation (SB) and (b) seaweed biochar post activation with the hydroxyapatite (HSB)

4.1.3 Fluoride Quantification in the Experimental Soil, Fertilizers and Seaweed

The availability, mobility, and toxicity of fluoride to plants and animals is not a function of Tot-F but the form in which it exists (Loganathan *et al.,* 2001). The soil had an average Tot-F of 422 ± 52.9 mg/kg. The bioavailable forms of fluoride present in the experimental soil were additionally extracted sequentially and found Ws-F of 39.5 ± 0.5 mg/kg which was the major quantity extracted followed by Or-F (9.1 ± 2.1 mg/kg), then Ex-F (3.5 ± 0.5 mg/kg), the minutest being Fe/Mn-F (3.1 ± 1.0 mg/kg). The extracted bioavailable fluoride fractions accounted for 13.5% of the Tot-F whereas 86.5% remains quantified as the residual amount (Res-F).

Moreover, the amount of fluoride in the seaweed material used for the study was quantified and DSW was found to contain 8 ± 2 mg/kg fluoride. This amount of fluoride could not be detected in either fermented seaweed (FSW) or seaweed-derived biochar (SB) as well as in the hydroxyapatite-activated seaweed biochar (HSB) and therefore further studies on the influence of fermentation and pyrolysis processes on fluoride concentration is recommended.

The amounts of forms of fluoride existing in fertilizers is presented in Table 7. There was a statistically significant difference ($p<0.05$) in the amount of all fluoride fractions in the fertilizers (Appendix 2). DAP had the highest concentration in all extracted fluoride fractions, followed by manure, whereas Urea displayed the least. The Ws-F concentration was 1.5 ± 0.1 mg/kg for Urea, 2.4 ± 0.5 g/kg for DAP, and 8.2 ± 1.9 mg/kg for manure. While other forms of fluoride were minimal (< 0.5 mg/kg) in Urea, manure contained 1.9 ± 1, 6.8 ± 0.4, 6.1 ± 0.6 mg/kg, and DAP, 52.8 ± 19.7, 370 ± 22.5 and 570 ± 44.0 mg/kg; Ex-F, Fe/Mn-F and Or-F, respectively.

Table 7: The quantity of fluoride fractions in the three commonly used fertilizers along the slopes of Mount Meru

Fertilizers	Tot-F (mg/kg)	Ws-F (mg/kg)	Ex-F (mg/kg)	Fe/Mn-F (mg/kg)	Or-F (mg/kg)
DAP	8,760 ± 246	2,410 ± 53.3	52.8 ± 19.7	370 ± 22.5	570 ± 44
Manure	98 ± 7	8.2 ± 1.9	1.92 ± 1	6.8 ± 0.43	6.12 ± 0.6
Urea	1.98 ± 0.9	1.5 ± 0.12	0.27 ± 0.1	N/A	N/A

The amount of the bioavailable fraction in the experimental soil was high enough to be absorbed by the plant roots and disseminated into the water in significant quantities enough to lead to fluorosis (FAO, 2003; Loganathan *et al.,* 2001). Each of the fluoride fractions exhibits an exceptional behavior dictated by factors such as; the place it is attached, human activities, soil properties, and the climate of the area (Arnesen, 1997; Zhao *et al.,* 2015).

The high fluoride concentration detected in the DAP fertilizer is principal since it is derived from phosphate rock. Phosphate-rock is known to contain fluorapatite ($Ca_5(PO_4)_3F$) and fluorite (CaF_2) (Loganathan *et al.,* 2001; O'hara *et al.,* 1982). DAP fertilizer is manufactured by a wet process through a reaction between ammonia and phosphoric acid (Equations 29 and 31). During this process, fluoride is lost into the atmosphere as HF, but some of it precipitates as CaF_2 (Equation 30) and remains in the fertilizer accounting for 2 - 3% of the phosphate-fertilizer (Ramteke *et al.,* 2018). The 2 - 3% CaF_2 introduced into the soil as Ex-F each time the phosphate-fertilizer is applied into agricultural soils which depending on the soil properties is converted to Ws-F as NaF, and SiF_4. Conversely, most of the HF does not escape into the atmosphere but deposited back into the fertilizer as the Ws-F.

$$Ca_5(PO_4)_3F + 5H_2SO_4 \rightarrow 3H_3PO_4 + 5CaSO_4 + HF \quad \ldots\ldots\ldots\ldots\ldots\ldots\ldots\ldots\ldots\ldots\ldots\ldots (29)$$

$$Ca^{2+} + 2HF \rightarrow CaF_2 + 2H^+ \ldots \ldots (30)$$

$$2NH_3 + H_3PO_4 \rightarrow (NH_4)_2HPO_4 \ldots \ldots (31)$$

Inversely, the existence of fluoride fractions in the manure used for this study, demonstrates the fluoride exposure to herbivorous in the contaminated area. The exposure footpaths to the animals is through grazing, soil ingestion, and/or drinking water (Hong *et al.,* 2016). Apart from water, exposure through grazing is minimal compared to direct soil ingestion (Cronin *et al.,* 2000). Acute fluorosis has been observed in domestic animals after immediate ingestion of fodder containing fluoride levels higher than 3000 mg/kg (O'hara *et al.,* 1982). Even further, deaths have been observed due to the ingestion of fluoride-containing volcanic ash dumped on pastures (Cronin *et al.,* 2003).

4.2 Soil Properties

4.2.1 General Soil Properties

The average values of the selected soil properties are presented in Table 8. The studied soil properties were targeted based on their known influence on fluoride behavior. The soil properties observed are in concordance with those obtained by Rizzu *et al.* (2020b) who used the same agricultural soil to investigate fluoride uptake by maize and bean plants (Rizzu *et al.,* 2020b). The soil is characterized as sandy loam with a Tot-F concentration of 422 ± 52.9 mg/kg and Ws-F of one order magnitude less thus very likely to cause toxicity to fluoride-sensitive plants and animals in the area. The pH of the experimental soil is strong alkaline and has a high concentration of exchangeable sodium as compared to the rest of the exchangeable bases. The quantity of sand in the experimental soil was also found to exceed 50% of other soil texture parameters. The extent of fluoride in this soil is linked to numerous soil properties (Rizzu *et al.,* 2020b). But, fluoride in the experimental soil could be associated with exchangeable sodium percentage (ESP), clay content, pH, irrigation, and contamination from long-term use of phosphate fertilizers.

The properties of the experimental soil after amendment with DSW and FSW are presented in Tables 9 and 10. The impact of DSW and FSW on the soil properties appeared to follow a similar pattern but at different efficiencies. Both amendments led to an increment in the water retention capacity, CEC, and SOM of the experimental soil which could be accounted to the decomposition process of organic matter. This increment observed was directly related to the

amendment dosages. The amendments were observed to decrease soil pH but had no statistically significant influence on the quantity of phosphorus in the soil.

Table 8: The selected soil properties of the experimental soil

Property	Quantity
CEC (meq/100g)	15.6
Clay (%)	6.4
Silt ((%)	18.2
Sand (%)	75.4
Ca^{2+} (mg/kg)	34 ± 8
Mg^{2+} (mg/kg)	7 ± 2
K^{+} (mg/kg)	98 ± 22
Na^{+} (mg/kg)	317 ± 102
PO_4^{3-}(mg/kg)	17.2 ± 3
ESP (%)	69.5 ± 9
O.M (g/kg)	11.2 ± 4
EC (µS/cm)	408.6 ± 13
Water retention (gH_2O/g soil)	0.02 ± 0.1
pH (H_2O)	9.3 ± 0.3

The pH drop observed was through the ionization of the organic compounds, HMWOC in DSW and LMWOC in FSW. Once the organic compounds are introduced into the alkaline soil (high pH) they become deprotonated loosing H^{+} into the soil solution interface. The released H^{+}reacts with OH^{-} to form H_2O (Mittal *et al.,* 2020). This reaction reduces the number of OH^{-} in the soil solution interface which inturn reduces the pH of the soil and increases the water retention capacity of the soil.

Table 9: The influence of dried seaweed (DSW) amendment dosage (%, *w/w*) on the experimental soil to the target soil properties at the 120th day

Soil Property	Initial	0%	1.25%	3%	5%
Water retention (gH_2O/g soil)	0.02 ± 0.1	0.02 ± 0.1	0.1 ± 0.1	0.27 ± 0.1	0.4 ± 0.1
CEC (meq/100g)	32.8 ± 0.9	30.5 ± 0.5	37.0 ± 1.4	37.1 ± 1.4	44 ± 3.1
PO_4^{3-}(mg/kg)	17.2 ± 0.4	15.8 ± 2	11.9 ± 3.3	10.2 ± 1.6	16.4 ± 3.9
EC (µS/cm)	453 ± 3	451 ± 2	440 ± 5	442 ± 4	432 ± 4
SOM (%)	2.5 ± 0.1	2.6 ± 0.4	2.7 ± 0.2	3.4 ± 0.3	3.8 ± 0.4

The protonated HMWOCs and LMWOCs in the soil solution interface becomes negatively charged ($R-COO^-$) and ($R-O^-$). Its existance as negatively charged ins in the soil leads to an increment in the cation exchange capacity of the soil (CEC). But once it interacts and reacts with the soil cations to attain stability it reduces the electric conductivity (EC) of the soil as observed. The seaweed materials also contains a significant amount of cations and anions which participate in a number of beneficial reactions with the soil solid phase (Cahyaningtyas *et al.,* 2021; Sharma *et al.,* 2014).

The LMWOAs plays an important role in the chemical, physical and biological properties of the rhizosphere (Ma *et al.,* 2021). It accelerates the bioavailability of carbon and micronutrients in the rhizosphere for plant utilization. Although the soil is capable of converting HMWOCs to LMWOCs, this process is fairly slow and could last long (Chew *et al.,* 2019; Craigie, 2011). Therefore, the fermentation process fuels this conversion thus speeding up the action of organic fertilizer in the soil (Krishnamoorthy & Malek, 2022).

Table 10: The influence of fermented seaweed (FSW) amendment dosage (%, *w/w*) to the experimental soil on selected soil properties at the 120th day

Soil Property	Initial	0%	1.25%	3%	5%
Water retention (gH_2O/g soil)	0.02 ± 0.1	0.02 ± 0.1	0.06 ± 0.1	0.17 ± 0.1	0.23 ± 0.1
CEC (meq/100g)	32.8 ± 0.9	30.5 ± 0.5	34.5 ± 1.7	35.3 ± 1.7	37 ± 1.3
PO_4^{3-} (mg/kg)	17.2 ± 0.4	15.8 ± 2	12.5 ± 0.4	14.0 ± 0.9	16.4 ± 0.8
EC (µs/cm)	453.9± 2.3	451 ± 1.6	444 ± 1.3	443 ± 0.4	440 ± 2
SOM (%)	2.5 ± 0.1	2.6 ± 0.4	3.5 ± 0.6	4.2 ± 0.3	5.4 ± 0.3

4.2.2 Soil pH

(i) Fertilizers and soil pH

Table 11 presents the influence of fertilizers on the pH of the soil. The pH is identified to affect most of the soil's biogeochemical characteristics. It pedals the interaction, translocation, transformation, and fate of diverse elements in the soil together with contaminants. It is therefore the architect behind the behavior of soil components and thereby properties of many soils (Minasny *et al.,* 2016). There was a significant difference ($p<0.05$) in the influence of the three fertilizers on the soil pH (Appendix 3). The pH change exhibited a slight positive correlation with the control (r = 0.31) and manure (r = 0.38), a weak positive with DAP (r = 0.19), and a strong negative correlation with Urea (r = -0.88) articulating the relationship between a specific fertilizer and the soil pH change.

Table 11: The influence of fertilizers on soil pH

Day	Control	DAP	Urea	Manure
0	9.3 ± 0.1	9.3 ± 0.1	9.3 ± 0.1	9.3 ± 0.1
30	9.1 ± 0.3	8.0 ± 0.3	8.8 ± 0.3	9.7 ± 0.3
60	9.6 ± 0.04	9.3 ± 0.5	8.8 ± 0.3	9.6 ± 0.0
90	9.4 ± 0.0	8.9 ± 0.2	9.6 ± 0.2	9.8 ± 0.1
120	9.3 ± 0.2	9.2 ± 0.3	9.3 ± 0.3	9.5 ± 0.2
150	9.3 ± 0.2	9.3 ± 0.2	9.4 ± 0.2	9.6 ± 0.3

In the soil, Urea liquifies and releases ammonium which rises the soil pH promoting an alkaline condition (in the first 14 days). Depending on the soil microbial activity, the released ammonium starts to progressively convert into nitrate through nitrification process ensuing consequent acidification observed by day 30 - 60 (Equations 32 - 35). Over time, ammonia-nitrogen is formed and is lost into the atmosphere through the ammonia volatilization process (Equation 36), this results in the pH rise observed on the 90th day attaining stability through 150th day (Ernst & Massey, 1960).

$$NH_2CONH_2 + 2H_2O \rightarrow (NH_4)_2CO_3 \quad (32)$$

$$(NH_4)_2CO_3 + H_2O \rightarrow 2NH_3 + CO_2 + 2H_2O \quad (33)$$

$$(NH_4)_2CO_3 + 3O_2 \rightarrow 2NO_2^- + CO_2 + 2H^+ + 3H_2O \ldots\ldots\ldots\ldots\ldots\ldots\ldots\ldots\ldots\ldots\ldots (34)$$

$$NO_2^- + 0.5O_2 \rightarrow NO_3^- \ldots\ldots\ldots\ldots\ldots\ldots\ldots\ldots\ldots\ldots\ldots\ldots\ldots\ldots\ldots\ldots\ldots\ldots\ldots\ldots\ldots\ldots\ldots\ldots (35)$$

$$2NO_3^- + 6C + 2H_2O + 2e^- \rightarrow N_2 + 4HCO^- + 2CO_2 \ldots\ldots\ldots\ldots\ldots\ldots\ldots\ldots\ldots\ldots\ldots (36)$$

While nitrogen undertakes revolutions in Equations 32 - 35, phosphorus similarly undergoes its chain of transitions in Equations 37 - 39. In the soil, Phosphorus pent-oxide dissociates into phosphoric acid which is its temporal transitional product. The formation of phosphoric acid lowers the soil's pH (day 30) before its disintegration into hydrogen and phosphate ions (McCann, 1953). The two ions are additionally neutralized by the OH^- from the soil solution interface endorsing the pH rise again observed from day 60 through day 150.

$$(NH_4)_2HPO_4 \rightleftharpoons NH_3 + (NH_4)H_2PO_4 \ldots\ldots\ldots\ldots\ldots\ldots\ldots\ldots\ldots\ldots\ldots\ldots\ldots\ldots\ldots\ldots\ldots (37)$$

$$(NH_4)H_2PO_4 \rightleftharpoons NH_4^+ + H_2PO_4 + e^- \ldots\ldots\ldots\ldots\ldots\ldots\ldots\ldots\ldots\ldots\ldots\ldots\ldots\ldots\ldots\ldots\ldots (38)$$

$$H_2PO_4 \rightleftharpoons PO_4^- + 2H^+ + e^- \ldots\ldots\ldots\ldots\ldots\ldots\ldots\ldots\ldots\ldots\ldots\ldots\ldots\ldots\ldots\ldots\ldots\ldots\ldots\ldots (39)$$

(ii) The influence of DSW and FSW on the soil pH

The influence of DSW and FSW on the pH of the soil is presented in Fig. 10 (a) and Fig. 10 (b), respectively. Within first 30 days of incubation, there was no pH change in the control samples however by the 60th day the pH dropped to 8.9 and remained fairly persistent thereafter but here was a significant difference in pH (*p<0.05*) between the treatments (both DSW and FSW) and the control samples (Appendix 4). The pH drop among DSW dosages was statistically noticeable (*p>0.05*) between day 30th and 60th then remained unnoticeable throughout the experiment (120th day) where pH reduced from 9.3 ± 0.3 to 7.5 ± 0.2, 7.3 ± 0.2 and 6.9 ± 0.3 following the 1.25, 3, and 5% amendment, respectively. While FSW exhibited the same behavior as that of DSW, yet its amendment within the first 24 h clear-cut the pH from 9.3 ± 0.3 to 9.1 ± 0.2, 9.0 ± 0.1, and 8.4 ± 0 and sustained a drop from 9.3 ± 0.3 to 7.8 ± 0.1, 7.4 ± 0.1 and 7.0 ± 0.0 by the 120th day, following, 1.25, 3, and 5% FSW amendment dosages, respectively. Even though the pH midst treatments were significantly different (*p<0.05*), the 3 and 5% amendments were not statistically different (*p>0.05*) throughout the experiment.

The pH drop observed was through the ionization of the organic compounds, HMWOC in DSW

and LMWOC in FSW. Once the organic compounds are introduced into the alkaline soil (high pH) they become deprotonated loosing H^+ into the soil solution interface. The released H^+reacts with OH^- to form H_2O (Mittal *et al.,* 2020). This reaction reduces the number of OH^- in the soil solution interface which inturn reduces the pH of the soil and increases the water retention capacity of the soil.

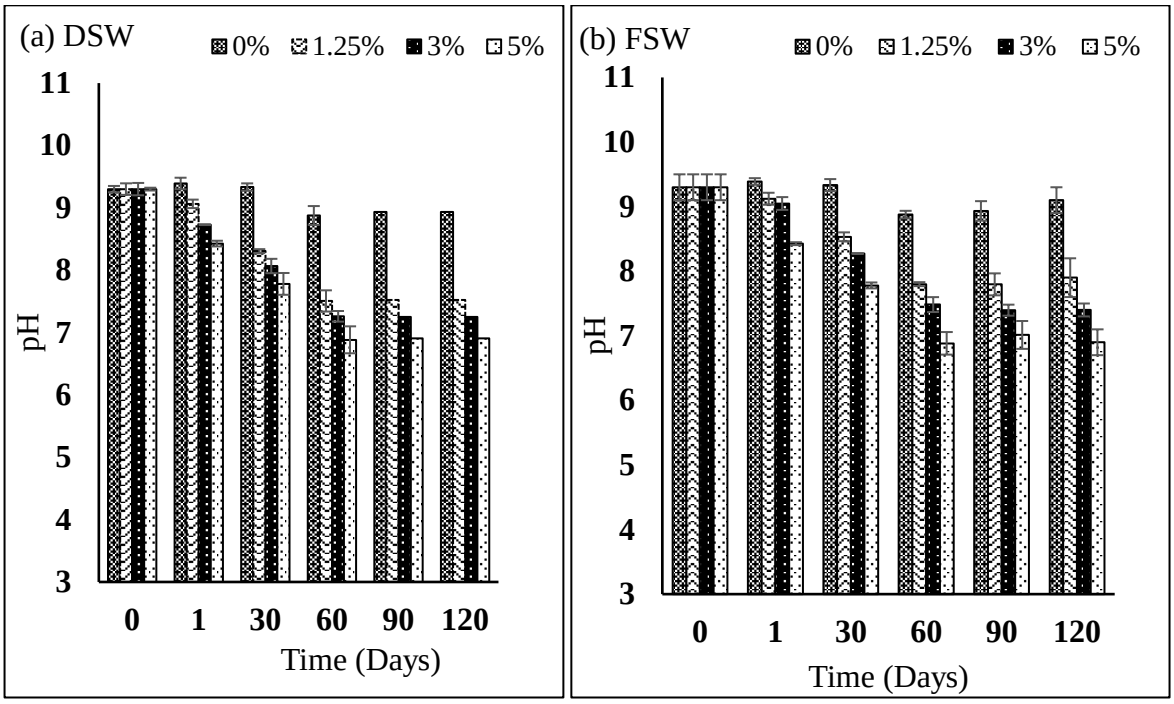

Figure 10 : (a) The impact of dried seaweed (DSW) amendment on soil pH, (b) The impact of fermented seaweed (FSW) on soil pH. Both studied every 30 days for 120 days at different amendment dosages

(iii) The influence of SB and HSB on the soil pH

Since the defluoridation efficiency of seaweed biochar derived (SB) was selective, its impact on soil pH was not studied but the impact of its fabricated HSB on the soil pH was studied and the results are presented in Fig. 11 (a). The influence of HSB on the soil pH was studied at 5 different soil pH values (3, 5, 7, 9, and 11). The findings on its impact on the soil pH were found to relate to its point-zero-charge (pH_{PZC}). The pH_{PZC} of HSB was 7.4 which means at this pH, HSB exists as a neutral material. Once HSB is introduced into a soil solution interface with a pH < pH_{PZC} the HSB will be protonated attracting the H^+in the soil thus rising the soil pH to create a new equilibrium of the soil solution. Conversely, when the pH of the soil > pH_{PZC}, HSB becomes deprotonated attracting the OH^- in the soil thereby lowering the soil pH as it creates a new equilibrium pH (Qiu *et al.,* 2020).

The impact of the soil pH on the defluoridation efficiency of seaweed biochar (SB) and hydroxyapatite-seaweed biochar (HSB) was further investigated employing five different pH values (3, 5, 7, 9, and 11) and the results are presented in Fig. 11 (b). The pH of the soil solution had a significantly higher influence on the defluoridation efficiency of SB as compared to its HSB. The maximum defluoridation efficiency of SB was noticed at pH 5 which was 37.7% and dropped abruptly to 8.4% at pH 7 hitting 0% at pH 9 and 3 and 10.2% at pH 11. Whereas the defluoridation efficiency of HSB was at its peak at pH 7 (65.5%), decreasing in an order 5 (65.2%), > 3 (53.8%), > 9 (49%), and > pH 11 (37.7%) indicating a significant improvement from its corresponding SB. The defluoridation behavior manifested by SB was analogous to the behavior of hydrous zirconium oxide which dropped from 12 mg/g at pH 5 to 2.7 mg/g at pH 7 to 0 mg/g at pH 9 (Das *et al.,* 2003).

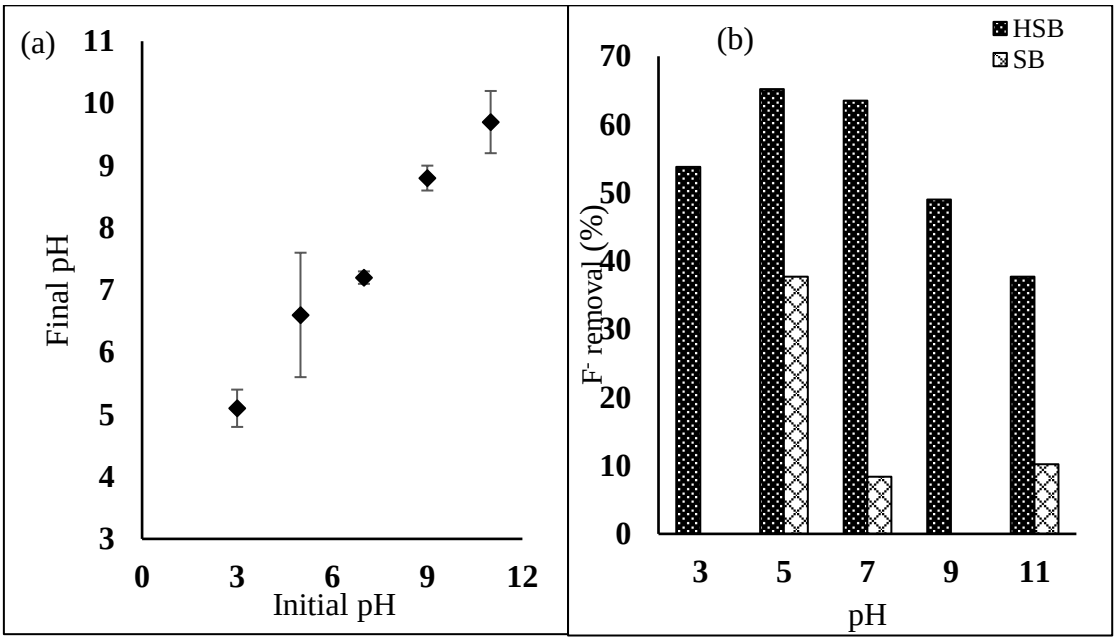

Figure 11: (a) The influence of HSB on the soil pH (b) The impact of pH on the defluoridation efficiency of seaweed biochar (SB) and hydroxyapatite-activated seaweed biochar (HSB) at an initial fluoride concentration of 103 ± 3.6 mg/kg, 0.2 g adsorbent dosages and contact time of 1 h

The observed fluoride adsorption by SB is non-specific, such that, its adsorption process is dependent on pH (Wambu & Kurui, 2018). At pH 3 fluoride could not be adsorbed because it exists mainly as HF. The soil is known to strongly adsorb fluoride at pH 5.5 - 6.5 and this together with the pH_{PZC} of SB which is 6.5 could have contributed to high fluoride adsorption observed at pH 5 (Hong *et al.,* 2016). At pH 7 adsorption is through ion-dipole-bonding and at pH 11 the concentration of OH^- in the interface is high and therefore fluoride adsorption into the SB is mainly through physisorption (Qiu *et al.,* 2020).

On the contrary, HSB exhibits both specific and nonspecific fluoride adsorption. Specific fluoride adsorption is observed through ion-exchange between F^- and OH^- in the hydroxyapatite, and the precipitation reaction between F^- and Ca^{2+} released from the dissolution of hydroxyapatite (Wambu & Kurui, 2018). At pH 4 – 12, hydroxyapatite exists as a stable calcium phosphate salt and therefore its OH^- can easily be exchanged with the soil anions. Although the soil solution encompasses a significant number of anions such as nitrate, sulfate, phosphate, and chlorides, hydroxyapatite displays selective adsorption towards the fluoride ions because the ionic radii of F^- (1.33 Å) are closer to that of OH^- (1.37 Å) and exchanges with fluoride to easily attain the stability of hydroxyapatite in form of fluorapatite ($Ca_5(PO_4)_3F$) which is insoluble, stronger, and tougher. The non-specific adsorption is observed in the SB active sites which were not attached with hydroxyapatite (Valdivieso *et al.,* 2006).

4.2.3 Microbial Community

Figures 12 and 13 present the influence of DSW and FSW amendment on (a) Bacteria, (b) Fungi, and (c) Actinomycetes. The soils treated with DSW and FSW revealed significantly higher quantities of bacteria as compared to those found in the control group. There was a statistically significant difference ($p<0.05$) in the number of bacteria cells between the control plates and the amendments as well as between individual amendments. While the amendment of 1.25% DSW led to a decrement in the number of bacteria by a factor of 0.62, the dosages of 3 and 5% led to an increase by a factor of 2.19 and 3.22, respectively. The DSW also increased the number of fungi by factors, 1.38, 1.54, and 2.23, which was following 1.25, 3, and 5% amendments, respectively. Moreover, the number of actinomycetes cells in 1.25 and 5% amendments was less by factors 0.56 and 0.87 compared to that in the control plate whereas, in 3 % amendment, an increment by a factor of 1.61 was observed.

The number of bacteria increased by a factor of 1 ± 7.2, 1.9 ± 4.3, 3.0 ± 9.0, following, 1.25, 3, and 5%, FSW amendment dosage, respectively. The addition of 5% FSW, was also observed to increase the amount of fungus in the soil by a factor of 1.6 ± 9.9 whereas, 3 and 1.25% amendments did not reveal a statistically significant difference ($p>0.05$) to that of the control. Moreover, while 3% FSW reduced the number of actinomycetes by a factor of 1.3 ± 8, the 5% FSW increased its number by 1.7 ± 17 and there was no significant difference ($p>0.05$) on the impact of 1.25% amendment dosage to that of the control.

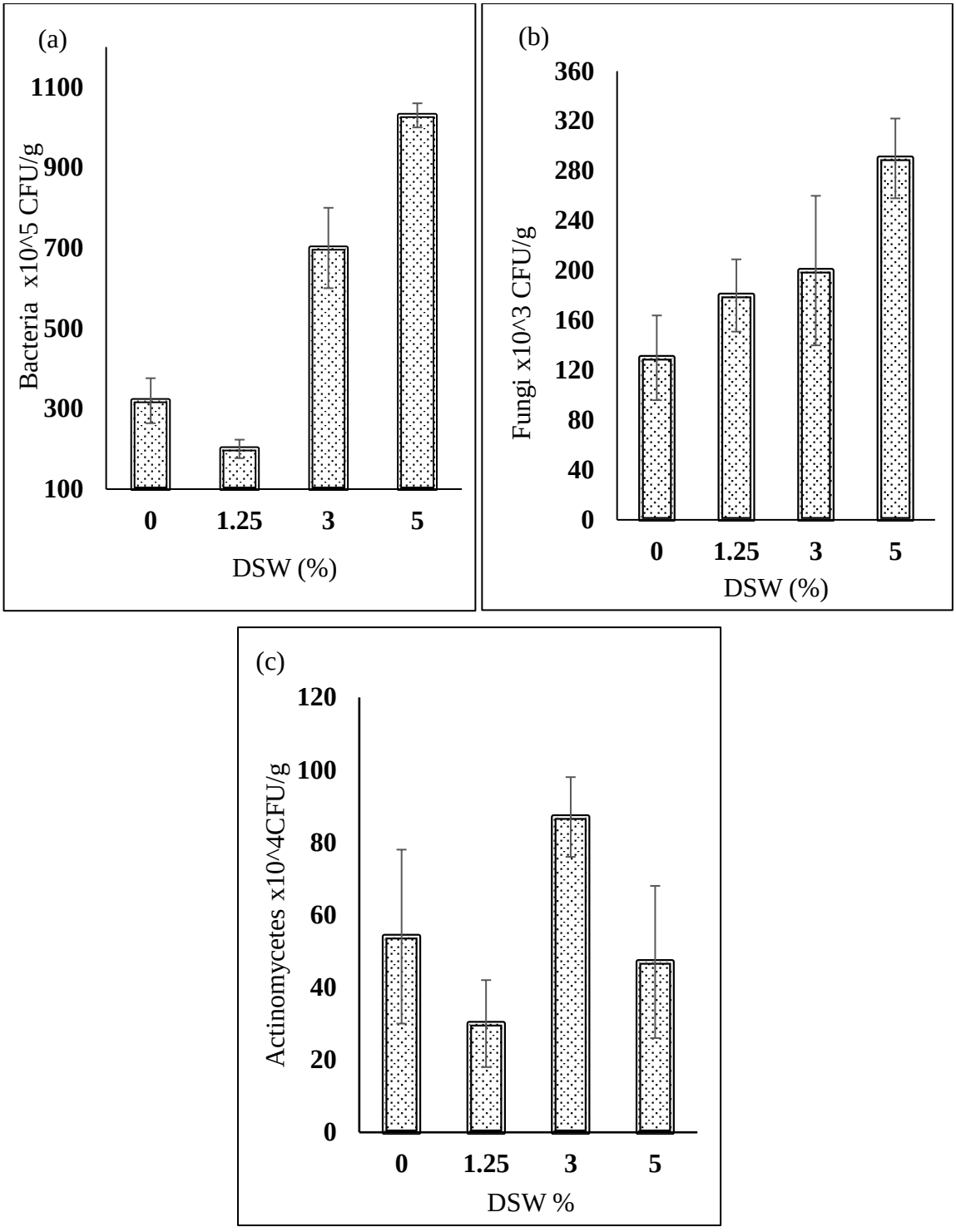

Figure 12: The Impact of Amendment of Different Concentrations of dried seaweed (DSW) on Microbial Quantity on the Soil (a) Bacteria, (b) Fungi (c) Actinomycetes

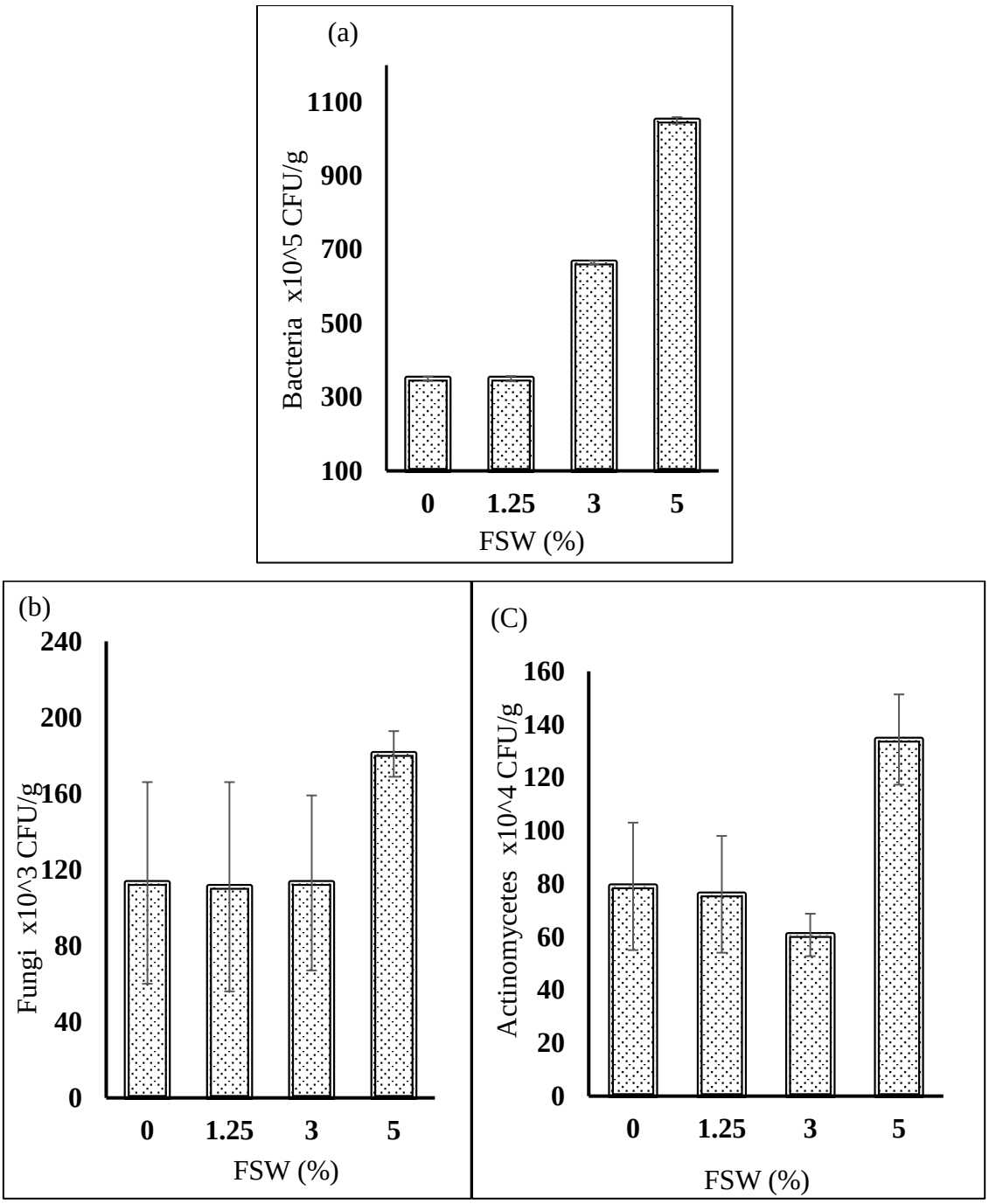

Figure 13: The Impact of Amendment of different concentrations of the fermented seaweed (FSW) on microbial quantity on the Soil (a) bacteria, (b) fungi (c) actinomycetes

4.3 Fluoride Adsorption

4.3.1 The Influence of Fertilizers on Soil Fluoride Adsorption and Release

The dynamics of the fractions of fluoride in the soil after adding fertilizers are presented in Fig. 14. Supplementing the soil with the fertilizers contributed to a rise in the average amount of

Ws-F from 39.5 ± 0.5 to 42.7 ± 2.0, 46.4 ± 2.6, and 48.2 ± 3.2 mg/kg for Urea, DAP, and manure, respectively, whereas in the control this amount reduced to 38.6 ± 1.7 mg/kg over 150 days. There was a significant difference ($p<0.05$) between the influence of the three fertilizer-amended soils and the control on the increase of Ws-F in the soil. The difference between Ws-F in Manure and Urea as well as DAP and Urea amended soils was significant ($p<0.05$) but there existed no significant relationship between manure and DAP ($p>0.05$) during the incubation period (supplementary data are attached as Appendix 3). When compared to the control, Ws-F concentration in the soils treated with fertilizers increased by 4.1 ± 0.2, 7.8 ± 0.6, and 9.6 ± 1.1 mg/kg for Urea, DAP, and manure, respectively. The increment in the amount of Ws-F observed when Urea was added into the soil is similar to the results obtained by Chen *et al.* (2010) on both fluvo-aquic and paddy soil (Chen, 2010). The increase in the amount of Ws-F was instant during the first 30 days followed by insignificant deviations thereafter in all samples. There was no significant difference observed in Ws-F from day 90 to 150 on all soil samples pointing to the establishment of the equilibrium of fluoride in the soil.

Manure and DAP contained fluoride and therefore the increment in fluoride observed in the soil could be through direct supplementation. But considering the quantity of fertilizers mixed into the soil, the amount released directly into the soil could be estimated to be as low as around 0.2 ± 0.7 mg/kg for DAP and 0.004 ± 0.02 mg/kg for manure and negligible for urea. Therefore, although the fertilizers could have augmented the bioavailability of fluoride in the soil directly, its impact is fairly low as equated to its indirect impact (alteration of the soil elemental composition and pH). The effect of fertilizers on the increase of fluoride fractions was pronounced more on the Ws-F fraction. The Ws-F in the experimental soil was the highest bioavailable fraction over the rest of the fractions and was reported in literature to directly correlate with fluoride uptake by *Trifolium repens* and *Lolium multiflorium* (Arnesen, 1997). The accretion of fluoride in tea leaves was also reported to linearly correlate with the quantity of Ws-F in the soil (Ruan *et al.,* 2003). The Ws-F is the form of fluoride that thaws in soil solution, one that has dimly been attached to the soil solid phase. The higher the amount of Ws-F, the higher its availability for plants and animals, and the higher the toxicity exposure levels (Gao *et al.,* 2012).

Similarly, while Urea did not reveal a noteworthy impact on the amount of Ex-F, manure exhibited a rise of 1.8 ± 0.5 mg/kg and DAP of 0.7 ± 0.5 mg/kg equated to the control soils as shown in Fig. 14 (b). There was no significant difference ($p>0.05$) on the amount of Ex-F

between the fertilizers and control samples except for manure samples. Similarly, a significant difference ($p<0.05$) was observed between the fertilizer-amended soils on the behavior of Ex-F except for DAP and Manure amended soils. The Ex-F exhibited a crisscross rise and fall changes due to its sensitivity to pH changes that were taking place in the soil-fertilizer solution interfaces however the crisscross pattern came to an end from the 90th day where the concentration of Ex-F in both samples became constant through the 150th day. Contrariwise, there was no significant difference ($p>0.05$) in Fe/Mn-F observed between fertilizer-amended soils and the control samples. The initial concentration of Fe/Mn-F in the soil before the addition of fertilizers was 3.1 ± 0.9 mg/kg which augmented to 4.0 ± 2.1, 6.2 ± 1.7, 3.5 ± 0.7, and 6.1 ± 1.9 mg/kg for control, DAP, Urea, and manure, respectively (Fig. 14 (c)). These values are equivalent to an increase of 2.2 ± 0.3 and 2.1 ± 0.2 mg/kg for DAP and manure and a decrease of 0.4 ± 0.2 mg/kg for Urea as equated to the variations in the control sample. Although the impact exerted by fertilizers on Fe/Mn-F was different from one another, the difference was not significant. Furthermore, the fluoride fractions were found to correlate to each other such that Ws-F-Ex-F showed a strong positive correlation (0.697), Ex-F-Fe/Mn-F a moderate positive correlation (0.449), and Ws-F-Fe/Mn-F a weak positive correlation (0.173).

Again, there was no significant variation in the quantity of all fluoride fractions from day 90 to 150, a similar behavior exerted by pH. These correlation between pH variation and the fluoride fractions is also reported by Huang *et al.* (2023). This is the point where the soil establishes its new fluoride distribution equilibrium succeeding fertilizer application. Fertilizers interfere with the fluoride cycle in the soil through the introduction of new ions, changes in pH, and direct introduction of fluoride. New ions present take part in chemical reactions in the soil to gain its stability which further affects the soil pH (Chen *et al.,* 2013; Huang *et al.,* 2023). The ability of the ions to participate in the chemical reactions in the soil can either hasten fluoride release or boost the fluoride holding capacity of the soil the same case being applied to pH changes. Therefore, once fertilizer is introduced into the soil, the soil undergoes these oscillations until a new equilibrium is established.

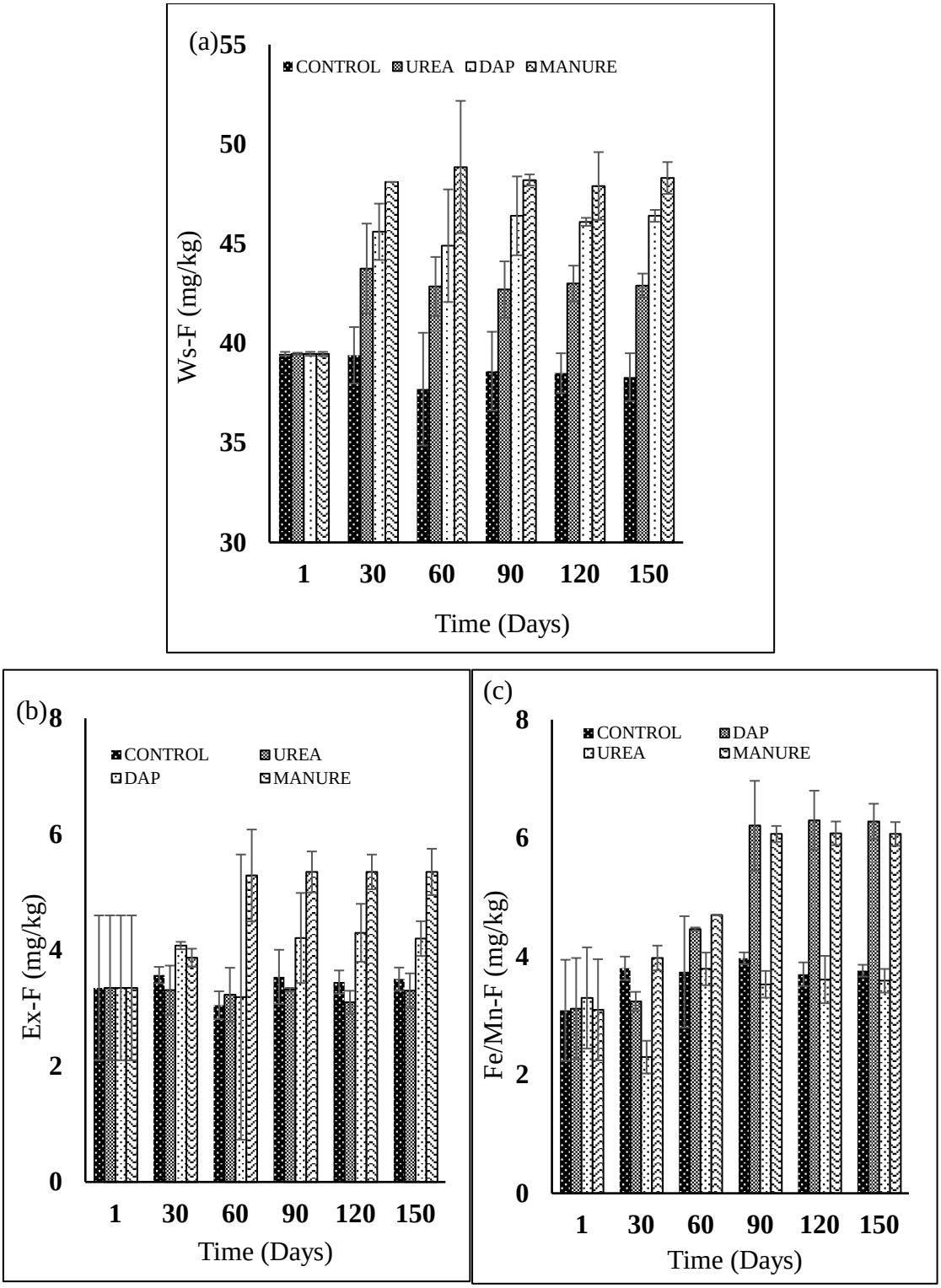

Figure 14: The influence of fertilizers on (a) water-soluble fluoride (Ws-F), (b) Exchangeable - fluoride (Ex-F), (c) fluoride bound to iron and manganese (Fe/Mn-F)

The Ex-F is held by exchangeable cations (Ca^{2+}, Mg^{2+}, Al^{3+}, K^{+}, and H^{+}) in the soil (Rayment & Higginson, 1992). These cations equilibrate charges of unstable clay minerals and are interchangeable with one another. Clay customarily comprises an electrical charge caused

by the imbalance of the quantity of electronegative and electropositive ion layers within the crystals. The imbalance is generated by the impurities integrated into the clay minerals during its development. The presence of an electrical charge attracts ions such as exchangeable cations to gain steadiness. Consequently, exchangeable cations are seized by the negatively charged clay minerals in the soil (Sumner, 1999). Therefore, the number of exchangeable cations and hence Ex-F is limited by the quantity of negatively charged clay particles. The presence of a substantial amount of permanently negatively charged clay minerals increases the number of exchangeable cations and vice versa.

The exposed surface of the Fe/Mn-OH group has an amphoteric character which permits it to lose or accept hydrogen ions contingent on the pH of the soil solution. At low pH, anions are strongly seized and the soil will participate in anion exchange capacity (AEC) whereas, at high pH, cations are strongly seized and become part of the soil CEC (Chen *et al.,* 2013; Sumner, 1999). Also, the carboxyl group associated with the surface of the oxide/hydroxide takes a share in anion exchange with the fluoride-containing ligands exchanging the $F^-$and OH^-liable to pH, the amount of Fe/Mn-OH, and fluoride present in the soil. This elucidates the increase of Fe/Mn-F in the experimental soil. The increase in the amount of Fe/Mn-F is beneficial since this form of fluoride is mostly unavailable for plant uptake (Chen, 2010).

4.3.2 Fluoride Adsorption Efficiency of Dried Seaweed (DSW)

The defluoridation efficiency of DSW at different dosages is presented in Fig. 15 (a). The Tot-F concentration of the experimental soil used for this experiment was 842 ± 26 mg/kg, Ws-F of 81.7 ± 3.1 mg/kg, Ex-F of 5.5 ± 0.1 mg/kg, Fe/Mn-F of 8.7 ± 0.1 mg/kg and Or-F of 11.7 ± 0.8 mg/kg. It is obvious that fluoride removal efficiency is directly proportional to the DWS amended dosage. The amount of Ws-F reduced from 81.7 ± 3.1 mg/kg to 54.2 ± 2.4, 43 ± 1.2, 30.1 ± 0.9, and 22.8 ± 1.3 mg/kg following 0, 1.25, 3, and 5%, DSW amendment at the incubation period of 120 days. The impact of contact time on the Ws-F reduction in the soil is presented in Fig. 15 (b). It is observable that Ws-F in the experimental soil decreased with increasing contact time for all the amendment dosages. Following the amendment of 0, 1.25, 3, and 5%, DSW, the Ws-F decreased from 81.7 ± 3.1 mg/kg to 78.4, 70.6, 67.8, and 54.0 mg/kg within 24 h, and 54.7, 43.2, 43.1 and 32.5 mg/kg by the 30th day, then to 54.7, 43.2, 32.7 and 28.5 mg/kg by the 60th day which remained fairly constant through the 120 days.

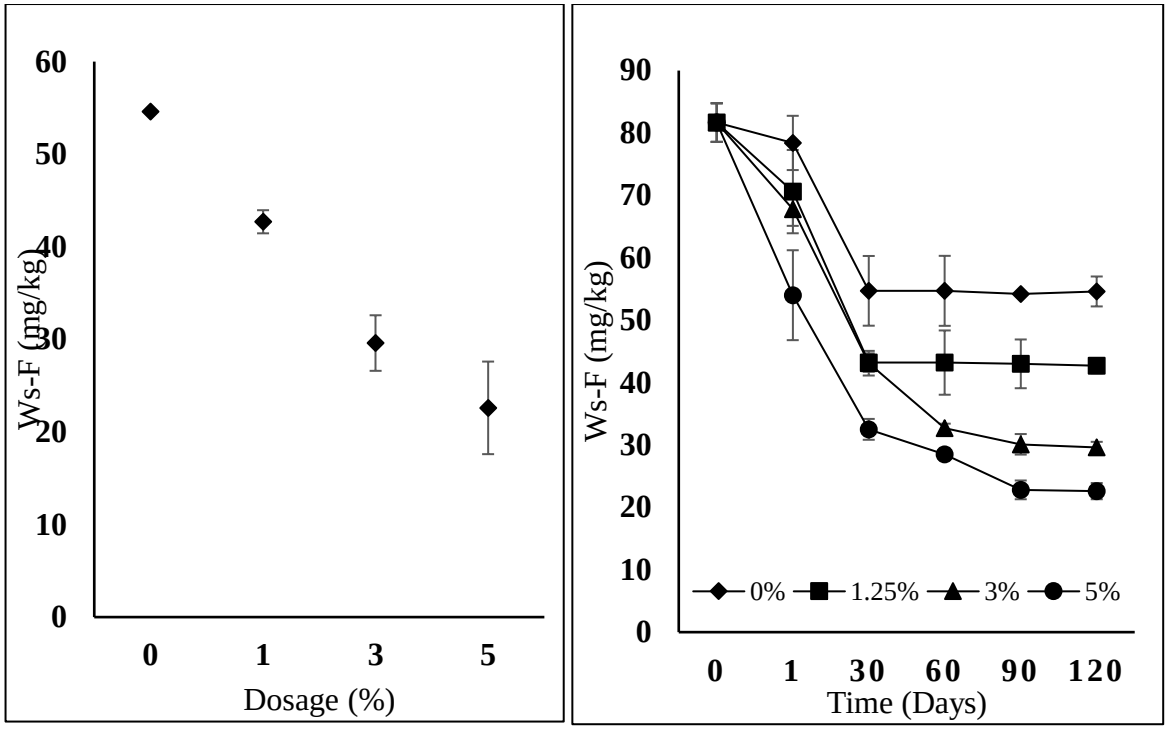

Figure 15: (a) The impact of dried seaweed (DSW) amendment dosage on the amount of water-soluble fluoride (Ws-F) in the soil at the 120th day (b) The impact of contact time/incubation period (0, 1, 30, 60, 90 and 120 days) on the removal of Ws-F in the soil

The influence of the DSW amendment on fluoride fractions in the soil is presented in Table 12. There was a significant difference ($P<0.05$) between the initial and the final concentration of fluoride fractions except for the Fe/Mn-F by the 120th day. While Ws-F decreased by 33.2, 47.7, 63.8, and 72.3%, the Ex-F increased by 64.3, 73.6, 73.8, and 77.5%, and the Fe/Mn-F increased by 6.5, 52.7, 52.5, and 61.5% following the 0, 1.25, 3, and 5% amendment dosages. The DSW amendment had no statistically significant ($p>0.05$) impact on the amount of Or-F as its concentration remained equal with that of the control samples whereas the amount of Res-F increased by 2.2, 3.0, 4.5, and 4.7% following 0, 1.25, 3, and 5% amendments.

Table 12: The influence of dried seaweed (DSW) on the soil fluoride fractions at different amendment dosages

Fluoride fractions	Initial conc.	0 %	1.25%	3%	5%
Ws-F (mg/kg)	81.7 ± 3	54.6 ± 2	42.7 ± 2	29.6 ± 2	22.6 ± 1
Ex-F (mg/kg)	5.5 ± 1	15.4 ± 3	20.9 ± 2	21.0 ± 2	24.4 ± 2
Fe/Mn-F (mg/kg)	8.7 ± 4	9.3 ± 2	18.4 ± 2	18.3 ± 3	22.6 ± 2
Or-F (mg/kg)	11.7 ± 1	4.6 ± 1	4.6 ± 1	4.9 ± 1	4.6 ± 1
Res-F (mg/kg)	734.4 ± 17	751.1 ± 18	757 ± 19	768.2 ± 18	770.8 ± 20

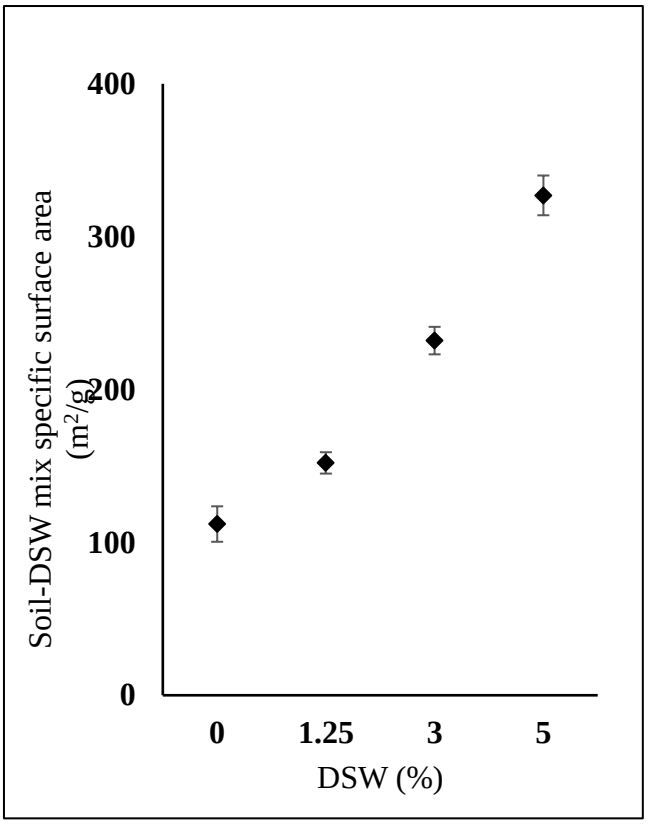

Figure 16: The impact of different DSW amendments (0, 1.25, 3, and 5%) on the soil-specific surface area by the 120th day of incubation

Figure 16 presents the influence of DSW to the soil-specific surface area (SSSA). It is within the solid phase of the soil that the fluoride ions are attached. The higher the amount of the solid phase of the soil the higher the surface area for fluoride ions to attach. By the 120th day, the surface area of the soil increased from 112 ± 11.6 to 152 ± 7, 232 ± 9, and 327 ± 13 following 0, 1.25, 3 and 5% amendments, respectively.

From the data collected, it is obvious that the Ws-F decreased but Ex-F, Fe/Mn-F and Res-F

increased. Therefore, DSW defluoridation mechanism is through conversion of Ws-F into unstable fluoride fractions which are Ex-F and Fe/Mn-F. But also, through conversion of Ws-F into stable/complex fluoride fractions represented as Res-F. The DSW contains different cations and multivalent ions which reacts with the free fluoride present in the soil solution interface leading to an increment in these fluoride fractions, Ex-F and Fe/Mn-F. But the HMWOCs in the seaweed reacts with the free fluoride in the solution interface to form $C-F$ bonds known as fluorocarbons and Organomettalicfluorcarbons as presented by Equations 40 - 41 (Valdivieso *et al.,* 2006; Wambu & Kurui, 2018).

$$\mathrm{R-COO^- + Ca^{2+} + F^- \rightarrow R-COO-Ca-F} \ldots\ldots\ldots\ldots\ldots\ldots\ldots\ldots\ldots\ldots\ldots\ldots\ldots\ldots\ldots\ldots (40)$$

$$R-OH + SiO_2 + 3F^- + 5H^+ + 2e^- \rightarrow R-SiF_3 + 3H_2O \ldots\ldots\ldots\ldots\ldots\ldots\ldots\ldots\ldots\ldots (41)$$

4.3.3 Fluoride Adsorption Efficiency of Fermented Seaweed (FSW)

The four fractions of fluoride were monitored throughout the experiment and the results are presented in Fig. 17. The supplementation decreased the Ws-F from 81. 7 ± 3.1 mg/kg to 42.7 ± 2.4, 33.7 ± 1.2, 19.6 ± 0.9, and 12 ± 1.3 mg/kg following 0, 1.25, 3, and 5%, FSW amendment dosages, respectively. The 5% amendment could reduce the amount of Ws-F below the recommended level of 16.4 mg/kg (Rizzu *et al.,* 2020b). Dissimilar to Ws-F, the Ex-F, and Fe/Mn-F increased following the FSW amendment. The Ex-F increased from 5.5 ± 0.1 mg/kg to 14.8 ± 0.7, 19.1 ± 2, 20.3 ± 0.8, and 21 ± 1.6 mg/kg after 0, 1.25, 3, and 5 %, amendments. The Fe/Mn-F increased from 8.7 ± 0.1 mg/kg to 16.3 ± 3.5, 24.4 ± 2, 24.8 ± 2.1, and 25.7 ± 1 succeeding 0, 1.25, 3, and 5%, FSW amendment which is the lesser bioavailable form compared to the above mentioned two but there was no observed impact of the amendments on Or-F.

There was a significant difference ($p<0.05$) in the amount of Ws-F observed between 0, 1.25, and 3%, to that of 5% amendment within the first 24 h of the incubation. The amendment dosage was inversely related to the amount of Ws-F in the soil such that, as the dosage increased, the Ws-F in the soil reduced. Within 30-day incubation, the amount of Ws-F was significantly different ($p<0.05$) amid the treatments and the control (0%). A significant difference between 1.25 and 3% to the 5% amendment was also observed but the two (1.25 and 3%) were not significantly different ($p>0.05$) up until the 60th day. From the 60th day to the 120th day, there was a significant difference in the amount of Ws-F among all treatments. Furthermore, Fig. 18 presents the influence of FSW amendments on the specific surface area of the soil. The addition

of FSW into the soil increased the soil's specific surface area by 28.2, 49.3, and 67.6% following 1.25, 3, and 5% amendment, respectively.

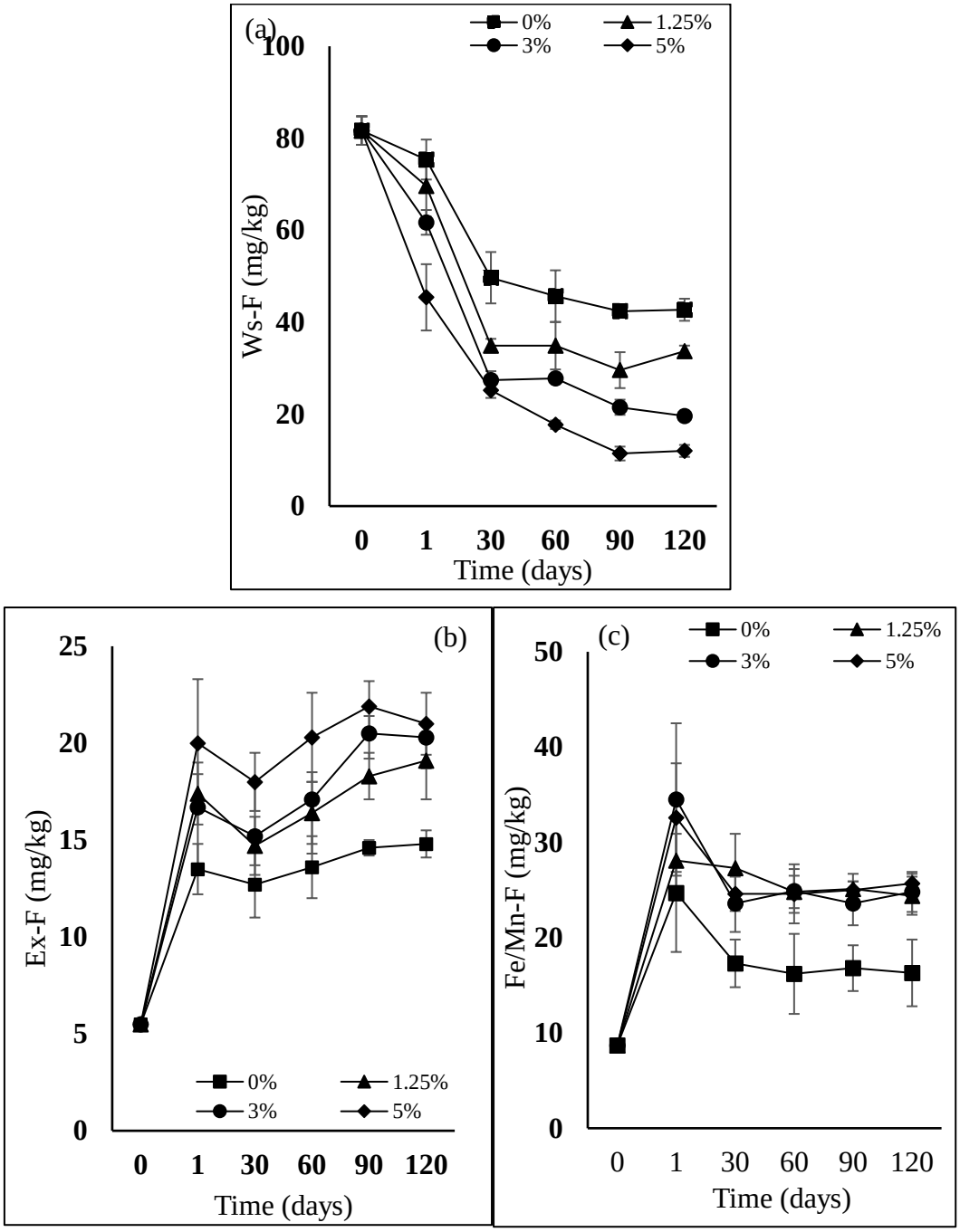

Figure 17: The Impact of Fermented Seaweed (FSW) Amendment on Fluoride Fractions of the Soil (a) Water Soluble-Fluoride (Ws-F), (b) Exchangeable-fluoride (Ex-F), (c) Fluoride-Bound to Iron/Manganese (Fe/Mn-F)

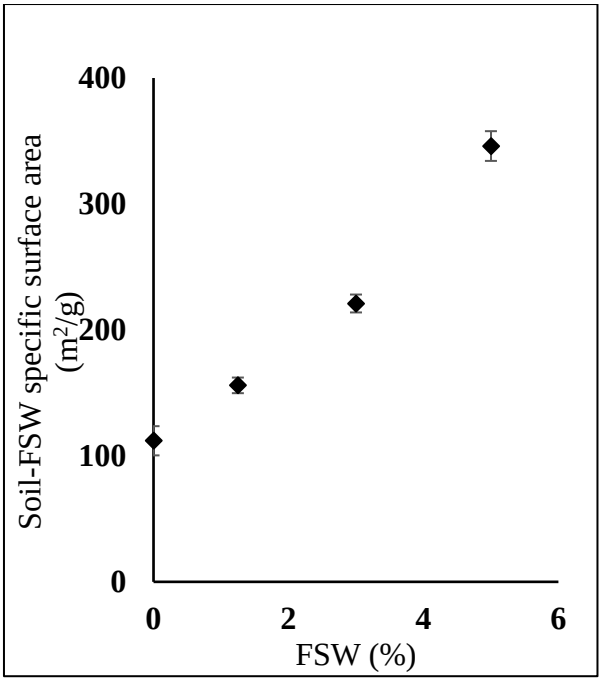

Figure 18: A scatter diagram showing a linear relationship between the FSW and the specific surface area of the soil on the 120th day

To further understand the adsorption mechanism of FSW, its defluoridation data at different initial fluoride concentration were fitted into three models, Langmuir, Freundlich and Temkins and Table 13 represents the calculated isotherm parameters of the three models.

Table 13: Isotherms parameters for the adsorption of fluoride in the soil succeeding fermented seaweed (FSW) amendment at 1.25% amendment dosage

Parameter	Langmuir	Freundlich	Temkin
$Q_{max}(\frac{mg}{g})$	15.67		
$K_L(\frac{L}{mg})$	0.009		
R^2	0.967		
R_L	0.52		
$\frac{1}{n}$		0.58	
K_f		3.733	
R^2		0.959	
$B_T(\frac{J}{mol})$			0.040
$K_T(\frac{L}{mg})$			1.92^22
R^2			0.996

When comparing the R^2 values of the three models, Temkin's model provided the best fit (0.996) for the adsorption data from the experiment. High R^2 signifies a strong contact between

the fluoride ions and the reactive groups in the FSW. According to Temkin's model, the K_T value describes the affinity of the adsorbent to soil ions. The K_T value for this study was extremely high 1.92^22 L/g which expresses the high affinity of fluoride ions to the FSW. The slightly positive value of B_T (0.040) also indicates that this process is somewhat exothermic. The study by Abasiyan *et al.* (2019) reported that the amount of Q_{max} was higher in the soil compared to the same material in the water system (Abasiyan *et al.,* 2019). The high adsorption in the soil is accounted for by the existence of other soil components containing a variety of functional groups such as carboxyl, phenolic, and carbonyl which interact and bind with the target ions in the soil acting as natural adsorbents.

Both HMWOCs and LMWOCs act as binding sites for soil ions. Their binding capacity depends on their length, flexibility, linearity, the number of $-OH$ groups, and the number of acid groups ($-COOH$) (Ruiz-Hitzky *et al.,* 2004). The binding capacity is also catalyzed by the multivalent ions in the soil which react with the negatively charged acidic functional groups of the organic acids generating positively charged compound that reacts with the clay. In both neutral and alkaline soils, the multi-valent ions involved in these reactions are Ca^{2+} and Mg^{2+}(Lützow *et al.,* 2006). Thus, the organic compounds containing acid groups, particularly carboxylic groups ($-COOH$) and the hydroxyl groups ($-OH$) partakes ionic binding with the multi-valent cations which then participate in the ion exchange sites on clay or with anionic adsorption to positively charged clay sites at the edges (Equations 42 - 44) (Ahmed *et al.,* 2021; Ruiz-Hitzky *et al.,* 2004). This could be a multifaceted way through which fluoride is adsorbed into the organic compounds of the FSW.

$$R - COO^{-} + Ca^{2+} \rightarrow R - COO - Ca^{+} \qquad (42)$$

$$R - COO - Ca^{+} + Clay \rightarrow R - COOCa - Clay^{+} \qquad (43)$$

$$R - COOCa - Clay^{+} + F^{-} \rightarrow R - COO - Ca - Clay - F \qquad (44)$$

The FSW also acts indirectly through the alteration of the soil properties. Apart from binding with the soil ions, the application of FSW reduces the bioavailability of fluoride in the soil indirectly by converting most of the Ws-F to either Ex-F, Fe/Mn-F and/or Res-F and also through pH change. The pH which remains an important soil property control the soil's chemical reactions and the activity of soil microorganisms was reduced from strong alkaline (pH 9.3 ± 0.3) to 7.8 ± 0.1, 7.4 ± 0.1, and 7.0 ± 0.0 after the amendments which is in contrast

to the control samples sustained at pH 8.9 ± 0.3.

Among the chemical reactions that pH controls are the sorption and desorption of fluoride in the soil. At high pH, the fluoride attached to either clay particles, exchangeable bases, SOM, or other multivalent elements is easily replaced by the OH^- ions accumulated on the soil solution interface. As the pH drops, the amount of OH^- ions in the soil solution interface diminutions dipping its competition with fluoride ions on the solid phase of the soil which results in more fluoride being held by the soil. At low pH, the F^- substitutes the OH^-, which decreases the number of F^- present in the soil solution interface. If the pH of the soil is high, the unconfined OH^- increases. The upsurge of OH^- further replaces the F^- until an equilibrium is established (Equation 45). But at neutral to low pH the H^+ reacts with the OH^- to form H_2O (Equation 46)

$$R - CO - OH^- + F^- \rightleftharpoons R - CO - F + OH^- \ldots\ldots\ldots\ldots\ldots\ldots\ldots\ldots\ldots\ldots\ldots\ldots\ldots\ldots\ldots\ldots (45)$$

$$R - CO - OH + F^- + H^+ \rightarrow R - CO - F + H_2O \ldots\ldots\ldots\ldots\ldots\ldots\ldots\ldots\ldots\ldots\ldots\ldots\ldots\ldots\ldots . (46)$$

The Ex-F is bound to the exchangeable bases (Ca^{2+}, Mg^{2+}, K^+, and Na^+) in the soil which is sensitive to pH changes whereas the Fe/Mn-F representing fluoride-bound to Fe, Mn, and Al exist in their steady forms (unreactive) at high pH and become reactive (unstable) as pH drops . Therefore, as pH drops, they easily react with the soil's anionic species particularly fluoride which is strong electronegative.

Although defluoridation mechanism of FSW is similar to that of its DSW, its defluoridation efficiency is higher. High defluoridation efficiency of FSW is because of the increment of its reaction surface area and sites. Breaking the HMWOC in the DSW to produce LMWOC does not only increase the reaction sites of a single compound but its surface area as well.

4.3.4 Fluoride Adsorption Efficiency of Seaweed Biochar (SB) and Hydroxyapatite Activated Seaweed Biochar (HSB)

The initial experiment for this section examined the defluoridation efficiency of SB and HSB at different adsorbent dosages (0.1, 0.2, 0.3, 0.4, and 0.5 g) using 5 g of naturally fluoride-polluted soil with a Ws-F concentration of 103.1 ± 3 mg/kg at a 24 h contact time. The results of the impact of adsorbent dosage on fluoride removal are presented in Fig. 19 (a).

As expected, the defluoridation efficiency of both SB and HSB increased with increasing

adsorbent dosage. The maximum defluoridation efficiency of HSB was observed at 0.5 g dosage which was 79%, 74.1% at 0.4 g, 70.8% at 0.3 g, 61.6% at 0.2 g the least being 39.3% at 0.1 g. whereas, SB had a defluoridation efficiency of 0.8%, 3.3%, 7.5%, 8.7%, and 11.5% at 0.1, 0.2,0.3, 0.4, and 0.5 g, respectively. It was obvious that HSB had a higher defluoridation capacity equated to its SB.

To further determine the maximum fluoride adsorption capacity and saturation point of the HSB, diverse initial fluoride concentrations were tested against a constant adsorbent dosage (0.2 g) and its results are presented in Fig. 19 (b). Inorder to obtain different initial fluoride concentration, four different NaF standards were prepared (25, 50, 75, and 100 mg/L). From Fig. 19 (b), the defluoridation capacity of HSB certainly increased with the increasing initial fluoride concentration. At the minimum initial fluoride of 89.1 mg/kg, the defluoridation capacity was 45.7% (C_e = 48.3 mg/kg) while at the initial fluoride concentration of 177.6 mg/kg, the defluoridation capacity increased to 53.8% (C_e = 82.2 mg/kg) without a saturation signal.

To intensely understand the defluoridation behavior of HSB, the defluoridation data were further fitted into the two adsorption isotherm models; Langmuir and Freundlich as presented in Fig. 20, and the model parameters for both models are presented in Table 14. The basic assumption of the Langmuir Theory is that adsorption arises at the homogeneous sites which are specific inside the adsorbent. Once a fluoride ion occupies a specific site, no additional fluoride adsorption happens to generate monolayer adsorption (Walsh *et al.,* 2020). Alternatively, Freundlich's Theory works in an assumption that there occurs an interaction between the fluoride ions and the adsorbent sites as well as with the adsorbed fluoride ions generating the multilayer adsorption (Sundaram *et al.,* 2008).

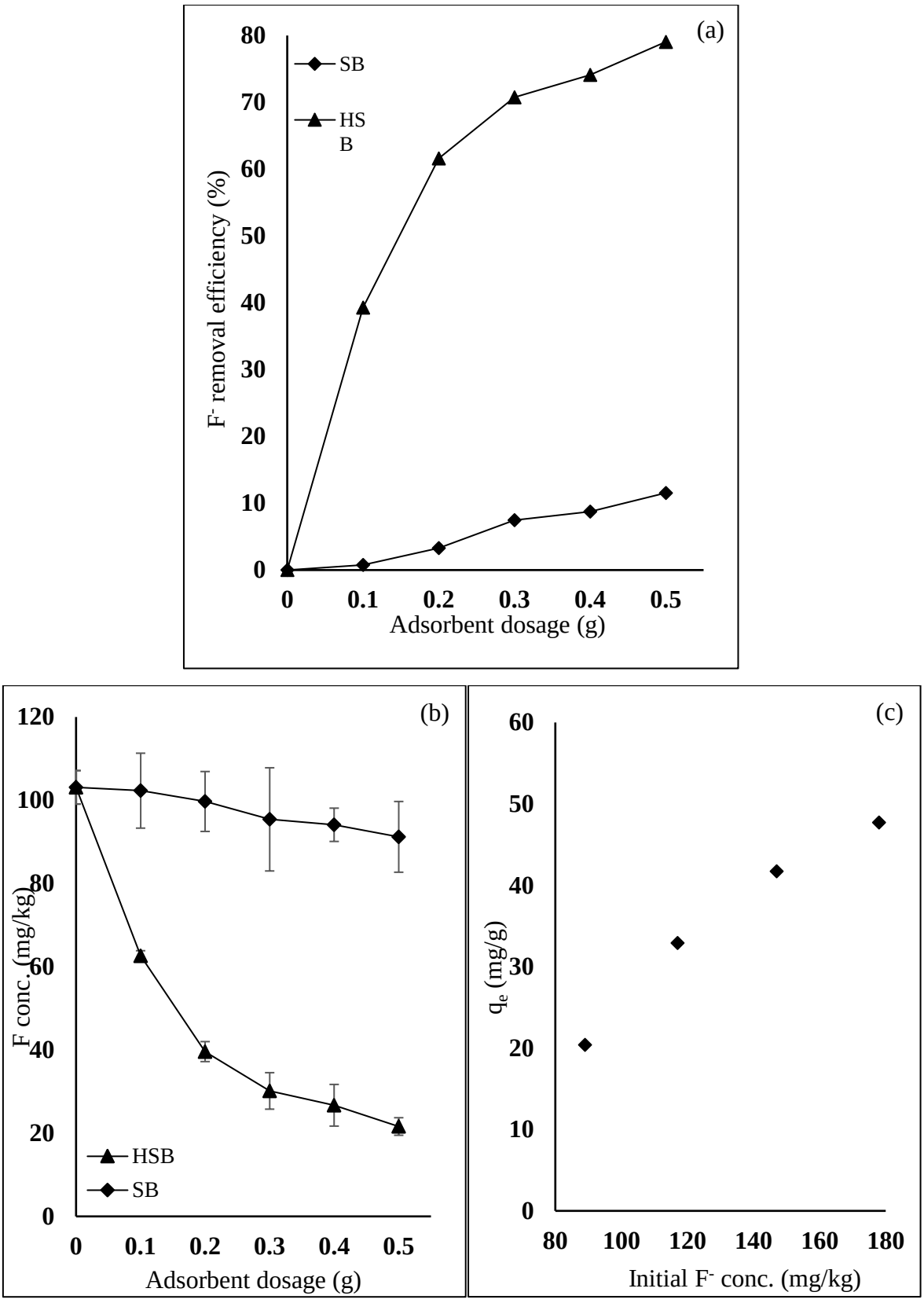

Figure 19: (a) Comparison of the defluoridation efficiency of the seaweed biochar (SB) and the hydroxyapatite-activated seaweed biochar (HSB) (b) comparison of fluoride removal rate (mg/kg) of SB and HSB (c) Defluoridation capacity of the HSB at different initial fluoride concentrations using 0.2 g adsorbent

Based on the coefficient of determination (R^2) results, the adsorption of fluoride onto HSB fits with the Langmuir model ($R^2 = 0.96$) trailed by the Freundlich model ($R^2 = 0.94$). The obtained values of $\frac{1}{n}$ (1) in the Freundlich model lie between 0 and 1 representing the favorable conditions for fluoride sorption and the value of R_L (0.85) in the Langmuir model were similarly in the range of 0 and 1 representing favorable fluoride adsorption conditions as well. From the experimental results, it looks that both models could be used to explain the fluoride adsorption process detected meaning some parts of the adsorbent exhibited a monolayer adsorption and other parts exhibited multilayer adsorption.

Studying the fluoride adsorption mechanism in the soil is tricky since soil itself is a natural adsorbent. But HSB adsorbent itself had different active sites from SB, and those attached with the hydroxyapatite. Thus, the HSB adsorbent had two diverse active sites from hydroxyapatite and its respective SB which have different fluoride adsorption mechanisms displaying the adsorption behaviors that fit both Langmuir and Freundlich models. The solid phase of the soil is also a natural fluoride adsorbent providing the attachment sites for fluoride adsorption and the elemental composition of the soil provides exchange reactions with the free fluoride contributing to the prevailing complex adsorption mechanism of the HSB amended. Therefore, the complex nature of the adsorbent and the soil creates a multifaceted fluoride adsorption mechanism which could either be multilayer or monolayer.

Table 14: The isotherm parameters for Langmuir and Freundlich's models describing the adsorption of fluoride on HSB

Parameters	Langmuir	Freundlich
$Q_{max}(\frac{mg}{g})$	23.3	
$K_L(\frac{L}{mg})$	0.002	
R^2	0.96	
R_L	0.85	
K_f		0.06
$\frac{1}{n}$		1
R^2		0.94

To understand the kinetics of the adsorption process, the kinetic experiments were conducted using 5 g of the soil with an initial fluoride concentration of 100.3 ± 3 mg/kg, and an adsorbent dosage of 0.2 g for contact times of 0.5, 1, 1.5, 2 and 2.5 h. the results for the impact of contact time on fluoride adsorption are presented by Fig. 21. Maximum fluoride was adsorbed within the first 30 minutes followed by a slight removal through an equilibrium. Fluoride concentration in the soil was reduced from 100 ± 3 mg/kg to 28. 8 ± 2 mg/kg equivalent to the HSB defluoridation capacity of 1.79 mg/g (71.3% removal) and the outstanding 3.8 ± 1 mg/kg (2.9% removal) was adsorbed in the subsequent 2 hours accounting for a total HSB defluoridation capacity of 1.88 mg/g (75.2% removal). The defluoridation kinetics of the HSB is analogous to adsorbents reported by Bhaumik *et al.* (2011), Meenakshi and Viswanathan (2007) and Montazeri *et al.* (2011). These results propose that the saturation of HSB is reached immediately after 30 minutes.

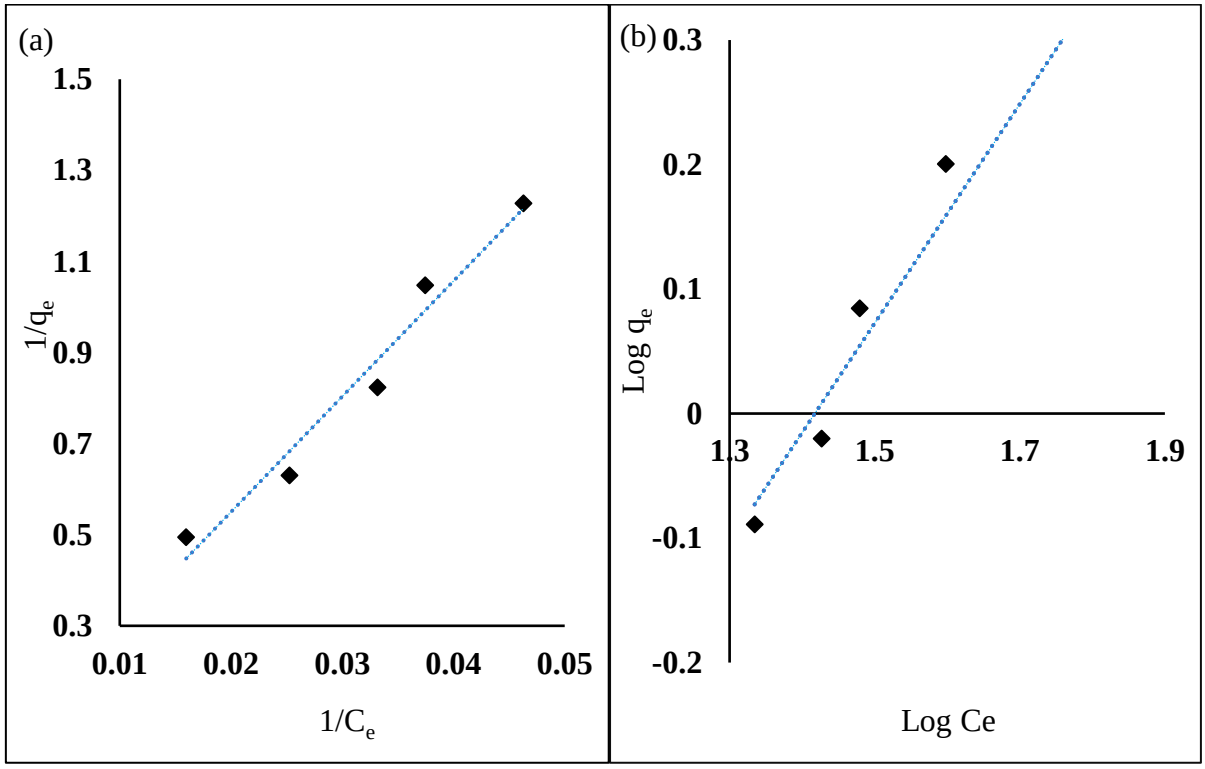

Figure 20: The adsorption model of fluoride into HSB composite at 0.2 g adsorbent dosage (a) Langmuir (b) Freundlich

The data obtained from the kinetic experiment was further fitted into the two common kinetic models; the pseudo-first (Ho, 2006) and the pseudo-second (Zhang *et al.,* 2017) models and the parameters for both models are presented in Table 15. The adsorption kinetics of fluoride ions into the HSB could not fit pseudo-first-order (R^2 = 0.057) but rather pseudo-second-order (R^2= 0.999). The chi-square value (X^2) for the pseudo-second-order model was 0.096 which

is smaller than the X^2 for the pseudo-first-order (1.74) proves to the appropriateness of the pseudo-second-order to the kinetic behavior of fluoride adsorption to the HSB. On another note, the value of q_e for the pseudo-second-order (1.905 mg/g) was closer to the experimental q_e which was 2.02 mg/g whereas the q_e for the pseudo-first-order was 0.834 mg/g showing that the pseudo-first-order is not an appropriate model to describe the kinetics of HSB fluoride adsorption but rather the pseudo-second-order of kinetics .

According to Meenakshi and Viswanathan (2007), the defluoridation process ruled by ion exchange is abruptly equated to the defluoridation process ruled by adsorption (Yang & Al-Duri, 2005). The saturation point of HSB was observed past 30 minutes which according to Sundaram (2008) is not abrupt (Díaz-Nava *et al.,* 2002) demonstrating both adsorption and ion-exchange processes were taking place concurrently. The two fluoride removal processes (adsorption and ion exchange) could be attributed to the presence of active sites of both attached hydroxyapatite, unattached seaweed biochar, and the solid part of soil capable of exchanging or adsorbing the free fluoride.

The defluoridation efficiency of adsorbents at different pH is related to the pH_{PZC} of the adsorbent (Valdivieso *et al.,* 2006). The pH_{ZPC} of SB was 6 and that of HSB was 7.4. The higher pH_{PZC} of HSB could be contributed by the activation of SB using hydroxyapatite. Defluoridation is favored when the pH of the soil-water interface is less than the pH_{PZC} of the adsorbent. If the $pH < pH_{PZC}$ the surface of the adsorbent is positively charged and exerts defluoridation through chemisorption and ion exchange which is stable, abrupt, and favors more fluoride removal. Therefore, rising the pH_{PZC} of the adsorbent enhances its defluoridation efficiency (Sundaram *et al.,* 2009b; Valdivieso *et al.,* 2006). Additionally, when the pH of the soil solution interface is more advanced than the pH_{PZC} of the adsorbent, the surface of the adsorbent develops negative charges exercising an electrostatic repulsion with fluoride ions. Under these conditions, defluoridation occurs through physisorption and to a lesser extent through ion exchange which is a slow and unstable process decreasing the fluoride adsorption capacity of the adsorbent. This elucidates the maximum defluoridation efficiency observed at pH 5 - 7 followed by the sharp diminution at pH 9 – 11 (Bhaumik *et al.,* 2011; McCann, 1953).

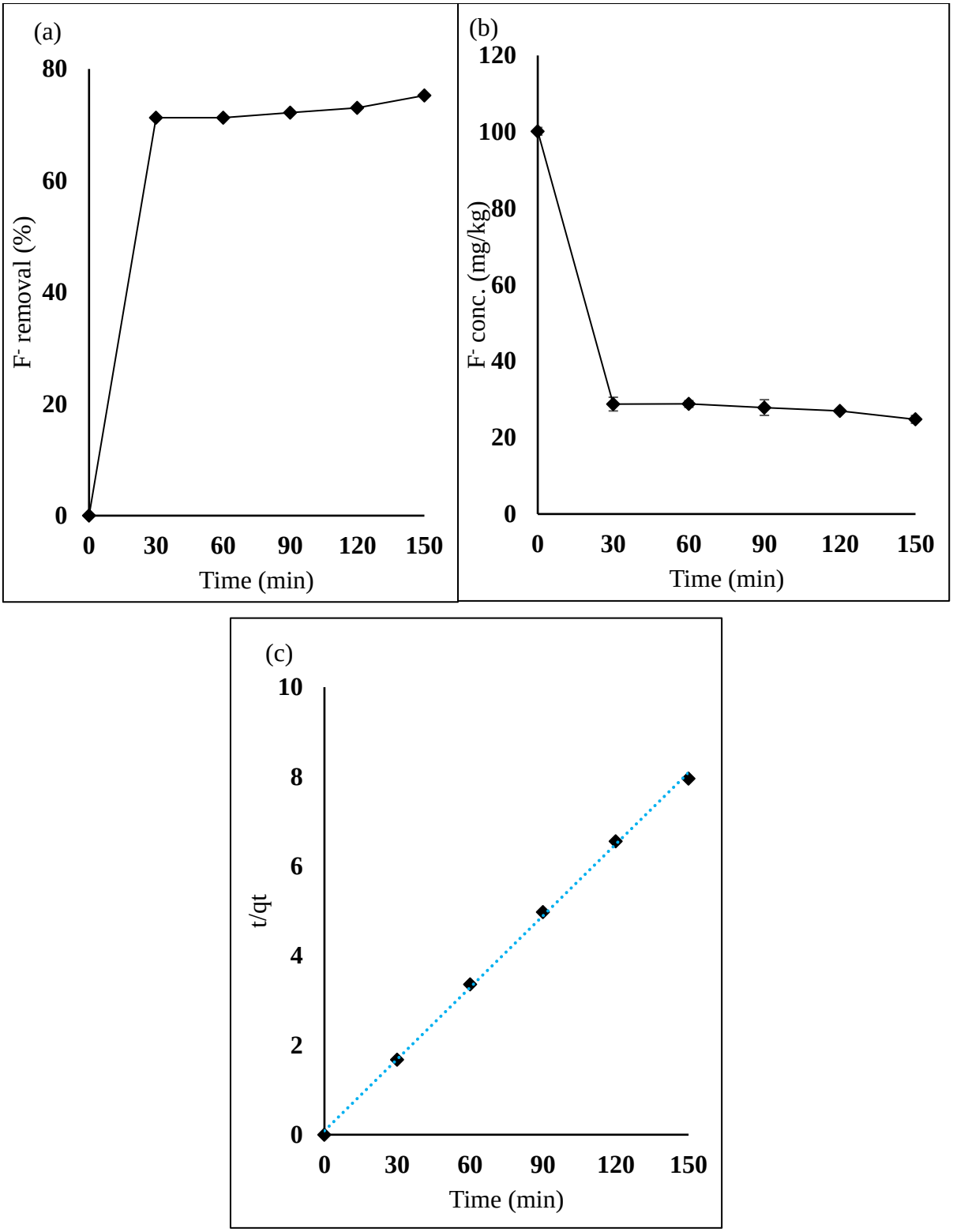

Figure 21: (a) The kinetics of fluoride removal efficiency of HSB at 0.2 g adsorbent dosage (b) The kinetics of fluoride adsorption on HSB at a 0.2 g adsorbent dosage (c) The pseudo-second-order kinetics of HSB

Table 15: Rate constants of the pseudo-first-order and pseudo-second-order

Parameter	Pseudo-first		Pseudo-second
K_1/min	-8.613E-05	$K_2(\frac{\frac{g}{mg}}{\min})$	0.015119
$q_e(\frac{mg}{g})$	0.834	$q_e(\frac{mg}{g})$	1.9048
R^2	0.051	R^2	0.99852
X^2	1.74	X^2	0.096

The soil fluoride removal by HSB was over adsorption and ion-exchange mechanism processes (McCann, 1953). The pH_{PZC} of HSB was 7.4 and below this pH, its surface attains a positive charge endorsing maximum fluoride removal through electrostatic attraction amid the positive HSB adsorbent surface and the negatively charged fluoride ions (Equation 47 - 48). At pH above 7.4, the HSB surface started to acquire a negative charge reducing its affinity to the negatively charged fluoride ions and thus low defluoridation capacity derived through physisorption.

$$Ca_5(PO_4)_3OH + n\,F^- \rightarrow Ca_5(PO_4)_6(OH)....F_n^- \quad (47)$$

$$Ca_5(PO_4)_3OH + n\,F^- \rightarrow Ca_5(PO_4)_3(OH^+)....F_n \quad (48)$$

The ion-exchange mechanism comprises the exchange with the hydroxyl (OH^-) ion obtainable in the hydroxyapatite attached to the HSB (McCann, 1953). The OH^- ion exchanges with the fluoride ion accessible in the soil solution to form fluorapatite (Equation 49 - 50). Furthermore, the soil could be a natural fluoride adsorbent at pH 5.5 - 6.5.

$$Ca_5(PO_4)_3OH + F^- \rightarrow Ca_5(PO_4)_3F + OH^- \quad (49)$$

$$Ca_5(PO_4)_3OH + F^- \rightarrow Ca_5(PO_4)_3FOH \quad (50)$$

CHAPTER FIVE

CONCLUSION AND RECOMMENDATIONS

5.1 Conclusion

The study quantified the amount of fluoride in the soil collected in agricultural soils located along the slopes of Mount Meru. The study presents the quantities of four (4) fluoride fractions present in the agricultural soils located along the slopes of Mount Meru. The four bioavailable fluoride fractions in the soil which was observed to decrease in an order Ws-F >> Or-F > Ex-F > Fe/Mn-F. This amount is higher for daily consumption by the grazing animal through direct soil consumption. Therefore, the result from this study highlights a need to control the bioavailability of fluoride in fluoride-contaminated agricultural soils.

A subsequent experiment focused on identifying whether agricultural practices enhance the bioavailable fluoride fraction in the agricultural soil. The study investigated the influence of the three commonly used fertilizers by farmers in the study area on the bioavailability of fluoride. The results concluded that the application of three fertilizers accelerates the bioavailability of fluoride in the soil at different rates and through different mechanisms in a decreasing order DAP >> manure > Urea. Therefore, it is important for the government authorities to take note and control the fertilizers used in the fluorinated zones of the country.

The study further presented the use of seaweed (*Eucheuma cottonii*)-derived materials for defluoridation purposes of fluoride contaminated soils. The seaweed materials investigated were prepared in four (4) different ways; dried seaweed (DSW), fermented (FSW), seaweed biochar (SB), and hydroxyapatite-activated seaweed biochar (HSB). The results suggest that the defluoridation mechanism of DSW and FSW is similar which is by conversion of Ws-F into Ex-F, Fe/Mn-F and Res-F. But FSW has high defluoridation efficiency compared to DSW because the fermentation process breaks the HMWOCs present in DSW into LMWOCs thereby increases the reaction sites.

Unlike DSW and FSW, the defluoridation efficiency of SB was sensitive to the pH of the soil solution interface. It could perform at pH 5 only, with a maximum defluoridation efficiency of 37.7%, however, its activation with the hydroxyapatite into HSB enhanced its defluoridation efficiency to a maximum of 79% using an initial Ws-F concentration of 103 mg/kg. Activation of SB with hydroxyapatite raised its point-zero-charge (pH_{PZC}) from 6 to 7.4 which further

broadened its fluoride adsorption spectra from strict acidic conditions (pH 5) to a variety of pH conditions (pH 3 - 11). The study envisions that the detected fluoride removal by HSB adsorbent is through chemisorption at pH below the pH_{PZC} of HSB, physisorption into the seaweed biochar at pH above pH_{PZC} of HSB or through ion exchange with the OH^-ion in the hydroxyapatite part of the HSB adsorbent. Therefore, all seaweed preparation methods proved effective for the remediation of fluoride-contaminated soils at decreasing efficiencies HSB >> FSW > DSW > SB.

5.2 Recommendations

Following the conclusions derived from this study, the researcher recommends further investigations on:

(i) The theoretical and experimental study on the performance of these seaweed materials in fluoride-contaminated soils of different pH and textures

(ii) The pot experiment as well as a field experiment to analyze fluoride uptake by crops following DSW, FSW, and HSB amendments

(iii) The lifecycle assessment of fermented seaweed (FSW) and hydroxyapatite activated seaweed biochar (HSB) for its use in the field

(iv) The socio-economic study indicating both social as well as economic feasibility of the use of seaweed (*Eucheuma cottonii)* derived materials

REFERENCES

Abasiyan, S. M. A., Dashbolaghi, F., & Mahdavinia, G. R. (2019). Chitosan cross-linked with κ-carrageenan to remove cadmium from water and soil systems. *Environmental Science and Pollution Research, 26*(25), 26254-26264.

Adamczyk, Z., & Warszyński, P. (1996). Role of electrostatic interactions in particle adsorption. *Advances in Colloid and Interface Science, 63*, 41-149.

Adesiyan, I. M., Bisi-Johnson, M., Aladesanmi, O. T., Okoh, A. I., & Ogunfowokan, A. O. (2018). Concentrations and human health risk of heavy metals in rivers in southwest Nigeria. *Journal of Health and Pollution, 8*(19), 180907.

Ahmad, M. A., Bibi, H., Munir, I., Ahmad, M. N., Zia, A., Mustafa, G., & Khan, I. (2018). Fluoride toxicity and its effect on two varieties of *Solanum lycopersicum*. *Fluoride, 51*(3), 267-277.

Ahmed, D. A. E. A., Gheda, S. F., & Ismail, G. A. (2021). Efficacy of two seaweeds dry mass in bioremediation of heavy metal polluted soil and growth of radish (*Raphanus sativus L.*) plant. *Environmental Science and Pollution Research, 28*(10), 12831-12846.

Al-Dhabaan, F. A. M., & Bakhali, A. H. (2017). Analysis of the bacterial strains using Biolog plates in the contaminated soil from Riyadh community. *Saudi Journal of Biological Sciences, 24*(4), 901-906.

Alexander, B., Olsen, G., Burris, J., Mandel, J., & Mandel, J. (2003). Mortality of employees of a perfluorooctanesulphonyl fluoride manufacturing facility. *Occupational and Environmental Medicine, 60*(10), 722-729.

Ameduri, B., & Boutevin, B. (2004). *Well-architectured fluoropolymers: synthesis, properties and applications*. Elsevier.

Annadurai, S. T., Arivalagan, P., Sundaram, R., Mariappan, R., & Munusamy, A. P. (2019). Batch and column approach on biosorption of fluoride from aqueous medium using live, dead and various pretreated *Aspergillus niger* (FS18) biomass. *Surfaces and Interfaces, 15*, 60-69.

Anukam, A., Mohammadi, A., Naqvi, M., & Granström, K. (2019). A review of the chemistry of anaerobic digestion: Methods of accelerating and optimizing process efficiency. *Processes, 7*(8), 504.

Arnesen, A. (1997). Availability of fluoride to plants grown in contaminated soils. *Plant and Soil, 191*(1), 13-25.

Arnesen, A., Abrahamsen, G., Sandvik, G., & Krogstad, T. (1995). Aluminium-smelters and fluoride pollution of soil and soil solution in Norway. *Science of the Total Environment, 163*(1-3), 39-53.

Asadi, M., Mohammadi, M. T., Moosakazemi, F., Esmaeili, M., & Zakeri, M. (2018). Development of an environmentally friendly flowsheet to produce acid grade fluorite concentrate. *Journal of Cleaner Production, 186*, 782-798.

Asakawa, A., Toyoshima, M., Fujimiya, M., Harada, K., Ataka, K., Inoue, K., & Koizumi, A. (2007). Perfluorooctane sulfonate influences feeding behavior and gut motility via the hypothalamus. *International Journal of Molecular Medicine, 19*(5), 733-739.

Awadia, A., Haugejorden, O., Bjorvatn, K., & Birkeland, J. (1999). Vegetarianism and dental fluorosis among children in a high fluoride area of northern Tanzania. *International Journal of Paediatric Dentistry, 9*(1), 3-11.

Ayub, A., Raza, Z. A., Majeed, M. I., Tariq, M. R., & Irfan, A. (2020). Development of sustainable magnetic chitosan biosorbent beads for kinetic remediation of arsenic contaminated water. *International Journal of Biological Macromolecules, 163*, 603-617.

Baek, K., & Yang, J. S. (2009). *Electrokinetic removal of nitrate and fluoride*. John Wiley & Sons: New Jersey.

Banerjee, A., Roychoudhury, A., & Ghosh, P. (2019). Differential fluoride uptake induces variable physiological damage in a non-aromatic and an aromatic indica rice cultivar. *Plant Physiology and Biochemistry, 142*, 143-150.

Banerjee, A., Samanta, S., & Roychoudhury, A. (2020). Spermine ameliorates prolonged fluoride toxicity in soil-grown rice seedlings by activating the antioxidant machinery and glyoxalase system. *Ecotoxicology and Environmental Safety*, *189*, 109737.

Banerjee, G., Sengupta, A., Roy, T., Banerjee, P. P., Chattopadhyay, A., & Ray, A. K. (2016). Isolation and characterization of fluoride resistant bacterial strains from fluoride endemic areas of west Bengal, India: Assessment of their fluoride absorption efficiency. *Fluoride*, *49*(4), 429.

Bashir, M., Salmiaton, A., Nourouzi, M., Azni, I., & Harun, R. (2015). Fluoride removal by chemical modification of palm kernel shell-based adsorbent: A novel agricultural waste utilization approach. *Asian Journal of Microbiology, Biotechnology, Environmental Sciences*, *17*(3), 533-542.

Baunthiyal, M., & Ranghar, S. (2015). Accumulation of fluoride by plants: potential for phytoremediation. *Clean Soil, Air, Water*, *43*(1), 127-132.

Baunthiyal, M., & Sharma, V. (2012). Phytoremediation of fluoride contaminated water and soil: A search for fluoride hyperaccumulators. *Journal of Agricultural Technology*, *8*(6), 1965-1978.

Bavda, A. R., Bapat, P. S., Joshi, V. B., & Thakur, R. S. (2018). Investigating the chemistry of alumina based defluoridation using safe H+ source. *International Journal of Hydrogen Energy*, *43*(47), 21699-21708.

Bhaumik, M., Leswifi, T. Y., Maity, A., Srinivasu, V., & Onyango, M. S. (2011). Removal of fluoride from aqueous solution by polypyrrole/Fe3O4 magnetic nanocomposite. *Journal of Hazardous Materials*, *186*(1), 150-159.

Bia, G., Borgnino, L., Zampieri, G., & Garcia, M. (2020). Fluorine surface speciation in South Andean volcanic ashes. *Chemical Geology*, *532*, 119402.

Bibi, S., Farooqi, A., Yasmin, A., Kamran, M. A., & Niazi, N. K. (2017). Arsenic and fluoride removal by potato peel and rice husk (PPRH) ash in aqueous environments. *International Journal of Phytoremediation*, *19*(11), 1029-1036.

Biswas, G., Thakurta, S. G., Chakrabarty, J., Adhikari, K., & Dutta, S. (2018). Evaluation of fluoride bioremediation and production of biomolecules by living cyanobacteria under fluoride stress condition. *Ecotoxicology and Environmental Safety*, *148*, 26-36.

Blanco-Flores, A., Arteaga-Larios, N., Pérez-García, V., Martínez-Gutiérrez, J., Ojeda-Escamilla, M., & Rodríguez-Torres, I. (2018). Efficient fluoride removal using Al-Cu oxide nanoparticles supported on steel slag industrial waste solid. *Environmental Science and Pollution Research*, *25*(7), 6414-6428.

Blondel, C., Cacciani, P., Delsart, C., & Trainham, R. (1989). High-resolution determination of the electron affinity of fluorine and bromine using crossed ion and laser beams. *Physical Review A*, *40*(7), 3698.

Bolan, N., Sarkar, B., Yan, Y., Li, Q., Wijesekara, H., Kannan, K., & Noll, H. (2021). Remediation of poly-and perfluoroalkyl substances (PFAS) contaminated soils to mobilize or to immobilize or to degrade? *Journal of Hazardous Materials*, *401*, 123892.

Bose, S., Yashoda, R., & Puranik, M. P. (2019). Novel materials for defluoridation in India: A systematic review. *Journal of Dental Research and Review*, *6*(1), 3.

Bowen, L., & Rood, R. (1966). Solvent extraction of 18F as tetraphenylstibonium fluoride. *Journal of Inorganic and Nuclear Chemistry*, *28*(9), 1985-1990.

Bower, C., & Hatcher, J. (1967). Adsorption of fluoride by soils and minerals. *Soil Science*, *103*(3), 151-154.

Cahyaningtyas, W., Kusumawati, R. & Basmal, J. (2021). Effect of molasses on the chemical characteristics of seaweed-based organic fertiliser. *IOP Conference Series: Earth and Environmental Science*, *733*(1). IOP Publishing, 2021.

Camarena-Rangel, N., Velázquez, A. N. R., & del Socorro Santos-Díaz, M. (2015). Fluoride bioaccumulation by hydroponic cultures of camellia (*Camellia japonica spp.*) and sugar cane (*Saccharum officinarum spp.*). *Chemosphere*, *136*, 56-62.

Chae, G. T., Yun, S. T., Kim, K., & Mayer, B. (2006). Hydrogeochemistry of sodium-bicarbonate type bedrock groundwater in the Pocheon spa area, South Korea: Water rock interaction and hydrologic mixing. *Journal of Hydrology*, *321*(1-4), 326-343.

Chai, L., Wang, Y., Zhao, N., Yang, W., & You, X. (2013). Sulfate-doped Fe_3O_4/Al_2O_3 nanoparticles as a novel adsorbent for fluoride removal from drinking water. *Water Research*, *47*(12), 4040-4049.

Chang, V., & Teo, S. (2016). Evaluation of heavy metal, antioxidant and anti-tyrosinase activities of red seaweed (*Eucheuma cottonii*). *International Food Research Journal*, *23*(6), 2370.

Chatterjee, N., Sahu, G., Bag, A. G., Plal, B., & Hazra, G. (2020). Role of fluoride on soil, plant and human health: A review on its sources, toxicity and mitigation strategies. *International Journal of Environment and Climate Change*, *10*(8), 77-90.

Chen, W. (2010). Effect of nitrogen fertilizer on fluorine species and soil pH in fluorine-contaminate soil. *2010 4th International Conference on Bioinformatics and Biomedical Engineering*, 1-4.

Chen, W., Pang, X., Li, J., & Hang, X. (2013). Effect of oxalic acid and humic acid on the species distribution and activity of fluoride in soil. *Asian Journal of Chemistry*, *25*(1), 469-474.

Chew, K. W., Chia, S. R., Yen, H. W., Nomanbhay, S., Ho, Y. C., & Show, P. L. (2019). Transformation of biomass waste into sustainable organic fertilizers. *Sustainability*, *11*(8), 2266.

Chidambaram, S., Jacob, N., Johnson Babu, G., Selvam, S., Anandhan, P., Rajeevkumar, E., & Tamizharasan, K. (2018). Origin of high fluoride in groundwater of the Tuticorin district, Tamil Nadu, India. *Applied Water Science*, *8*(2), 1-14.

Chowdhury, A., Adak, M. K., Mukherjee, A., Dhak, P., Khatun, J., & Dhak, D. (2019). A critical review on geochemical and geological aspects of fluoride belts, fluorosis and natural materials and other sources for alternatives to fluoride exposure. *Journal of Hydrology*, *574*, 333-359.

Costarramone, N., Tellier, S., Grano, B., Lecomte, D., & Astruc, M. (2000). Effect of selected conditions on fluorine recovery from a soil, using electrokinetics. *Environmental Technology*, *21*(7), 789-798.

Craigie, J. S. (2011). Seaweed extract stimuli in plant science and agriculture. *Journal of Applied Phycology*, *23*, 371-393.

Cronin, S., Manoharan, V., Hedley, M., & Loganathan, P. (2000). Fluoride: A review of its fate, bioavailability, and risks of fluorosis in grazed-pasture systems in New Zealand. *New Zealand Journal of Agricultural Research*, *43*(3), 295-321.

Cronin, S. J., Neall, V., Lecointre, J., Hedley, M., & Loganathan, P. (2003). Environmental hazards of fluoride in volcanic ash: A case study from Ruapehu volcano, New Zealand. *Journal of Volcanology and Geothermal Research*, *121*(3-4), 271-291.

Dagnaw, L. A., Chandravanshi, B. S., & Zewge, F. (2017). Fluoride content of leafy vegetables, irrigation water, and farmland soil in the rift valley and in non-rift valley areas of Ethiopia. *Fluoride*, *50*(4), 409-429.

Das, D. P., Das, J., & Parida, K. (2003). Physicochemical characterization and adsorption behavior of calcined Zn/Al hydrotalcite-like compound (HTlc) towards removal of fluoride from aqueous solution. *Journal of Colloid and Interface Science*, *261*(2), 213-220.

Dehbandi, R., Moore, F., & Keshavarzi, B. (2017). Provenance and geochemical behavior of fluorine in the soils of an endemic fluorosis belt, central Iran. *Journal of African Earth Sciences*, *129*, 56-71.

Dehghani, M. H., Farhang, M., Alimohammadi, M., Afsharnia, M., & Mckay, G. (2018). Adsorptive removal of fluoride from water by activated carbon derived from $CaCl_2$-modified Crocus sativus leaves: Equilibrium adsorption isotherms, optimization, and influence of anions. *Chemical Engineering Communications*, *205*(7), 955-965.

Del-Socorro, M. S,, & Zamora-Pedraza, C. (2010). Fluoride removal from water by plant species that are tolerant and highly tolerant to hydrogen fluoride. *Fluoride*, *43*(2), 150-156.

Delmelle, P., Lambert, M., Dufrêne, Y., Gerin, P., & Óskarsson, N. (2007). Gas/aerosol–ash interaction in volcanic plumes: New insights from surface analyses of fine ash particles. *Earth and Planetary Science Letters*, *259*(1-2), 159-170.

Díaz-Nava, C., Olguin, M., & Solache-Ríos, M. (2002). Water defluoridation by Mexican heulandite–clinoptilolite. *Separation Science and Technology*, *37*(13), 3109-3128.

Distantina, S., & Fahrurrozi, M. (2011). Carrageenan properties extracted from *Eucheuma cottonii*, Indonesia. *International Journal of Chemical and Molecular Engineering*, *5*(6), 501-505.

Dong, S., & Wang, Y. (2016). Characterization and adsorption properties of a lanthanum-loaded magnetic cationic hydrogel composite for fluoride removal. *Water Research*, *88*, 852-860.

Dugyala, V. R., Muthukuru, J. S., Mani, E., & Basavaraj, M. G. (2016). Role of electrostatic interactions in the adsorption kinetics of nanoparticles at fluid–fluid interfaces. *Physical Chemistry Chemical Physics*, *18*(7), 5499-5508.

El-Said, G. F., El-Sadaawy, M. M., & Aly-Eldeen, M. A. (2018). Adsorption isotherms and kinetic studies for the defluoridation from aqueous solution using eco-friendly raw marine green algae, Ulva lactuca. *Environmental Monitoring And Assessment*, *190*(1), 1-15.

Elliott, H., & Huang, C. (1979). The effect of complex formation on the adsorption characteristics of heavy metals. *Environment International*, *2*(3), 145-155.

Enriquez, V. A. (2017). Growth performance of water spinach, Ipomoea aquatica on seaweed, *Eucheuma cottonii* compost treated soil and other commercial growing media. *International Journal of Agriculture and Economic Development*, *5*(1), 29.

Ernst, J., & Massey, H. (1960). The effects of several factors on volatilization of ammonia formed from urea in the soil. *Soil Science Society of America Journal*, *24*(2), 87-90.

Evangeline, C., & Pragasam, V. (2015). Adsorptive fluoride removal from aqueous solution by using saponified orange peel residue immobilized sorbent. *International Journal of Pharma and Bio Sciences*, *6*(1).

FAO. (2003). Toxicological Profile of Fluorides, Hydrogen fluoride and Fluorine

Fawell, J., Bailey, K., Chilton, J., Dahi, E., & Magara, Y. (2006). *Fluoride in drinking-water*. IWA publishing.

Fendi, F., Lili, L., Rakhfid, A., & Rochmady, R. (2019). The growth of seaweed (*Eucheuma cottoni*) at different fertilizing doses in the waters of the village of Ghonebalano, Duruka District, Muna Regency, Indonesia. *Akuatikisle: Jurnal Akuakultur, Pesisir dan Pulau-Pulau Kecil*, *3*(1), 17-22.

Fidanci, U. R. S., Tevhide. (2001). The industrial fluorosis caused by a coal-burning power station and its effects on sheep. *Turkish Journal of Veterinary and Animal Sciences*, *25*(5), 735-741.

Fiedler, H. (2007). National PCDD/PCDF release inventories under the Stockholm convention on persistent organic pollutants. *Chemosphere*, *67*(9), S96-S108.

Fuge, R. (1988). Sources of halogens in the environment, influences on human and animal health. *Environmental Geochemistry and Health*, *10*(2), 51-61.

Fung, K., Zhang, Z., Wong, J., & Wong, M. H. (2003). Aluminium and fluoride concentrations of three tea varieties growing at Lantau Island, Hong Kong. *Environmental Geochemistry and Health*, *25*(2), 219-232.

Fuwa, K. (1986). Analytical chemistry and biogeochemistry of fluorine: An historical view. In *Studies in Environmental Science, 27*, 3-14. Elsevier.

Gan, C. D., Jia, Y. B., & Yang, J. Y. (2021). Remediation of fluoride contaminated soil with nano-hydroxyapatite amendment: Response of soil fluoride bioavailability and microbial communities. *Journal of Hazardous Materials*, *405*, 124694.

Ganvir, V., & Das, K. (2011). Removal of fluoride from drinking water using aluminum hydroxide coated rice husk ash. *Journal of Hazardous Materials*, *185*(2-3), 1287-1294.

Gao, H., Zhang, Z., & Wan, X. (2012). Influences of charcoal and bamboo charcoal amendment on soil-fluoride fractions and bioaccumulation of fluoride in tea plants. *Environmental Geochemistry and Health*, *34*(5), 551-562.

Gebrewold, B. D., Kijjanapanich, P., Rene, E. R., Lens, P. N., & Annachhatre, A. P. (2019). Fluoride removal from groundwater using chemically modified rice husk and corn cob activated carbon. *Environmental Technology*, *40*(22), 2913-2927.

Ghiglieri, G., Balia, R., Oggiano, G., & Pittalis, D. (2010). Prospecting for safe (low fluoride) groundwater in the Eastern African Rift: The Arumeru District (Northern Tanzania). *Hydrology and Earth System Sciences*, *14*(6), 1081-1091.

Gilpin, L., & Johnson, A. H. (1980). Fluorine in agricultural soils of southeastern Pennsylvania. *Soil Science Society of America Journal*, *44*(2), 255-258.

Gogoi, S., & Dutta, R. K. (2016). Fluoride removal by hydrothermally modified limestone powder using phosphoric acid. *Journal of Environmental Chemical Engineering*, *4*(1), 1040-1049.

Guntur, D. C. P., Yona, D., Pratiwi, N., & Alifi, Y. Phytoremidiation of Pb and Cd using indigenous *Eucheuma cottonii* Madura Island, Indonesia. *Ecology, Environment and Conservation Journal, 26* (1), 310-313.

Gupta, A. K., & Ayoob, S. (2016). *Fluoride in drinking water: Status, issues, and solutions*. CRC Press.

Hani, H. (1978). Interactions by fluoride with a mineral soil containing illite and alterations of maize plants grown in this soil. *Fluoride*, *11*(1), 18-24.

Harada, K. H., & Koizumi, A. (2009). Environmental and biological monitoring of persistent fluorinated compounds in Japan and their toxicities. *Environmental Health and Preventive Medicine, 14*(1), 7-19.

Harsanyi, A., & Sandford, G. (2015). Organofluorine chemistry: Applications, sources and sustainability. *Green Chemistry*, *17*(4), 2081-2086.

He, H., & Suito, H. (2001). Immobilization mechanism of fluorine in aqueous solution with calcium aluminates. *Iron and Steel Institute of Japan International*, *41*(5), 506-512.

He, J., Cai, X., Chen, K., Li, Y., Zhang, K., Jin, Z., & Kong, L. (2016). Performance of a novelly-defined zirconium metal-organic frameworks adsorption membrane in fluoride removal. *Journal of Colloid and Interface Science*, *484*, 162-172.

He, J., Yang, Y., Wu, Z., Xie, C., Zhang, K., Kong, L., & Liu, J. (2020). Review of fluoride removal from water environment by adsorption. *Journal of Environmental Chemical Engineering*, *8*(6), 104516.

Hegde, R. M., Rego, R. M., Potla, K. M., Kurkuri, M. D., & Kigga, M. (2020). Bio-inspired materials for defluoridation of water: A review. *Chemosphere*, *253*, 126657.

Ho, Y.-S. (2006). Second-order kinetic model for the sorption of cadmium onto tree fern: A comparison of linear and non-linear methods. *Water Research*, *40*(1), 119-125.

Hodge, H., & Smith, F. A. (1977). Occupational fluoride exposure. *Journal of Occupational Medicine*, *19*(1), 12-39.

Hong, B. D., Joo, R. N., Lee, K. S., Lee, D. S., Rhie, J. H., Min, S. W., & Chung, D. Y. (2016). Fluoride in soil and plant. *Korean Journal of Agricultural Science*, *43*(4), 522-536.

Hoogers, G. (2002). *Fuel cell technology handbook*. CRC press.

Hu, Y., Lu, Y., Veeramasuneni, S., & Miller, J. (1997). Electrokinetic behavior of fluoride salts as explained from water structure considerations. *Journal of Colloid and Interface Science*, *190*(1), 224-231.

Huang, S., Guo, J., Xie, Y., Bian, R., Wang, N., Qi, W., & Liu, H. (2023). Distribution, sources, and potential health risks of fluoride, total iodine, and nitrate in rural drinking water sources of North and East China. *Science of the Total Environment*, 165561.

Huq, N. A., Hafenstine, G. R., Huo, X., Nguyen, H., Tifft, S. M., Conklin, D. R., & Heyne, J. S. (2021). Toward net-zero sustainable aviation fuel with wet waste–derived volatile fatty acids. *Proceedings of the National Academy of Sciences*, *118*(13), e2023008118.

Hussein, H., Farag, S., & Moawad, H. (2003). Isolation and characterization of Pseudomonas resistant to heavy metals contaminants. *Arab journal of Biotechnology*, *7*, 13-22.

Ibrahim, Y., Abuaffan, A. H., & Bjorvatn, K. (1995). Prevalence of dental fluorosis in Sudanese children from two villages with 0.25 and 2.56 ppm fluoride in the drinking water. *International Journal of Paediatric Dentistry*, *5*(4), 223-229.

Ingle, N. A., Dubey, H. V., Kaur, N., & Sharma, I. (2014). Defluoridation techniques: Which one to choose. *Journal of Health Research and Reviews*, *1*(1), 1.

Jarvis, H. G., Heslop, P., Kisima, J., Gray, W. K., Ndossi, G., Maguire, A., & Walker, R. W. (2013). Prevalence and aetiology of juvenile skeletal fluorosis in the south-west of the

H ai district, Tanzania: A community-based prevalence and case–control study. *Tropical Medicine & International Health*, *18*(2), 222-229.

Jayarathne, T., Stockwell, C. E., Yokelson, R. J., Nakao, S., & Stone, E. A. (2014). Emissions of fine particle fluoride from biomass burning. *Environmental science & technology*, *48*(21), 12636-12644.

Jha, S., Nayak, A., Sharma, Y., Mishra, V., & Sharma, D. (2008). Fluoride accumulation in soil and vegetation in the vicinity of brick fields. *Bulletin of Environmental Contamination and Toxicology*, *80*(4), 369-373.

Jha, S. K., Mishra, V. K., Sharma, D. K., & Damodaran, T. (2011). Fluoride in the environment and its metabolism in humans. *Reviews of Environmental Contamination and Toxicology*, *211*, 121-142.

Jones, D. L. (1998). Organic acids in the rhizosphere–a critical review. *Plant and Soil*, *205*(1), 25-44.

Jumaidin, R., Sapuan, S., Jawaid, M., Ishak, M., & Sahari, J. (2017). Characteristics of *Eucheuma cottonii* waste from East Malaysia: Physical, thermal and chemical composition. *European Journal of Phycology*, *52*(2), 200-207.

Jung, K., Kim, W., Park, G. W., Seo, C., Chang, H. N., & Kim, Y. C. (2015). Optimization of volatile fatty acids and hydrogen production from Saccharina japonica: Acidogenesis and molecular analysis of the resulting microbial communities. *Applied Microbiology and Biotechnology*, *99*(7), 3327-3337.

Justo, A. J., Junfeng, L., Lili, S., Haiman, W., Lorivi, M. R., Mohammed, M. O., &Yujie, F. (2016). Integrated expanded granular sludge bed and sequential batch reactor treating beet sugar industrial wastewater and recovering bioenergy. *Environmental Science and Pollution Research*, *23*(20), 21032-21040.

Kalyani, G., Rao, G. B., Vijaya, B., & Kumar, Y. P. (2009). Biosorption isotherms of fluoride from aqueous solution on Ulva fasciata sp.: A waste material. *International Journal of Applied Environmental Sciences*, *4*(2), 177-186.

Kamathi, M. C. (2017). *Defluoridation Of Water by Adsorption with Triethylamine Modified Maize Tassels* (Doctoral dissertation, Kenyatta University).

Khandare, A. L., & Rao, G. S. (2006). Uptake of fluoride, aluminum and molybdenum by some vegetables from irrigation water. *Journal of Human Ecology*, *19*(4), 283-288.

Kihampa, C., Mato, R. R., & Mohamed, H. (2010). Residues of organochlorinated pesticides in soil from tomato fields, Ngarenanyuki, Tanzania. *Journal of Applied Sciences and Environmental Management*, *14*(3).

Kim, D. H., Jeon, C. S., Baek, K., Ko, S. H., & Yang, J. S. (2009). Electrokinetic remediation of fluorine-contaminated soil: Conditioning of anolyte. *Journal of Hazardous Materials*, *161*(1), 565-569.

Kim, Y., Kim, J. Y., & Kim, K. (2011). Geochemical characteristics of fluoride in groundwater of Gimcheon, Korea: Lithogenic and agricultural origins. *Environmental Earth Sciences*, *63*(5), 1139-1148.

Koretsky, C. (2000). The significance of surface complexation reactions in hydrologic systems: A geochemist's perspective. *Journal of Hydrology*, *230*(3-4), 127-171.

Krishnamoorthy, M., & Malek, S. A. (2022). Application of Seaweed (*Eucheuma cottonii*) Extract and Shrimp Waste as Biofertilizer for Mustard (*Brassica juncea L.*). *AgroTech-Food Science, Technology and Environment*, *1*(2), 14-19.

Kumar, B., Naaz, A., Shukla, K., Narayan, C., Singh, G., Kumar, A., & Ramanathan, A. (2016). Spatial variability of fluorine in agricultural soils around Sidhi District, Central India. *Journal of the Geological Society of India*, *87*(2), 227-235.

Kvande, H., & Drabløs, P. A. (2014). The aluminum smelting process and innovative alternative technologies. *Journal of Occupational and Environmental Medicine*, *56*(5), S23.

Larsen, S., & Widdowson, A. (1971). Soil fluorine. *Journal of Soil Science*, *22*(2), 210-221.

Li, Y., Wang, S., Sun, H., Huang, W., Nan, Z., Zang, F., & Li, Y. (2020). Immobilization of fluoride in the sediment of mine drainage stream using loess, Northwest China. *Environmental Science and Pollution Research*, *27*(7), 6950-6959.

Liang, C., Gascó, G., Fu, S., Méndez, A., & Paz-Ferreiro, J. (2016). Biochar from pruning residues as a soil amendment: Effects of pyrolysis temperature and particle size. *Soil and Tillage Research*, *164*, 3-10.

Ligate, F. J. (2023). *Hydrogeochemistry of arsenic, fluoride, and other trace elements in groundwater in northern Tanzania: Occurrence, distribution, and impacts on drinking water quality* (Doctoral dissertation, KTH Royal Institute of Technology).

Lindsay, W., & Walthall, P. (2020). The solubility of aluminum in soils. In *The Environmental Chemistry of Aluminum*, 333-361. CRC Press.

Loganathan, P., Hedley, M., Wallace, G., & Roberts, A. (2001). Fluoride accumulation in pasture forages and soils following long-term applications of phosphorus fertilisers. *Environmental Pollution*, *115*(2), 275-282.

Lützow, M. v., Kögel-Knabner, I., Ekschmitt, K., Matzner, E., Guggenberger, G., Marschner, B., & Flessa, H. (2006). Stabilization of organic matter in temperate soils: Mechanisms and their relevance under different soil conditions: A review. *European Journal of Soil Science*, *57*(4), 426-445.

Ma, J., Shen, Y., Shen, C., Wen, Y., & Liu, W. (2014). Al-doping chitosan–Fe (III) hydrogel for the removal of fluoride from aqueous solutions. *Chemical Engineering Journal*, *248*, 98-106.

Ma, X., Li, H., Xu, Y., & Liu, C. (2021). Effects of organic fertilizers via quick artificial decomposition on crop growth. *Scientific Reports*, *11*(1), 1-7.

Maadid, H., El Mzouri, E. H., Mabrouk, A., & Koulali, Y. (2017). Fluoride content in well waters for human and animal consumption with reported high incidence levels of endemic fluorosis in Beni Meskine (Morocco). *Euro-Mediterranean Journal for Environmental Integration*, *2*(1), 1-6.

Mack, G. (1961). Toxicity of Decomposition Products of "Teflon". *Canadian Medical Association Journal*, *85*(17), 955.

Madera-Parra, C. A. (2016). Treatment of landfill leachate by polyculture constructed wetlands planted with native plants. *Ingeniería Y Competitividad*, *18*(2), 183-192.

Mahmić-Kaknjo, M., & Marušić, A. (2015). Analysis of evidence supporting the Federation of Bosnia and Herzegovina reimbursement medicines lists: Role of the WHO Essential Medicines List, Cochrane systematic reviews and technology assessment reports. *European Journal of Clinical Pharmacology*, *71*(7), 825-833.

Malde, M. K., Maage, A., Macha, E., Julshamn, K., & Bjorvatn, K. (1997). Fluoride content in selected food items from five areas in East Africa. *Journal of Food Composition and Analysis*, *10*(3), 233-245.

Mbugua, G., Mwangi, I., Wanjau, R., Ollengo, M. A., Nthiga, E. W., & Ngila, J. C. (2020). Facile removal of Fluoride Ions from water using Triethylamine Modified Polyethylene Adsorbent. *Asian Journal of Research in Chemistry*, *13*(1), 60-64.

McCann, H. G. (1953). Reactions of fluoride ion with hydroxyapatite. *Journal of Biological Chemistry*, *201*(1), 247-259.

McQuaker, N. R., & Gurney, M. (1977). Determination of total fluoride in soil and vegetation using an alkali fusion-selective ion electrode technique. *Analytical Chemistry*, *49*(1), 53-56.

Meenakshi, S., & Viswanathan, N. (2007). Identification of selective ion-exchange resin for fluoride sorption. *Journal of Colloid and Interface Science*, *308*(2), 438-450.

Minasny, B., Hong, S. Y., Hartemink, A. E., Kim, Y. H., & Kang, S. S. (2016). Soil pH increase under paddy in South Korea between 2000 and 2012. *Agriculture, Ecosystems & Environment*, *221*, 205-213.

Mittal, Y., Srivastava, P., Kumar, N., & Yadav, A. K. (2020). Remediation of fluoride contaminated water using encapsulated active growing blue-green algae, Phormidium sp. *Environmental Technology & Innovation*, *19*, 100855.

Mjengera, H., & Mkongo, G. (2003). Appropriate deflouridation technology for use in flourotic areas in Tanzania. *Physics and Chemistry of the Earth, Parts A/B/C*, *28*(20-27), 1097-1104.

Mkungu, J., Machunda, R. L., & Muzuka, A. N. N. (2014). Application of soil composition for inferring fluoride variability in volcanic areas of Mt. Meru, Tanzania. *International Journal of Environmental Monitoring and Analysis*, *2*(5), 231.

Mohamed, W. S. E.-D., Hamad, M. T. M. H., & Kamel, M. Z. (2020). Application of statistical response surface methodology for optimization of fluoride removal efficiency by *Padina sp.* alga. *Water Environment Research*, *92*(7), 1080-1088.

Mohan, S. V., Ramanaiah, S., Rajkumar, B., & Sarma, P. (2007). Biosorption of fluoride from aqueous phase onto algal *Spirogyra* IO1 and evaluation of adsorption kinetics. *Bioresource Technology*, *98*(5), 1006-1011.

Mondal, D., & Gupta, S. (2015). Fluoride hydrogeochemistry in alluvial aquifer: An implication to chemical weathering and ion-exchange phenomena. *Environmental Earth Sciences*, *73*(7), 3537-3554.

Montazeri, N., Jahandideh, R., & Biazar, E. (2011). Synthesis of fluorapatite–hydroxyapatite nanoparticles and toxicity investigations. *International Journal of Nanomedicine*, *6*, 197.

Mukherjee, S., & Halder, G. (2016). Assessment of fluoride uptake performance of raw biomass and activated biochar of Colocasia esculenta stem: Optimization through response surface methodology. *Environmental Progress & Sustainable Energy*, *35*(5), 1305-1316.

Murray, F. (1984). Fluoride retention in highly leached disturbed soils. *Environmental Pollution Series B, Chemical and Physical*, *7*(2), 83-95.

Nehra, S., Raghav, S., & Kumar, D. (2020). Biomaterial functionalized cerium nanocomposite for removal of fluoride using central composite design optimization study. *Environmental Pollution*, *258*, 113773.

O'Hagan, D., Schaffrath, C., Cobb, S. L., Hamilton, J. T., & Murphy, C. D. (2002). Biosynthesis of an organofluorine molecule. *Nature*, *416*(6878), 279-279.

O'hara, P., Fraser, A., & James, M. (1982). Superphosphate poisoning of sheep: The role of fluoride. *New Zealand Veterinary Journal*, *30*(12), 199-201.

Okamoto, Y. (2001). Determination of fluorine in aqueous samples by electrothermal vaporisation inductively coupled plasma mass spectrometry (ETV-ICP-MS). *Journal of Analytical Atomic Spectrometry*, *16*(6), 539-541.

Olsson, B. (1978). Dental caries and fluorosis in Arussi province, Ethiopia. *Community Dentistry and Oral Epidemiology*, *6*(6), 338-343.

Omueti, J., & Jones, R. L. (1980). Fluorine distribution with depth in relation to profile development in Illinois. *Soil Science Society of America Journal*, *44*(2), 247-249.

Ono, Y., Hayashi, Y., Urashima, S. H., & Yui, H. (2022). Glass etching with gaseous hydrogen fluoride: Rapid management of surface nano-roughness. *International Journal of Applied Glass Science*.

Óskarsson, N. (1980). The interaction between volcanic gases and tephra: Fluorine adhering to tephra of the 1970 Hekla eruption. *Journal of Volcanology and Geothermal Research*, *8*(2-4), 251-266.

Patil, S., Jagdale, A., Patil, D., Kulkarni, A., & Govindwar, S. (2014). Evaluation of fluoride uptake and accumulation by *Portulaca grandiflora Hook.* and *Brassica oleracea Linn.* from water. *International Journal od Science, Engineering and Technology Research*, *3*(12), 3474-3477.

Percival, W. (1957). Quantitative determination of fluorinated hydrocarbons by gas chromatography. *Analytical Chemistry*, *29*(1), 20-24.

Perrott, K., Smith, B., & Inkson, R. (1976). The reaction of fluoride with soils and soil minerals. *Journal of Soil Science*, *27*(1), 58-67.

Piccin, J., Dotto, G., & Pinto, L. (2011). Adsorption isotherms and thermochemical data of FD&C Red n 40 binding by chitosan. *Brazilian Journal of Chemical Engineering*, *28*, 295-304.

Pickering, W. (1985). The mobility of soluble fluoride in soils. *Environmental Pollution Series B, Chemical and Physical*, *9*(4), 281-308.

Plácido, J., & Zhang, Y. (2018). Production of volatile fatty acids from slaughterhouse blood by mixed-culture fermentation. *Biomass Conversion and Biorefinery*, *8*(3), 621-634.

Pomes, V., Fernandez, A., Costarramone, N., Grano, B., & Houi, D. (1999). Fluorine migration in a soil bed submitted to an electric field: Influence of electric potential on fluorine removal. *Colloids and Surfaces A: Physicochemical and Engineering Aspects*, *159*(2-3), 481-490.

Popat, K., Anand, P., & Dasare, B. (1994). Selective removal of fluoride ions from water by the aluminium form of the aminomethylphosphonic acid-type ion exchanger. *Reactive Polymers*, *23*(1), 23-32.

Poulsen, R. (2011). *The effect of fluoride pollution on soil microorganisms*

Prabhu, S. M., Yusuf, M., Ahn, Y., Park, H. B., Choi, J., Amin, M. A., & Jeon, B. H. (2023). Fluoride occurrence in environment, regulations, and remediation methods for soil: A comprehensive review. *Chemosphere*, 138334.

Purnamasari, L., Rostaman, T., Widowati, L. R., & Anggria, L. (2021). Comparison of appropriate cation exchange capacity (CEC) extraction methods for soils from several regions of Indonesia. In *IOP Conference Series: Earth and Environmental Science*, *648*(1), 012209.

Qiu, H., Ye, M., Zhang, M.-D., Zhang, X., Zhao, Y., & Yu, J. (2020). Nano-hydroxyapatite encapsulated inside an anion exchanger for efficient defluoridation of neutral and weakly alkaline water. *ACS ES&T Engineering*, *1*(1), 46-54.

Rafique, T., Naseem, S., Ozsvath, D., Hussain, R., Bhanger, M. I., & Usmani, T. H. (2015). Geochemical controls of high fluoride groundwater in Umarkot sub-district, Thar Desert, Pakistan. *Science of the Total Environment*, *530*, 271-278.

Ramteke, L., Sahayam, A., Ghosh, A., Rambabu, U., Reddy, M., Popat, K., & Ghosh, P. (2018). Study of fluoride content in some commercial phosphate fertilizers. *Journal of Fluorine Chemistry*, *210*, 149-155.

Ranjith, M., Sridevi, S., Rao, K. J., Ramesh, T., & Bhave, M. (2017). Fluoride Content of Agricultural Soils and it's Relation with Physicochemical Properties in Kalwakurthy Mandal, Mahabubnagar District, Telangana State. *International Journal of Pure and Applied Bioscience*, *5*(4), 1588-1598.

Rayment, G., & Higginson, F. R. (1992). *Australian laboratory handbook of soil and water chemical methods*. Inkata Press Pty Ltd.

Rizzu, M., Tanda, A., Canu, L., Masawe, K., Mtei, K., Deroma, M. A., & Seddaiu, G. (2020a). Fluoride uptake and translocation in food crops grown in fluoride-rich soils. *Journal of the Science of Food and Agriculture*, *100*(15), 5498-5509.

Rizzu, M., Tanda, A., Canu, L., Masawe, K., Mtei, K., Deroma, M. A., & Seddaiu, G. (2020b). Fluoride uptake and translocation in food crops grown in fluoride-rich soils. *Journal of the Science of Food and Agriculture*, *100*(15), 5498-5509.

Rizzu, M., Tanda, A., Cappai, C., Roggero, P. P., & Seddaiu, G. (2021). Impacts of soil and water fluoride contamination on the safety and productivity of food and feed crops: A systematic review. *Science of the Total Environment*, *787*, 147650.

Rooeda-van-Eysinga, J. (1974). The uptake of fluoride by the root and its effect on various crops, particularly freesias.

Ruan, J., Ma, L., Shi, Y., & Han, W. (2003). Uptake of fluoride by tea plant (*Camellia sinensis L.*) and the impact of aluminium. *Journal of the Science of Food and Agriculture*, *83*(13), 1342-1348.

Ruan, J., Ma, L., Shi, Y., & Han, W. (2004). The impact of pH and calcium on the uptake of fluoride by tea plants (*Camellia sinensis L.*). *Annals of Botany*, *93*(1), 97-105.

Ruiz-Hitzky, E., Aranda, P., & Serratosa, J. M. (2004). *Clay-organic interactions: Organoclay complexes and polymer-clay nanocomposites*. Marcel Dekker: New York.

Saeed, A. A. H., Harun, N. Y., Sufian, S., Siyal, A. A., Zulfiqar, M., Bilad, M. R., & Almahbashi, N. (2020). *Eucheuma cottonii* seaweed-based biochar for adsorption of methylene blue dye. *Sustainability*, *12*(24), 10318.

Sawangjang, B., Induvesa, P., Wongrueng, A., Pumas, C., Wattanachira, S., Rakruam, P., & Khan, E. (2021). Evaluation of fluoride adsorption mechanism and capacity of different types of bone char. *International Journal of Environmental Research and Public Health*, *18*(13), 6878.

Schröder, H. F. (2003). Determination of fluorinated surfactants and their metabolites in sewage sludge samples by liquid chromatography with mass spectrometry and tandem mass spectrometry after pressurised liquid extraction and separation on fluorine-modified reversed-phase sorbents. *Journal of Chromatography A*, *1020*(1), 131-151.

Sedayu, B. B., Erawan, I. M. S., & Assadad, L. (2014). Pupuk cair dari rumput laut *Eucheuma cottonii, Sargassum sp. dan Gracilaria sp.* menggunakan proses pengomposan. *Jurnal Pascapanen dan Bioteknologi Kelautan dan Perikanan*, *9*(1), 61-68.

Selassie, Y. G., Molla, E., Muhabie, D., Manaye, F., & Dessie, D. (2020). Response of crops to fertilizer application in volcanic soils. *Heliyon*, *6*(12).

Shaji, H., Chandran, V., & Mathew, L. (2021). Organic fertilizers as a route to controlled release of nutrients. *Controlled Release Fertilizers for Sustainable Agricultur*, 231-245.

Shanker, A. S., Srinivasulu, D., & Pindi, P. K. (2020). A study on bioremediation of fluoride-contaminated water via a novel bacterium *Acinetobacter sp.* (GU566361) isolated from potable water. *Results in Chemistry*, *2*, 100070.

Sharma, H. S., Fleming, C., Selby, C., Rao, J., & Martin, T. (2014). Plant biostimulants: A review on the processing of macroalgae and use of extracts for crop management to reduce abiotic and biotic stresses. *Journal of Applied Phycology*, *26*, 465-490.

Sharmila, A., Amruthavarshini, V., Chandana, K., & Shreenidhi, H. (2019). Trichoderma Harzianum: An Effective Biosorbent for Defluoridation. *Water and Energy International*, *62*(6), 56-60.

Shu, W., Zhang, Z., Lan, C., & Wong, M. H. (2003). Fluoride and aluminium concentrations of tea plants and tea products from Sichuan Province, PR China. *Chemosphere*, *52*(9), 1475-1482.

Singh, A., Sharma, R., Pant, D., & Malaviya, P. (2021). Engineered algal biochar for contaminant remediation and electrochemical applications. *Science of the Total Environment*, *774*, 145676.

Singh, G., Kumari, B., Sinam, G., Kumar, N., & Mallick, S. (2018). Fluoride distribution and contamination in the water, soil and plants continuum and its remedial technologies, an Indian perspective: A review. *Environmental Pollution*, *239*, 95-108.

Strobel, B. W. (2001). Influence of vegetation on low-molecular-weight carboxylic acids in soil solution: A review. *Geoderma*, *99*(3-4), 169-198.

Sumner, M. E. (1999). *Handbook of soil science*. CRC press.

Sun, E., & Su, H. (1985). Fluoride injury to rice plants caused by air pollution emitted from ceramic and brick factories. *Environmental Pollution Series A, Ecological and Biological*, *37*(4), 335-342.

Sundaram, C. S., Viswanathan, N., & Meenakshi, S. (2008). Uptake of fluoride by nano-hydroxyapatite/chitosan, a bioinorganic composite. *Bioresource Technology*, *99*(17), 8226-8230.

Sundaram, C. S., Viswanathan, N., & Meenakshi, S. (2009a). Defluoridation of water using magnesia/chitosan composite. *Journal of Hazardous Materials*, *163*(2-3), 618-624.

Sundaram, C. S., Viswanathan, N., & Meenakshi, S. (2009b). Fluoride sorption by nano-hydroxyapatite/chitin composite. *Journal of Hazardous Materials*, *172*(1), 147-151.

Supriyono, E., Hastuti, Y. P., & Arifka, A. R. (2022). Combination effect of atonic growth regulator with PES (Provasoli Enrich Seawater) on Seaweed (*Eucheuma Cottonnii*) growth. In *IOP Conference Series: Earth and Environmental Science*, 1033(1), 012019.

Susilorini, R. M. R., Hardjasaputra, H., Tudjono, S., Hapsari, G., Wahyu, S. R., Hadikusumo, G., & Sucipto, J. (2014). The advantage of natural polymer modified mortar with seaweed: Green construction material innovation for sustainable concrete. *Procedia Engineering*, *95*, 419-425.

Suzuki, T., Nakamura, A., Niinae, M., Nakata, H., Fujii, H., & Tasaka, Y. (2013). Immobilization of fluoride in artificially contaminated kaolinite by the addition of commercial-grade magnesium oxide. *Chemical Engineering Journal*, *233*, 176-184.

Symonds, R. B., Rose, W. I., & Reed, M. H. (1988). Contribution of C1- and F- bearing gases to the atmosphere by volcanoes. *Nature*, *334*(6181), 415-418.

Tafu, M., & Chohji, T. (2006). Reaction between calcium phosphate and fluoride in phosphogypsum. *Journal of the European Ceramic Society*, *26*(4-5), 767-770.

Tafu, M., & Manaka, A. (2016). Immobilization of fluoride and heavy-metals in polluted soil. *Environmental Remediation Technologies for Metal-Contaminated Soils*, 147-159.

Tomar, V., Prasad, S., & Kumar, D. (2014). Adsorptive removal of fluoride from aqueous media using *Citrus limonum* (lemon) leaf. *Microchemical Journal*, *112*, 97-103.

Tscherko, D., & Kandeler, E. (1997). Ecotoxicological effects of fluorine deposits on microbial biomass and enzyme activity in grassland. *European Journal of Soil Science*, *48*(2), 329-335.

Udeigwe, T. K., Eze, P. N., Teboh, J. M., & Stietiya, M. H. (2011). Application, chemistry, and environmental implications of contaminant-immobilization amendments on agricultural soil and water quality. *Environment International*, *37*(1), 258-267.

Valdivieso, A. L., Bahena, J. R., Song, S., & Urbina, R. H. (2006). Temperature effect on the zeta potential and fluoride adsorption at the α-Al_2O_3/aqueous solution interface. *Journal of Colloid and Interface Science*, *298*(1), 1-5.

Villalba, G., Ayres, R. U., & Schroder, H. (2007). Accounting for fluorine: Production, use, and loss. *Journal of Industrial Ecology*, *11*(1), 85-101.

Virkutyte, J., Sillanpää, M., & Latostenmaa, P. (2002). Electrokinetic soil remediation: Critical overview. *Science of the Total Environment*, *289*(1-3), 97-121.

Viswanathan, N., Sundaram, C. S., & Meenakshi, S. (2009). Sorption behaviour of fluoride on carboxylated cross-linked chitosan beads. *Colloids and Surfaces B: Biointerfaces*, *68*(1), 48-54.

Waghmare, S. S., & Arfin, T. (2015). Fluoride removal from water by various techniques. *International Journal of Innovative Science, Engineering and Technology, 2*(3), 560-571.

Walsh, K., Mayer, S., Rehmann, D., Hofmann, T., & Glas, K. (2020). Equilibrium data and its analysis with the Freundlich model in the adsorption of arsenic (V) on granular ferric hydroxide. *Separation and Purification Technology*, *243*, 116704.

Wambu, E. W., & Kurui, A. J. (2018). Fluoride adsorption onto soil adsorbents: The role of pH and other solution parameters. *Soil pH for Nutrient Availability and Crop Performance*. IntechOpen.

Wang, J., Zhao, F. J., Meharg, A. A., Raab, A., Feldmann, J., & McGrath, S. P. (2002). Mechanisms of arsenic hyperaccumulation in Pteris vittata. Uptake kinetics, interactions with phosphate, and arsenic speciation. *Plant physiology*, *130*(3), 1552-1561.

Wang, X., Li, Q., Ding, J., Luo, M., Zhang, T., & Zhou, Y. (2007). An improved method for the extraction of low molecular weight organic acids in variable charge soils. *Analytical Sciences*, *23*(5), 539-543.

Wang, Y., Chen, N., Wei, W., Cui, J., & Wei, Z. (2011). Enhanced adsorption of fluoride from aqueous solution onto nanosized hydroxyapatite by low-molecular-weight organic acids. *Desalination*, *276*(1-3), 161-168.

WHO, G. (1984). *Fluorine and fluorides*. World Health Organization.

WHO, G. (2003). Toxicological profile of fluorides, hydrogen fluoride and fluorine

Wyszkowski, M., Chełstowski, A., Ciećko, Z., & Szostek, R. (2014). Long-time effect of hard coal ash on the content of some elements in soil. *Journal of Ecological Engineering*, *15*(1), 55-60.

Yang, X., & Al-Duri, B. (2005). Kinetic modeling of liquid-phase adsorption of reactive dyes on activated carbon. *Journal of Colloid and Interface Science*, *287*(1), 25-34.

Yeung, L. W., & Mabury, S. A. (2015). Are humans exposed to increasing amounts of unidentified organofluorine? *Environmental Chemistry*, *13*(1), 102-110.

Yi, X., Qiao, S., Ma, L., Wang, J., & Ruan, J. (2017). Soil fluoride fractions and their bioavailability to tea plants (*Camellia sinensis L.*). *Environmental Geochemistry and Health*, *39*(5), 1005-1016.

Yousefi, M., Arami, S. M., Takallo, H., Hosseini, M., Radfard, M., Soleimani, H., & Mohammadi, A. A. (2019). Modification of pumice with HCl and NaOH enhancing its

fluoride adsorption capacity: kinetic and isotherm studies. *Human and Ecological Risk Assessment: An International Journal*, *25*(6), 1508-1520.

Yuan, L. Z., Wang, J. N., Ma, C. Y., & Guo, S. H. (2019). Fluorine spéciation in soil and the remediation of fluorine contaminated soil. *Ying Yong Sheng tai xue bao. The Journal of Applied Ecology*, *30*(1), 10-20.

Yukselen, Y., & Kaya, A. (2006). Comparison of methods for determining specific surface area of soils. *Journal of Geotechnical and Geoenvironmental Engineering*, *132*(7), 931-936.

Zang, J., Wang, N., Huang, N., Wang, H., Sui, B., Zhao, C., & Liu, J. (2022). Improved adsorption of fluorine on three typical saline-sodic soils by increasing functional groups with $Al_2(SO_4)_3$ incorporation. *Research Sqaure.*

Zhang, X., Zhang, L., Li, Z., Jiang, Z., Zheng, Q., Lin, B., & Pan, B. (2017). Rational design of antifouling polymeric nanocomposite for sustainable fluoride removal from NOM-rich water. *Environmental Science & Technology*, *51*(22), 13363-13371.

Zhao, S., Liu, Y., Ma, J., Mao, H., Lan, T., Jiang, Y., & Liao, Y. (2015). Influence of fertilizers on fluoride accumulation in tea leaves and its remediation using polyphenol–Ce adsorbents. *Rsc Advances*, *5*(8), 6085-6091.

Zhou, M., Zhu, S., Liu, Y., & Wang, H. (2014). Electrokinetic Remediation of Fluorine-C ontaminated Soil Using Approaching Cathodes. *Clean Soil, Air, Water*, *42*(12), 1771-1775.

Zhu, S., Zhang, J., & Dong, T. (2009). Removal of fluorine from contaminated field soil by anolyte enhanced electrokinetic remediation. *Environmental Earth Sciences*, *59*(2), 379-384.

APPENDICES

Appendix 1: A preliminary study quantifying fluoride fractions, EC, and pH of the soils along the study area

Location	Ws-F	Ex-F	Fe/Mn-F	Or-F	Tot-F	pH	EC
Olkung'wado	52.59±18.5	3.4±2.9	3.18±1.2	6.65±1.7	422.9±0.14	9.3±0.4	208.6
Uwiro	54.63±30.6	5.04±3.7	7.08±2.7	7.17±2.4	327±9.89	8.9±1	254.5
Ngabobo	143.45±100.2	10.2±6.5	3.89±1.7	5.24±0.4	147.9±7.2	8.7±0.3	484
Kireeni	36.57±18.5	4.56±4.6	12.65±4	16.32±2.7	50.7±3.3	9.4±0.5	320.6
Mwakey	62.25±14.7	4.27±4.1	4.43±2.7	6.98±1.4	179.83±11.5	7±0.2	189.5

Appendix 2: Analysis of the differences between the influence of fertilizers on the soil pH with a confidence interval of 95% (pH)

Contrast	Difference	Standardized difference	Critical value	Pr > Diff	Significant
Manure vs Urea	5.656	8.402	2.759	**<0.0001**	Yes
Manure vs DAP	0.889	1.320	2.759	0.560	No
Manure vs Control	0.329	0.488	2.759	0.961	No
Control vs Urea	5.327	7.914	2.759	**<0.0001**	Yes
Control vs DAP	0.560	0.832	2.759	0.839	No
DAP vs Urea	4.767	7.082	2.759	**<0.0001**	Yes
Tukey's d critical value:			3.901		

Appendix 3: Summary of the least square (LS) means for the fertilizers

Fertilizer	Ws-F	Ex-F	Fe/Mn-F	pH
Manure	46.690 a	4.463 a	4.858 a	9.676 a
DAP	45.047 ab	3.847 ab	4.566 a	8.787 a
Control	38.704 c	3.183 b	4.764 a	9.347 a
Urea	43.161 b	3.117 b	3.026 a	4.020 b
Pr > F(Model)	<0.0001	0.057	0.168	<0.0001
Significant	Yes	No	No	Yes

Appendix 4: Raw data (Ws-F) of the defluoridation efficiency of dried seaweed (DSW)

DSW (%)	day 1	day 30	day 60	Day 90	Day 120
0	78.6	53.6	52.3	53.7	54.2
0	77.4	55.7	56.8	55	53.5
0	79.3	54.9	54.9	53.8	56.1
1.25	74	49.2	43.7	45.4	46.7
1.25	69.8	41	42.9	41.5	39.6
1.25	67.9	39.4	42.9	42.1	41.7
3	68.7	39.4	32.2	31.8	31.5
3	67.8	41.9	36.4	28.4	27.6
3	66.9	48.1	29.6	30.1	29.8
5	53	31.3	27	24.8	23.2
5	55.8	33.1	29.4	21.9	21.9
5	53.3	33	29.2	21.6	22.8

Appendix 5: Raw data (Ws-F) of the defluoridation efficiency of Fermented seaweed (FSW)

FSW (%)	day 1	day 30	day 60	Day 90	Day 120
0	79.3	54.6	39.2	42.3	42.7
0	76.1	43.6	48.6	42.3	41.5
0	70.7	50.8	49.2	42.5	43.8
1.25	75.4	33.6	40.5	33.6	36.6
1.25	71.1	34.6	30.4	29.3	32.1
1.25	62.3	36.5	33.7	25.8	32.3
3	60.3	27	27.9	20.5	18.1
3	60	25.6	28.4	23.4	21.1
3	64.8	29.5	27	20.6	19.6
5	53.5	27	18.02	13	12
5	43	24.9	16.65	10	11.3
5	39.7	23.7	18.4	11.3	12.6

RESEARCH OUTPUTS

(i) Journal Papers

Moirana, R. L., Kivevele, T., Mkunda, J., Mtei, K., & Machunda, R. (2021). Trends towards Effective Analysis of Fluorinated Compounds Using Inductively Coupled Plasma Mass Spectrometry (ICP-MS). *Journal of Analytical Methods in Chemistry*, 2021.

Moirana, R. L., Mkunda, J., Perez, M. P., Machunda, R., & Mtei, K. (2021). The influence of fertilizers on the behavior of fluoride fractions in the alkaline soil. *Journal of Fluorine Chemistry*, 250, 109883.

Moirana, R. L., Mkunda, J., Paradelo Perez, M., Perez, R., & Mtei, K. (2022). Remediation of soils contaminated by fluoride using a fermentation product of seaweed (*Eucheuma cottonii*). *Applied and Environmental Soil Science*, 2022.

Moirana, R. L., Mkunda, J., Machunda, R., Paradelo, M., & Mtei, K. (2023). Hydroxyapatite-activated seaweed biochar for enhanced remediation of fluoride-contaminated soil at various pH ranges. *Environmental Advances, 11*, 100329.

(ii) Poster Presentation

Appendix 6: Poster Presentation

Remediation of Soils Contaminated with Fluoride using Seaweed-Derived Materials: Case of Slopes of Mount Meru

Abstract

Exposure to low fluoride is essential for stronger bones and teeth but exposure to high levels (> 3 mg/L/day) leads to hyperostosis and osteoporosis. This study investigated the effectiveness of using seaweed (*Eucheuma cottonii*) derived materials for fluoride contaminated soil remedial purposes. Soil amendment with dried seaweed (DSW) and fermented seaweed (FSW) led to a decrement of Ws-F from 81.7 ± 3.1 mg/kg to 28.5 mg/kg and 12 ± 1.3 mg/kg following 5% (*w/w*) amendments, respectively. But while seaweed-derived biochar (SB) adsorbs fluoride at specific pH values only, its activated product with hydroxyapatite (HSB) exhibited a maximum Ws-F reduction from 103.1 mg/kg to 21.6 ± 2.1 mg/kg at 0.2 g dosage.

Problem Statement

While several defluoridation techniques are dedicated to defluoridation of drinking water, less attention is directed towards other potential fluoride exposure routes particularly soil which harbors most of the fluoride present in the ecosystem. Although most of the fluorides in the soil are sparingly soluble in the presence of water, some such as SiF_4, NaF, and HF are quite soluble constituting the bioavailable fluoride fraction. The bioavailable fluoride in the soil ends up in the food chain directly through uptake and accumulation by plants who are the bottom members of the food chain exposing the rest of the chain to fluoride toxicity. While this is a case, techniques such as electrokinetic, soil washing, biological remediation and immobilization/adsorption have been investigated for soil defluoridation but majority of these techniques are either not economical, have unsatisfactory results or unrealistic for implementation in actual environment calling for more feasible remedial approaches which is the focus of this study.

Methods

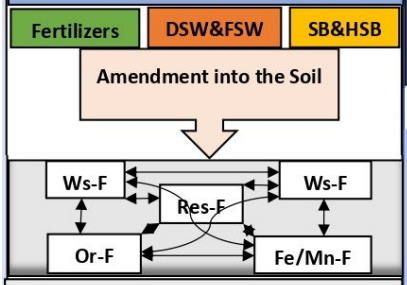

DSW-Dried Seaweed, **FSW**-Fermented Seaweed, **SB**-Seaweed Biochar, **HSB**-Hydroxyapatite Activated SB, **Ws-F**-Water-Soluble Fluoride, **Ex-F** Exchangeable Fluoride, **Fe/Mn-F** Fluoride Bound to Iron and Manganese, **Res-F**-Residual Fluoride, **Or-F**-Organic Matter Bound Fluoride

Results and Discussion

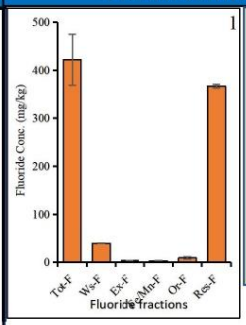

Figure 1: The amount of Total fluoride (Tot-F) and fluoride Fractions (Water-Soluble Fluoride (Ws-F), Exchangeable Fluoride (Ex-F), Fluoride Bound to Iron and Manganese (Fe/Mn-F), Residual Fluoride (Res-F), and Organic Matter Bound Fluoride (Or-F)) in the experimental soil

The soil is characterized by high amount of Ws-F equated to other fluoride fractions and is linked to strong alkalinity property of the soil, low clay content (6%) and high ESP

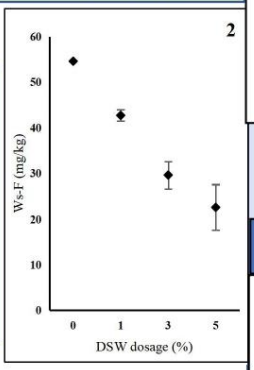

Figure 2: The impact of dried seaweed (DSW) amendment dosage on the amount of water-soluble fluoride (Ws-F) in the soil on the 120th day

DSW defluoridation is through the conversion of Ws-F into Ex-F and Fe/Mn-F and through the formation of C-F bonds and Organometallic complexes between high molecular weight organic compounds (HMWOCs) and fluoride

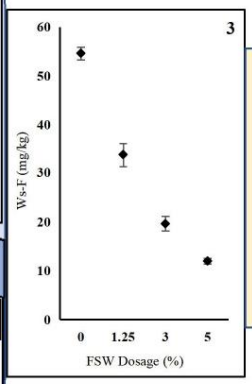

Figure 3: The impact of fermented seaweed (FSW) amendment dosage on the amount of water-soluble fluoride (Ws-F) in the soil on the 120th day

FSW defluoridation is through the conversion of Ws-F into Ex-F and Fe/Mn-F and through the formation of C-F bonds and Organometallic complexes between low molecular weight organic compounds (LMWOCs) and fluoride

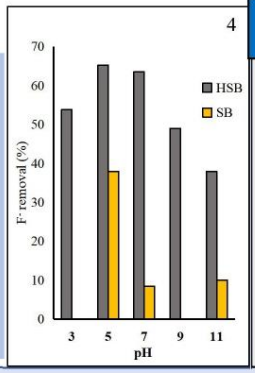

Figure 4: The Defluoridation efficiency of seaweed biochar (SB) and Hydroxyapatite activated seaweed biochar (HSB) at different pH values

SB exerts non-specific adsorption which means it is pH sensitive whereas HSB exerts both specific and non-specific fluoride adsorption meaning some parts are pH dependent and other parts are exerts chemisorption

Conclusion

The results suggest that the defluoridation mechanism of DSW and FSW is similar which is by conversion of Ws-F into Ex-F, Fe/Mn-F, and Res-F.

The FSW has high defluoridation efficiency compared to DSW because the fermentation process breaks the HMWOCs present in DSW into LMWOCs thereby increases the reaction sites.

Likewise, fluoride removal by HSB is through chemisorption at pH below the pH_{PZC} of HSB, physisorption into the

Recommendations

The study recommends further investigations on:

The theoretical and experimental study on the performance of these seaweed materials in fluoride-contaminated soils of different pH and textures

The pot experiment as well as a field experiment to analyze fluoride uptake by crops following DSW, FSW, and HSB amendments

Acknowledgments

This work was funded by the Partnership for Applied Skills in Sciences, Engineering, and Technology-Regional Scholarship Innovation Fund (PASET-RSIF) and the East and West Africa Farming system-BELT (EWA-BELT) Horizon 2020 project No. 862848.